Phosphor Thermometry

" Preliminary Development of a Phosphor Thermometry System"

Master Thesis

Aarhus University
Department of Engineering

Aarhus, Denmark
2018

Author: Javier I. Camacho

Supervisor: Xuping Zhang

Co-Supervisor: Søren Lindholt Andersen

Abstract

The present thesis is based on the contribution from Dansk Teknologisk Institut (DTI) to the EMPRESS Project("European Project to Enhance Process Control Through Improved Temperature Measurement"). In the project(work package#3), one of the objectives involves the development of a surface temperature measurement system, based on a phosphor Thermometry technique. Phosphor Thermometry is a temperature-sensing method, which can determine the temperature remotely through the use of sensor materials known as thermographic phosphors. In contrary to other techniques that are considered non-invasive, such IR method (infrared Thermometry), phosphor Thermometry is considered semi-invasive. This is based on that is required the deposition of a sensing layer on the substrate surface under test. The phosphors are considered thermographic when at least one or more of their luminescence properties show a dependency (or sensitivity) to the change in temperature. The temperature dependence of the emitted light intensity or the decay time(τ) provides the temperature sensing capability of thermographic phosphors.

In this work describes the development of a phosphor Thermometry system (decay time-based), that is composed primarily of a pulsed excitation light source (LED with a waveform controller), a phosphor layer sensor ($Mg_4FGeO_6 : Mn$) applied to the substrate surface, a photo-detector assembly, and a data acquisition system (oscilloscope). The decay time-based phosphor Thermometry procedure starts with a pulsed light source directed towards the phosphor layer sensor deposited onto the substrate surface under test, in order to excite the phosphor material. After the excitation the emitted luminescence from the thermographic phosphor it collected by a photo-sensor assembly. The photo-sensor convert the input emitted luminescence signal into a useful electrical output signal that it acquired by an oscilloscope and storage by software interface. The acquired data require a post-processing that involves the extraction of the information about the decay time and that it is associated with the specific temperature during the calibration.

In the experiential work of this thesis, two phosphor layer sensors have been prepared on top of a stainless steel substrate (thickness < 25 [μm]). The phosphor layers have been exposed to a temperature range from 23 [°C] up to 250 [°C] in a cyclic manner(heating and cooling phase). It is observed that the decay time results in both phosphor sensor layers exhibit a linear relationship with respect to the temperature. However, after the first thermal exposure, the emitted luminescence intensity has shown a significant reduction that consequently affects the SNR (signal-noise ratio) producing an increment in the uncertainty. Furthermore, a detailed explanation of the fabrication of a phosphor layer sensor is included. The quantification of the fabricated phosphor layer thickness has been performed on several different samples. In the preparation of the samples, three operators have been involved achieving a set of layers with a thickness mean value that does not exceed 27.5 [μm](uncertainty values up to 14.1[%])(the process still requires further improvements).

Keywords: Surface Temperature Measurements · Phosphor Thermometry · Thermographic Phosphors · Decay Time Estimation.

DANISH TECHNOLOGICAL INSTITUTE

EMPRESS TEMPERATURE METROLOGY FOR PROCESS EFFICIENCY

EMPIR EURAMET
The EMPIR initiative is co-funded by the European Union's Horizon 2020 research and innovation programme and the EMPIR Participating States

Contents

List of Figures

List of Tables

1
Introduction

This Master Thesis Project in Mechanical Engineering is based on the contribution from Dansk Teknologisk Institut (DTI) to the EMPRESS Project("European Project to Enhance Process Control Through Improved Temperature Measurement" [1]). The EMPRESS project is divided into work packages(WP) in which there are different goals in terms of temperature measurement improvements.

In this particular case, the aim of the related work package(WP3) is to develop traceable surface temperature measurement methods (contact methods) to enhance materials/chemical processing to around 500 [°C] with a target uncertainty of better than 5 [°C] [1].

Furthermore, the temperature measurement methods should allow the calibration of surface temperature sensors, using a novel surface temperature approach, which in this case the technique is based on phosphor Thermometry [1].

The phosphor Thermometry is a remote sensing technique (semi-invasive) in which the temperature is measured without physical connections. The technique makes use of the properties of the thermographic phosphors (phosphor layer sensor) that display a change in their characteristic luminescence as a result of changes in their temperature. Consequently, the method is classified as a semi-invasive, since it requires the deposition of a thermal sensor layer on top of the surface of the object under study [3][6].

1.1 Importance of Surface Temperature Measurements

Temperature measurements play a significant role in many engineering applications.
The reliability of the temperature control in a process it is crucial, especially in the high-value manufacturing process, for example in the aerospace sector. Accurate and traceable temperature measurement are essential for applications up to and above 1300 [°C](casting, forging and sintering)[2]. The industry needs involve achieving improved manufacturability and also energy efficiency quantification.
The manufacturing process such a forming of metal and composites, that works at temperatures below 500 [°C], requires tight temperature control. As a consequence, this small tolerance imposes a challenge in terms of the temperature measurements [2].

1.2 Literature Review

In the literature review will be presented two main topics. The first one, "Contact Surface Measurement" that is considered relevant to this project in order to illustrate the limitations of the method. The second topic deals with the theme of "Phosphor Thermometry", which in this case will be a brief introduction, since this topic will be discussed in detail in a further chapter.

1.2.1 Contact Surface Temperature Measurements

The objective of this section is to illustrate the effect of a contact thermometer on the surface temperature of an object. In order to do that a simplified simulation[1] it is performed based on an example from the book "Temperature Measurement"(ch16) in which it is discussed the "Temperature Measurement of Solid Bodies by Contact Method" [9].

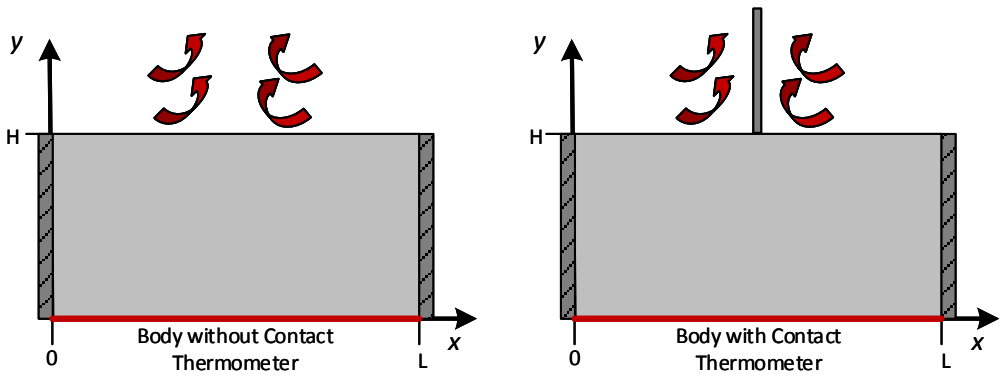

Figure 1.1: 2D Body Diagram

Governing Equation

$$\nabla.(-k\nabla T) = 0 \tag{1.1}$$

Boundary Condition

$$\begin{aligned} &at \quad x = 0 \quad and \quad x = L \quad \forall \quad y \quad q_x = 0 \\ &at \quad y = 0 \quad \forall \quad x \quad T = T_{Set} \\ &at \quad y = H \quad \forall \quad x \quad q = h_{conv}.(T - T_{amb}) \end{aligned} \tag{1.2}$$

Main Assumptions

- Thermal steady state.
- 1D Heat transfer in the block(with boundary conditions that are adiabatic on the lateral sides(no heat flux in the x-coordinates direction),
- Constant temperature at the bottom of the body ($T_{Set} = 150$ [°C]).

[1] In this report: Diagrams(Misosoft-Visio 2016), Technical Drawings(Autodesk Inventor 2018), FEM Simulations (COMSOL 5.2a), Graphical Representation (Plots) and Calculations MATLAB R2017b

- Convective heat flux at the upper surface of the body and around the contact thermometer. ($h_{conv} = 11.13[W/m^2K]$)
- Material properties such as thermal conductivity remain constant.
- Ambient temperature $T_{amb} = 23$ [°C].

The simplified simulations are performed on 2D rectangular body(Aluminium) with a height of $H = 250[mm]$ and a length of $L = 500[mm]$). The dimensions of the contact thermometer sensor(Chromel)are $130[mm]$ of length, and $6[mm]$ length at the contact with the body.

Simulation Results and Discussion

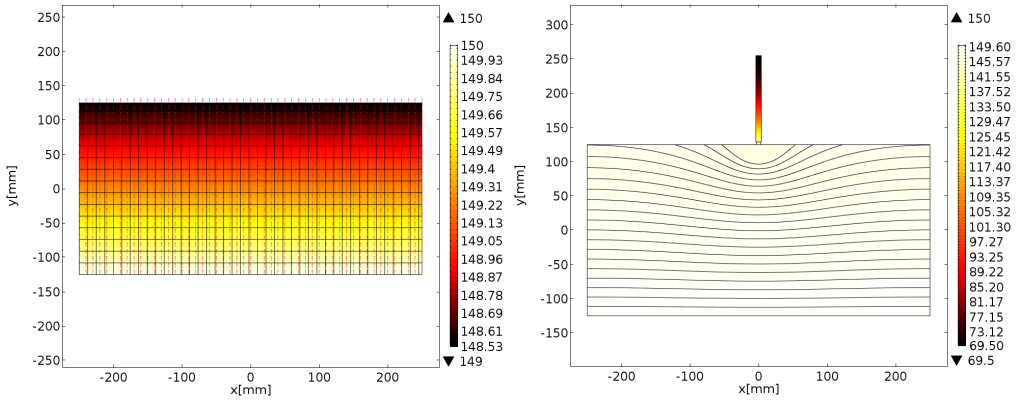

Figure 1.2: 2D Body Temperature Distribution

The figure 1.2 illustrates the contour plot of the isotherms of the undisturbed temperature distribution of the body and the effect of the sensor on the thermal field. It is observed that when the contact sensor is introduced, the thermal field it is perturbed.

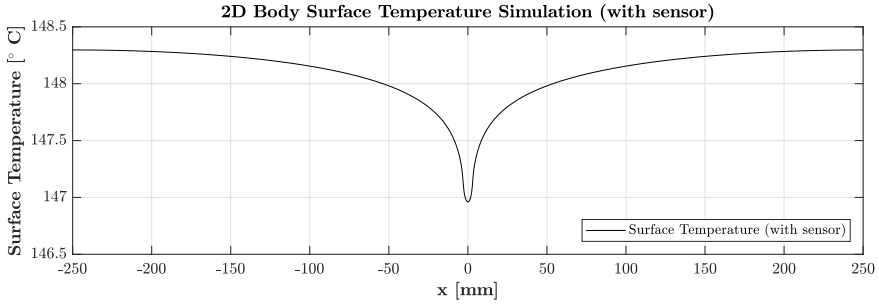

Figure 1.3: 2D Body Top Surface Temperature Distribution

The temperature distribution of the top surface of the body that it is in contact with the thermometer it is shown in the figure 1.3. The contact with the sensor produce an increment on the heat flow from the surface, resulting in a drop in the surface temperature from its original value of approximately 148.53 [°C], down to 146.96 [°C]. This temperature difference is called "*First Partial Error*" of the measurement, caused by the disturbance of the original temperature field. Thermal contact resistance between the thermometer and the surface of interest,produce a temperature drop due to a non-ideal contact. This temperature drop is called "*Second Partial Error*" of the measurement [9].

1.2.2 Phosphor Thermometry

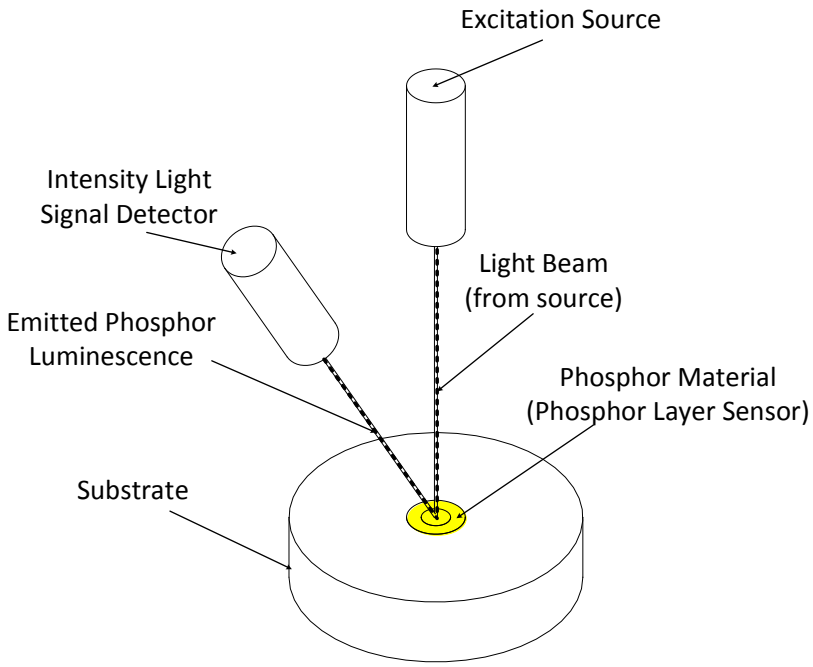

Figure 1.4: Phosphor Thermometry System Simplified Diagram

The purpose of this review about phosphor Thermometry, it is to briefly describe an standard system configuration. Phosphor Thermometry, it is a non-contact temperature measurement method, based on the temperature-dependent properties of phosphors. In figure 1.4, it is illustrated a simplified diagram of an standard phosphor Thermometry system. It is shown the main components of the system that can be classified according their functionality as follow:

- **Substrate**

  In general, it is an object on which the surface temperature is under study. However, for calibration purpose which is in this particular case, the substrate is an object with well defined geometry and temperature at the surface.

- **Phosphor Layer Sensor(Phosphor Material)**

  The phosphor layer material, it is the thermal sensor that responds(luminescence process) to a light input(excitation). The responds (luminescence) emission property, it is the temperature dependent characteristic that is required to quantify in order to estimate the temperature on the substrate surface.
  The excitation and respond, are governed by a combination of multiples process that occurs at different time-scale (Light Absorption(Excitation), Internal Conversion, Vibration Relaxation, Fluorescence, Phosphorescence, Non-Radiative Decay)("Jablonski energy-level diagram")[19].

- **Excitation Source**

  The excitation source, provide the required energy to excite the phosphor layer sensor. There is a variety of equipment to provide this source of energy, for example a laser or LEDs. The type of excitation can be classified in terms temporal functionality, pulsed or continuous.

- **Signal Detector Device**

  The main function is of the devices is to capture the luminescence emitted from excited thermal phosphor layer. There is different equipments to perform the detection of the signal, for Point Detection(Photomultiplier Tube (PMT)), Photo-diodes and also Imaging systems [6].

Thermographic Properties

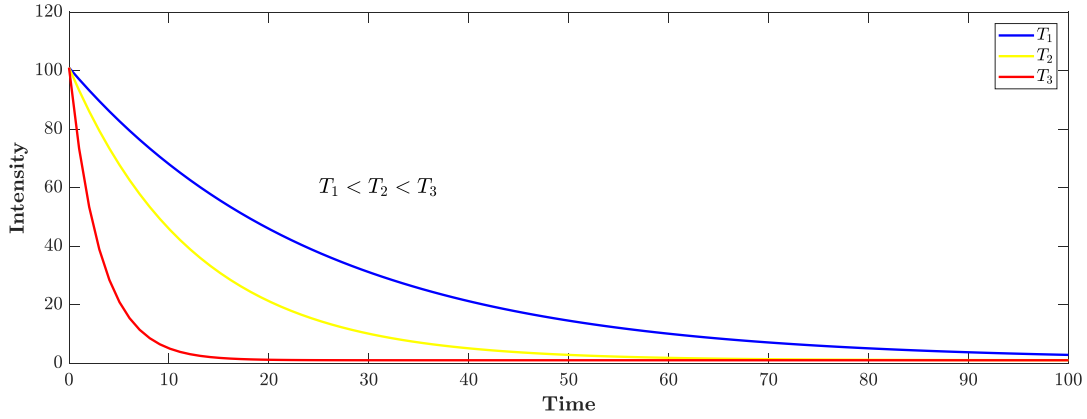

Figure 1.5: Decay Time Temperature Dependence

$$I(t) = I_0.e^{\frac{-t}{\tau}} + c \tag{1.3}$$

The excitation[2] of the phosphor layer induce the electrons to a higher energy state that produce the luminescence effect when return to a ground state. The luminescence property is temperature-dependent and one method to quantify this dependency, it is by estimating the decay time (τ)[6] (see figure 1.5). The equation 1.3 represent the fitting function where I_0 is the initial luminescence intensity at time $t = 0$ and c is an optional offset constant. However, in order to utilize the thermographic phopshor for thermometry, it is required an appropriate calibration measurements[3], considering that the involved photo-physics of these materials is complex for a model-based data evaluation[21]. The system that provide this calibration in surface temperature is the "Surface Temperature Reference" that it s described in the next section.

[2] Exerted by light source according to the specific type of phosphor.
[3] In order to correlate the estimate decay time (τ[ms]) to an specific temperature (T[°C])

1.3 Surface Temperature Reference System

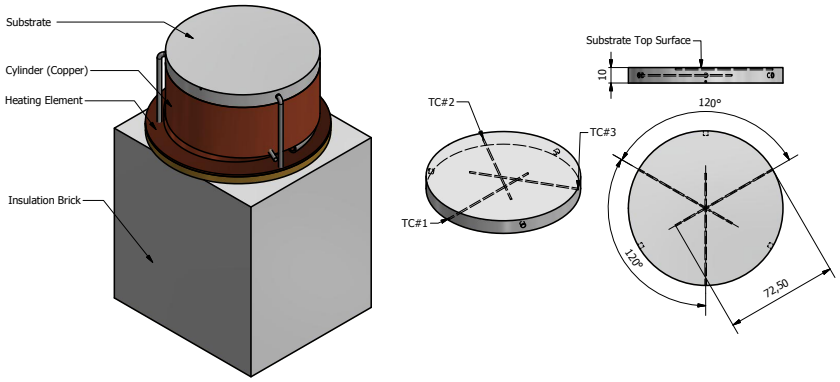

Figure 1.6: Surface Temperature Reference System*(Prior start the thesis project) (for more details see chapter: "Surface Temperature Reference System")*

This section is a brief introduction, that summarizes the importance of the Temperature Reference System and the configuration conditions before the Master Thesis Project start. The "Surface Temperature Reference"(see figure 1.6) is a key system, in a surface temperature calibration process of a device under test(DUT), such as a contact thermometer or a phosphor Thermometry system.

Furthermore, the expression key system refers to that the traceability[4] of the measurements are incorporated from the thermocouples (sensor embed in the substrate to estimate surface temperature) and the DAQ system[5]. The traceability of the measurements is acquired through the calibration of the thermocouples in a salt bath or furnace and by taking into account the reproducibility of the method. In other words, the calibration of the thermocouples it is performed with the same DAQ System in order to avoid any potential introduction of unknown source of errors.
In addition to that, the obtained measurements from the thermocouples on the substrate at different points are the basis for the implementation of an extrapolation method. This method, it is used in order to obtain the temperature at the surface of the substrate.

It is considered relevant to mention that prior the Master Thesis start, some improvements have been suggested regarding the Surface Temperature Reference System. In particular and most important, it is in terms of the number of thermocouples in which have been recommended an increment of at least one thermocouples.

Consequently, it is expected that the increment in the number of measurements points (thermocouples measurements) should be reflected as a reduction in the uncertainty of the estimated temperature at the substrate surface. Furthermore, the improvements in the uncertainty will be analysed during the Master Thesis by comparing the two different configuration conditions (3TC vs 4TC uncertainty).

[4] *"Metrological Traceability: property of a measurement result whereby the result can be related to a reference through a documented unbroken chain of calibrations, each contributing to the measurement uncertainty."*[18]

[5] Data Acquisition System(Fluke 1586A SUPER-DAQ Precision Temperature Scanner)

1.4 Specification of Purpose

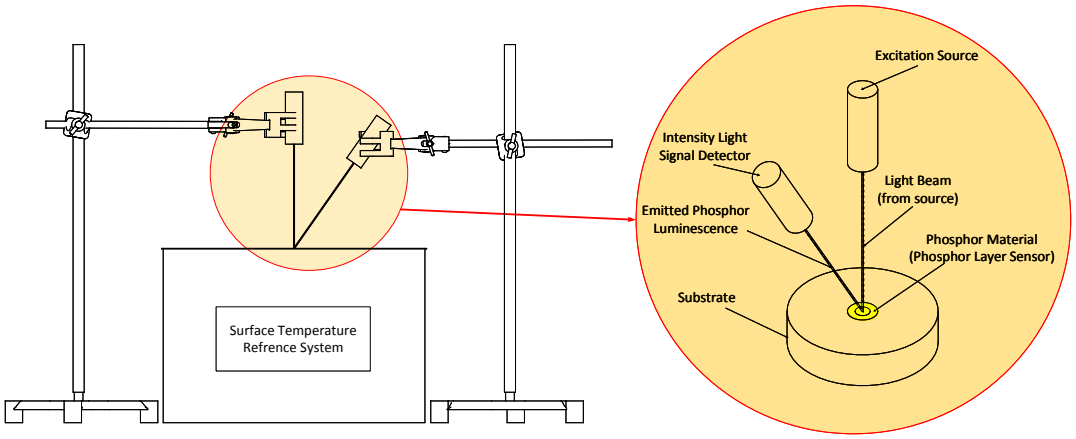

Figure 1.7: Schematic Phosphor Thermometry System

The main purpose of the master thesis is to cooperate in the development of a Phosphor Thermometry System.
The Phosphor Thermometry is a remote sensing (semi-invasive) technique in which the temperature is measured without physical connections (see figure 1.7). It is expected that the system can operate up to 500 [°C]. The acquisition and selection of the instrumentation to built the Phosphor Thermometry set-up is a task performed by DTI.
However, in the selection of the instrumentation, some inputs have been already provided based on the performed literature review. The main purpose of the project can be summarized in the following points.

- **Surface Temperature Reference.**

  The traceability of the Phosphor Thermometry System relies on the Surface Temperature Reference. Consequently, it is considered necessary to dedicate a certain amount of time to analyse the system. Prior to start the thesis, some improvements on this system has been suggested such as an increment on the number of thermocouples used to estimate the surface temperature of the substrate.
  The recommended increment on the number of thermocouples have an impact on the uncertainty of the estimated substrate surface temperature. In order to quantify the effect of the increased number of the thermocouples, the following tasks will be performed:

  – Perform measurements at different temperature ranges.

  – Preliminary uncertainty estimation.

- **Determine a suitable phosphor layer deposition method.**

  The thickness of the phosphor layer is an important parameter that could conduct to a potential error in the estimation of the surface temperature of an object. The potential error is due to thermal intrusion, this means that in a thick layer thermal gradients are created on the deposited layer. Consequently, the thermal properties of the object under study are disturbed introducing an error in the measured surface temperature. Furthermore, the recommended thickness of a sensing layer is around 20 [μm] in order to achieve a negligible thermal intrusiveness[29], this information provides an initial thickness target.
  The implemented fabrication method of the phosphor layer sensor should be able to provide a phosphor layer with a reproducible thickness and minimize as much as possible the thermal intrusiveness effect (thickness $\sim$ 20 [μm]).

  - Determine an adequate method to quantify the phosphor layer thickness.

  - Determine reproducibility of the phosphor layer fabrication process.

- **Assembly of the Phosphor Thermometry System.**

  The objective of this part of the project involves the assembly of the system and makes ready for normal operation.

- **Phosphor Thermometry System Performance Test.**

  It is expected to perform a set of measurements at different temperatures in order to estimate decay time (τ_μ) of the emitted luminescence from the thermal sensing layer. This could be considered as a preliminary characterization of the system in which the main limitations can be identified.

- **Study of the temperature exposure effect in the phosphor layer.**

  - Potential luminescence properties degradation of the sensing layer due thermal exposure.

  - Investigate the presence of thermal history effects.

1.5 Problem Formulation

The main focus in this section is the phosphor layer since it is the thermal sensor in which the method rely. The problem formulation will be presented as a set of question that could interesting to have an answer at the end of this thesis.

- What are parameters that define a suitable phosphor layer deposition method? (in a phosphor thermometry system).

- Is the phosphor layer affected by the temperature?
  (by phosphor layer affected by the temperature, here means any potential change in the molecular structure that could affect the expected luminescence time decay property for an specific temperature.)

- Is this change in the phosphor layer due to the temperature affecting the measurements results?

- if previous question turns out to be affirmative. Can be neglected this effect in terms of metrology?
  (That means by the incorporation of an extra uncertainty parameter that can deal with the problem.)

- if previous question turns out to be negative. Is the phosphor layer affected by all the temperature ranges in the same manner?

- Is it a permanent effect in the molecular structure or can be reversed?

- Which are the main limitations of the developed "Phosphor Thermometry System"?

1.6 Project Scope or Delimitations

The project is aiming for a specific uncertainty target value of 5 [°C] at 500 [°C]. It is required to consider, that the uncertainty estimation is a complex process and maybe during the time frame of this project this target will not be achieved. Besides that, it is important to mention that the expected temperature range up to 500 [°C] for the Phosphor Thermometry system will be highly dependent on the available equipment ($$$) at the time that the experiments will be performed.

Furthermore, since this Master Thesis is heavily research-oriented it is expected that some of the questions in the problem formulation will not be possible to have an answer at the end of the project and maybe new ones appear due to the knowledge acquired during the process of finding answers. However, if that is the case, the future work will be the finding of an answer to those questions.

1.7 Thesis Outline

- **Chapter #1: Introduction**
  In the introduction has been described two different techniques for surface temperature measurements of an object. Furthermore, the main purpose, problem formulation and limitations of the Master Thesis has been presented.

- **Chapter #2: Basics in Phosphor Thermometry**
  The Phosphor Thermometry chapter will be focused on describing, in general, the theoretical principles in terms of luminescence and related concepts based on the literature review. It is considered relevant since the Phosphor Thermometry technique relies on the luminescence phenomenon.

- **Chapter #3: Surface Temperature Reference System**
  The main components of the Surface Temperature Reference System will be described in this chapter. As mentioned in the purpose of the thesis, the effect of the number of thermocouples in the estimated uncertainty of the surface temperature will be analysed and discussed.

- **Chapter #4: Development of a Phosphor Thermometry System**
  In this chapter, the developed Phosphor Thermometry system will be presented and the main selection criteria for the different types of equipment will be described. Furthermore, the implemented algorithm to determine the decay time from the experiments data is described.

- **Chapter #5: Phosphor Sensing Layer Manufacture**
  The phosphor layer sensor is one of the most important components of the Phosphor Thermometry system. In this chapter, the fabrication process of the phosphor layer will be described and the achieved level of thickness reproducibility will be discussed.

- **Chapter #6: Phosphor Thermometry Experiments**
  The Phosphor Thermometry experimental results are presented in this chapter. Furthermore, the results will be accompanied by a small discussion about the estimated reason for the different outcomes. The main focus will be in terms of reproducibility of the results, sensing layer performance (emissivity permanent change) due to thermal effect and the identification of a potential thermal history effect.

- **Chapter #7: Discussion and Conclusion**
  The discussion and conclusion chapter will summarize all the work that has been performed during the Master Thesis. Additionally, the main limitations of the system and suggestions for future improvements will be explained.

- **Chapter #8: Future Work**
  As mentioned before, there is a level of uncertainty in terms of achieving an objective in a heavily research-oriented project. This means that maybe some of the questions that are proposed in the problem formulation cannot be answered in the project time frame or could be that new questions arise. Consequently, the main focus of this chapter will be to describe this issues.

1.8 Thesis Contribution

The main contribution from thesis can be summarized as follow:

- **Surface Temperature Reference System**
  Collaboration in the improvements of the Surface Temperature Reference System, such as design of a new substrate that incorporate an extra thermocouple and quantification of the impact of adding a thermocouple in the uncertainty associated to the surface temperature extrapolation method.

- **Development of a Phosphor Thermometry System**
  Assembly of the system, design of an excitation light source controller (Arduino Based) for a luminescence decay-time based experimental work. Implementation of an algorithm that extracts the information from the data acquired by the oscilloscope in order to estimate the decay-time of the emitted luminescence from the phosphor layer sensor.

- **Phosphor Layer Sensor Fabrication**
  Implementation of a deposition method and a detailed description of the required steps in order to fabricate phosphor layer sensor and quantification of the thickness layer.

2

Basics in Phosphor Thermometry

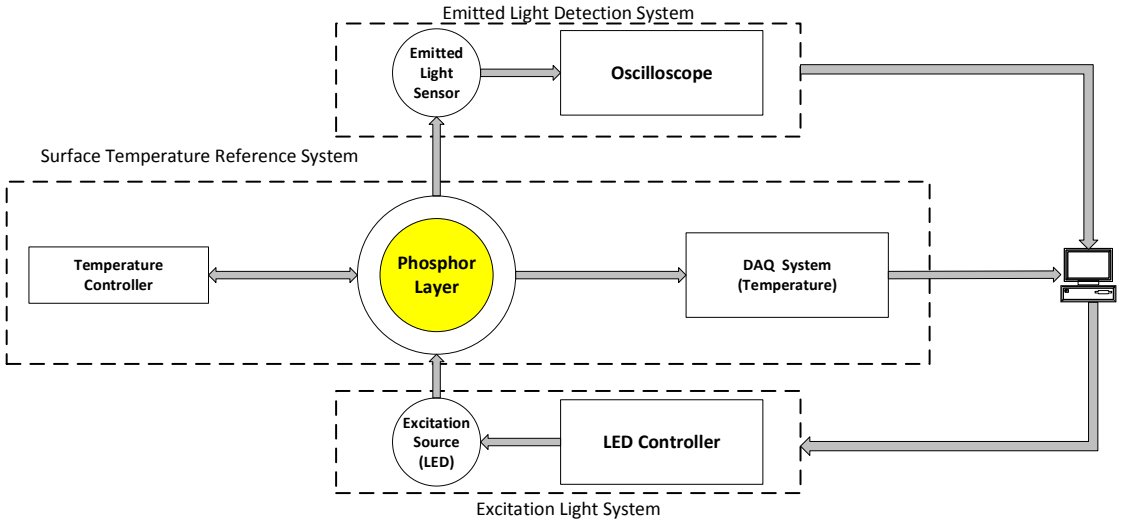

Figure 2.1: Phosphor Thermometry System (General Schematic Layout)

This chapter is an overview of the concepts involved in Phosphor Thermometry, that are considered relevant for this project. It is described briefly the luminescence mechanism of thermographic phosphor and the general methodology implemented in temperature-dependent decay time to estimate the temperature of the phosphor layer sensor attached to the surface of an object.

Phosphor Thermometry is a temperature-sensing method, which can determine the temperature remotely through the use of sensor materials known as thermographic phosphors. In contrary to other techniques that are considered non-invasive, such IR methods (infrared Thermometry), phosphor Thermometry is considered semi-invasive[3]. This is based on that it requires the deposition of a sensing layer on the substrate surface under test. The details about the phosphor layer sensor are discussed in the chapter "Phosphor Layer Sensor Fabrication".

The figure 2.1 shows the general layout of a Phosphor Thermometry system, which is comprised of three subsystems. The surface temperature reference (more details in the next chapter) is required in phosphor Thermometry to provide an appropriate temperature calibration measurement, in order to correlate[1], for the example, the estimated decay time(τ[ms]) to a specific temperature. This a relevant subsystem, considering that the involved photo-physics in the thermographic phosphors material (layer sensor) are complex for a model-based data evaluation[21]. The excitation light system triggers the luminescence phenomenon and the emitted light detection system is required to quantify, as mentioned before, for example, the decay time in function of the temperature.

[1] The correlation of the reference temperature to a specific measured parameter depend on the different approaches(Temporal,Spectral or Spectral Intensity)

2.1 Thermographic Phosphors & Luminescence

2.1.1 Thermographic Phosphors

In order to obtain information concerning the temperature of an object the Phosphor Thermometry technique makes practical use of materials known as thermographic phosphors.
The phosphors are considered thermographic when at least one or more of their luminescence properties show a dependency (or sensitivity) to the change in temperature. The temperature dependence of the emitted light intensity or the decay time(τ) provides the temperature sensing capability of thermographic phosphors.

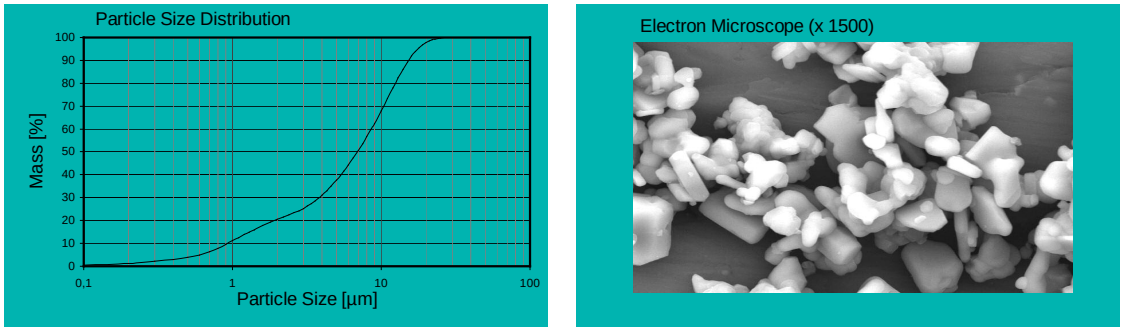

Figure 2.2: Particle Size Distribution
($Mg_4FGeO_6 : Mn$)(see Appx. B)

In figure 2.2 is shown the particle size distribution (6.5-10.5 [μm])[2] for Magnesium fluorogermanate doped with manganese $Mg_4FGeO_6 : Mn$, which is the phosphor material used during this thesis (this phosphor material exhibit a yellowish body color not visible in the figure).

Thermographic phosphors are usually a powder with a fine particle size distribution that shows a white or slightly coloured aspect. They mainly consist of two components: host material (a ceramic, inorganic micro-crystalline) and an activator (or dopant)[3] from which the light is emitted when it is excited by a suitable radiation[4].
The host material in thermographic phosphors is usually optically inactive when irradiated by UV light and the activator makes the mixture optically active, by emitting electromagnetic radiation extending over the visible range(see optical properties figure 2.2). However, if the activator ions exhibit a low degree of absorption of the excitation energy, impurities (sensitizers) can be added in order to enhance the luminescence generated by the activator ions.

[2] Details about optical properties (excitation and emission wavelength)(see chapter "Development of a Phosphor Thermometry System")
[3] Usually a rare-earth or transition metals.[6]
[4] Excitation light source at the appropriated wavelength according to the type of phosphor.

2.1.2 Principles of Thermographic Phosphors Luminescence

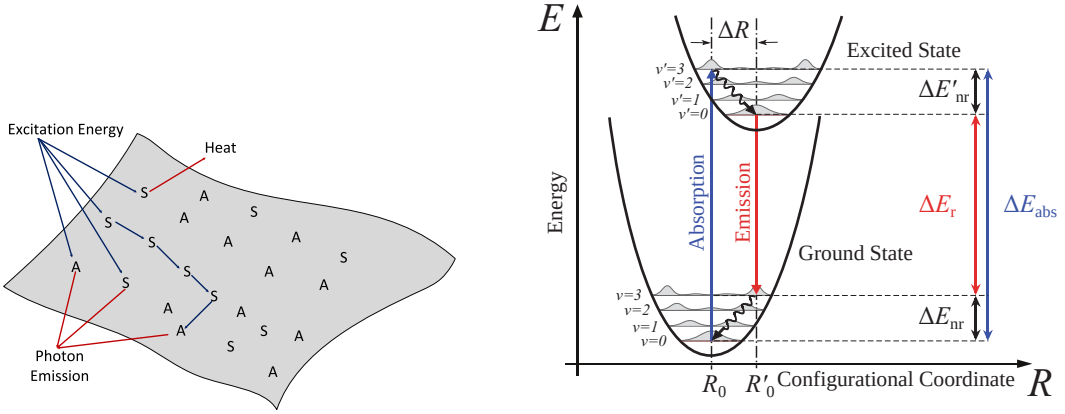

(a) Illustration of absorption of excitation energy and emission

(b) Configurational Coordinate Diagram (adopted from [6])

Figure 2.3: Thermographic Phosphors Luminescence

In the figure 2.3(a)[5] is illustrated the process of energy absorption and emission within a luminescent material in the presence of the activator and sensitizer ions. The sensitizer ions absorb part of the excitation energy and transfer it to the activator ions which then emit the transferred energy into a photon. Sensitizers can also emit a photon instead.
The configurational diagram is shown in figure 2.3(b), is a simplified model which represents the potential energy of a luminescence centre (activator)[6] as a function of the configurational coordinate R(deviation from the ion equilibrium distance).
After the excitation by an appropriate radiation (usually UV light)($v = 0 \rightarrow v' = 3$), the activator atoms are promoted from the ground state($v = 0$) to a higher energy level (excited state)($v' = 3$). In the pathway (relaxation) from the excited state (excited states are unstable) back to the ground state, the energy is liberated in the form of either light(radiant transition $v' = 0 \rightarrow v = 3$) or heat[7] (thermal dissipation non-radiant transitions($v' = 3 \rightsquigarrow v' = 0(\Delta E'_{nr})$ and $v = 3 \rightsquigarrow v = 0(\Delta E_{nr})$) or both [3].
The emission wavelength is usually red-shifted in relation to the absorption wavelength, due to the difference in absorption and emission energy levels, that is know as a Stokes-shift($\Delta E_{abs} - \Delta E_r$) [6] [19]. In terms of energy balance, the Stokes-shift between the absorption and the emission is equilibrated by the sum of the energy from the non-radiative relaxation processes.
Furthermore, during relaxation to the ground state, radiant and non-radiant transitions are in direct competition with each other due to interactions with the host material.
Phosphor thermometry is based on the fact that this competition is temperature-dependent, for example, if the temperature high enough the energy transfer will reduce radiative emission, producing a reduction of the luminescence intensity (thermal quenching)[6].

[5] Activator ions (A) and sensitizer ions (S)(based on an illustration from [3](page 14)).
[6] *"Luminescent centres are considered to be isolated based on that the dopant concentrations are a few percent. Although this most often the case, the host lattice has a profound effect on the thermal response of the phosphor"* [6].
[7] Losing energy via the release of phonons: *"this can be seen as vibrations occurring in the crystal lattice, sometimes referred as the emission of phonons in quantum physical terms, so that energy is lost as heat"* [19]

2.1.3 Temperature Dependency of Temporal Luminescence Properties

In a context of a short pulsating excitation, the persistence of luminescence after excitation is known as after-glow. The luminescence can be classified as fluorescence or as phosphorescence depending on the temporal length of the after-glow.
The electron population (in a simple two-level system), in the excited state $N^{'}$, after the excitation has been removed, decreases in accordance with [6]:

$$\frac{dN'}{dt} = -N^{'}.(k_r + k_{nr}) \tag{2.1}$$

$$N^{'}(t) = -N_0^{'}.exp[-(k_r + k_{nr}).t] \tag{2.2}$$

Where k_r and k_{nr} are rates for radiative and non-radiative transitions. The solution of the differential equation (2.1), presented in equation (2.2), represent a single exponential decay of the excited state population.
The decay in the population of the excited state, is directly proportional to the observed phosphorescence intensity decay. The emitted light intensity in function of time, after the excitation has been removed, can be approximated by a single exponential function[8], see equation 2.3.

$$I(t) = I_0.exp\left(-\frac{t}{\tau}\right) \tag{2.3}$$

Where $I(t)$ is the emission intensity at a specific time t after the excitation termination, I_0 is the initial emission intensity (at $t = 0$) after the excitation is removed, and τ is the decay time of the luminescence.
The dependence of the decay time (τ) with respect to the transition rates (k_r and k_{nr}) can be observed by comparing the equations (2.2) and (2.3).

$$\tau = \frac{1}{k_r + k_{nr}} \tag{2.4}$$

The non-radiative transitions (k_{nr}) are generally much more probable than radiative transitions (k_r)[9] are, because of radiative transitions being restricted by quantum mechanical selection rules[10]. The k_r is largely insensitive to temperature variations, while the relaxation by a non-radiative transition rate (k_{nr}) is a temperature-dependent quantity[11].
Consequently, taking into account the equation 2.4, indicate that the increment in temperature will be reflected as a reduction in the luminescence decay time.

[8] This is a simplified approach, that does take into account the interactions with other luminescence centres or with impurities in the host material lattice. However, this interaction could introduce additional relaxation mechanisms that produce multi-exponential luminescence decays [6].
[9] The radiative transition rate k_r is also known as the Einstein coefficient for spontaneous emission.
[10] *"Selection rule, in quantum mechanics, any of a set of restrictions governing the likelihood that a physical system will change from one state to another or will be unable to make such a transition." [37]*
[11] The probability of occurrence for a non-radiative mechanisms increases with temperature [6].

2.2 Temperature Sensing using Thermographic Phosphors

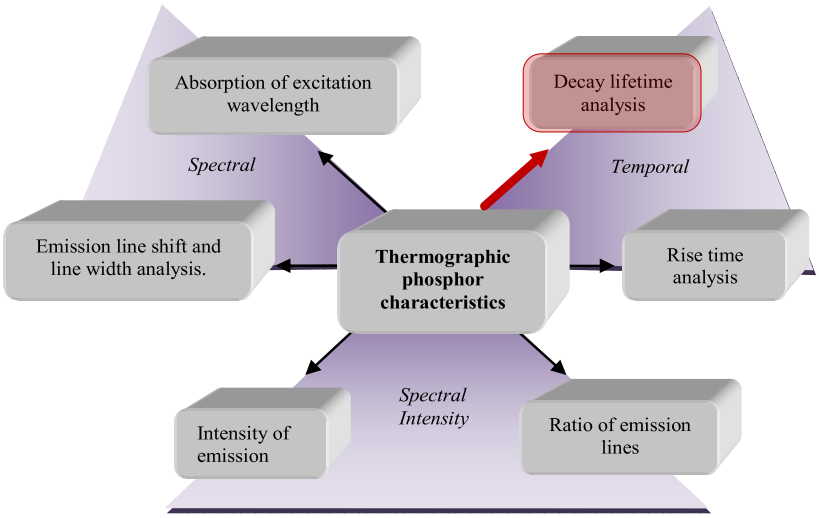

Figure 2.4: Different response modes for thermographic phosphors. *(Adopted from [19])*

The phosphors are considered thermographic when at least one or more of their luminescence properties show a dependency (or sensitivity) to the change in temperature. The response of a thermographic phosphor can be affected by the temperature change in several different ways, that gives the temperature sensing characteristics. There are different approaches in Phosphor Thermometry to extract the information carried within the temperature-dependent luminescence from a thermographic phosphor (see figure 2.4). In this section, an overview of a temporal method (Decay Time Analysis)[12] is presented. The implemented algorithm to obtain the decay time in order to evaluate the experimental results will be described in the next chapter.

2.2.1 Analysis of Temporal Luminescence Characteristic

The temporal methods in order to determine the temperature involve the detection of luminescence decay lifetime[13]. There are two known methods that are classified depending on the excitation light source as follow:

- **Pulsed Excitation Scheme**
  This technique utilizes a pulsating excitation light source to measure intensity decays (after-glow) by means of an optical detectors.

- **Continuous Excitation Scheme(Amplitude-Modulated)**
  The phosphor layer sensor is continuously excited by a well known modulated signal. The phase shift (ϕ) between the source and the emitted light correlates to the decay time (τ).

[12]Recommended further reading about other response methods [3][6] [19]
[13]Depending on the application and the type of phosphor materials rise time could be used instead of decay time.

2.2.2 Pulsed Excitation Scheme

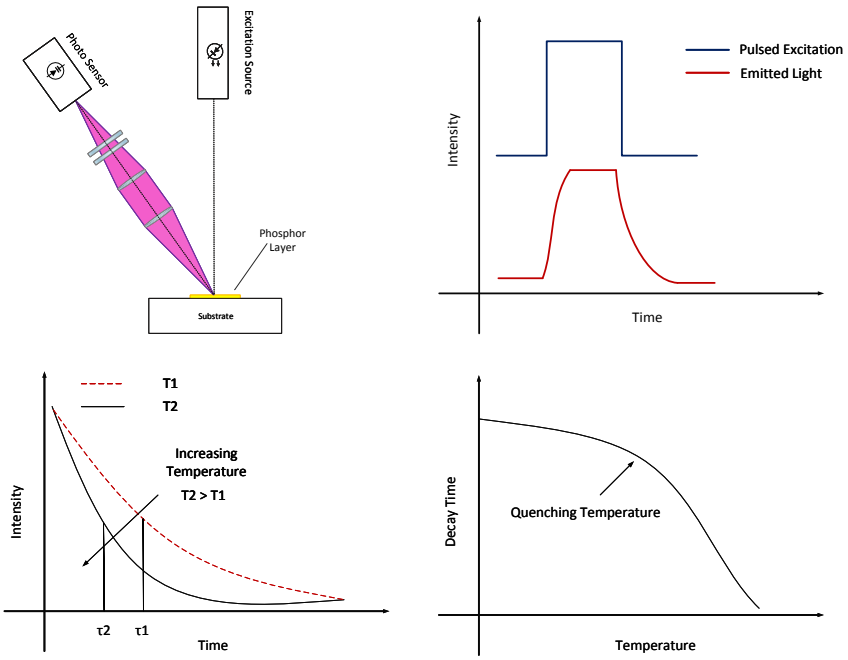

Figure 2.5: Pulsed Excitation Scheme & Decay Time Method Diagram

In this project, the implemented method is the Decay Time Method with Pulsed Excitation Scheme(see figure 2.5). In this method, the pulsed light source (square waveform in this case) excite the phosphor layer sensor and the decay time is estimated from the emitted luminescence (afterglow). The decay time becomes shorter with an increase in the temperature at which the phosphor layer sensor it is exposed. The quenching temperature, is a characteristic temperature for each individual phosphor at which the decay time temperature sensitivity increase. The decay time method is preferred for this project considering that eliminates many of the issues related with the intensity based approaches. The main advantages of the decay time method with respect to the intensity-ratio approach can be summarized as follow [3] [19]:

- Higher precision and accuracy than the intensity ratio.[14]
- Insensitive to variations in the positioning of the detector, excitation light energy and it is possible to use in high ambient light environments. That provides a flexible implementation in terms of reproducibility.
- The use of an appropriated high-gain detector provide the ability of measuring higher temperature ranges.
- Higher temperature sensitivity, that helps in the reduction of the errors that the decay time calculations produce in evaluating the temperatures involved.

In terms of disadvantages, in the the decay method the signal strength could be deficient due to the pulsating excitation scheme, that it is only present during a fraction of the time. In order to overcome this issue, high-powered laser pulses are used [19].

[14] *"The highest level of possible temperature accuracy, that can be achieved in a phosphor thermometry experiment, is limited by the accuracy of the temperature reference measurement, obtained during calibration."*.[6]

2.3 Potential Source of Errors in Phosphor Thermometry

The following section summarized the main potential source of errors that are involved in the Phosphor Thermometry technique based on the literature review.

- **Thermal Intrusiveness from Phosphor Layer Sensor**

  The thickness of the phosphor layer sensor could be a potential source of error. A thick layer could cause a thermal perturbation creating a thermal gradient between the substrate surface and the phosphor layer sensor. The thermal intrusiveness effect can be negligible, from a layer of approximately 20 μm [3] [20].

- **Excitation Continuous Operation**

  During a continuous operation mode of the excitation source, instead of a pulsating mode, this could introduce a potential error if the wavelength of the excitation and the emitted luminescence are close to each other.

- **Distortion due to Detector Saturation**

  If the signal detector operates in a saturation mode can disturb the form of the generated waveform, leading as consequence to an erroneous time decay rate, which also will influence in the estimated temperature.

- **Multi-Exponential Decay Waveforms**

  Depending on the selected thermographic phosphors, some could display multi-exponential decay waveforms. An special attention it is required at the time of fitting multi-exponential decay waveforms, the fitting error can cause an erroneous temperature determination [3].

- **Experimental Environment Influences(Contamination or Impurities)**

  The substances that could be present in an experimental environment (lubricants or other types of impurities) could lead to an erroneous temperature estimation.

- **Time Decay Drift due to Thermal Cycling or Excessive Temperature.**

  Degradation of the phosphor properties could be induced due to the exposure of the phosphor layer sensor to a thermal cycling or temperature that exceed a specific threshold. This effect could introduce a drift in the time decay rate and as consequence an erroneous temperature estimation [3].

3

Surface Temperature Reference System

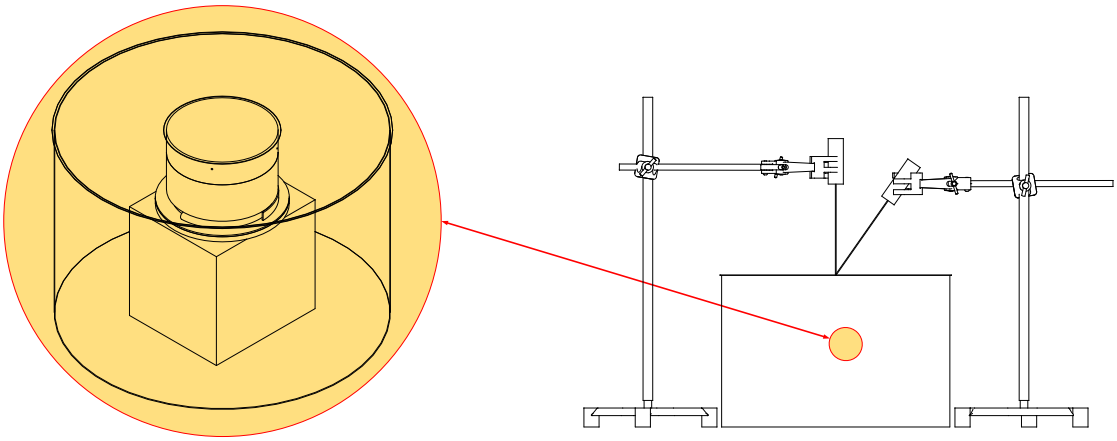

Figure 3.1: Surface Temperature Reference System

The "Surface Temperature Reference System[1]"(see figure 3.1), as mentioned in the introduction, is one of the key systems in the development of a phosphor Thermometry system. The reference system provides a well-defined surface temperature of a substrate, that will be correlated[2] to the decay time (τ) measurement performed by the phosphor Thermometry system. Furthermore, the traceability of the measurements is acquired through the calibration of the thermocouples embedded at different levels in the substrate. This means that the lowest level of uncertainty in the phosphor Thermometry system is restricted by the uncertainty of the surface temperature reference system during the calibration process, that gives significant relevance to the surface temperature reference system.
In order to determine the temperature at the surface of the substrate, the obtained measurements from the thermocouples on the substrate at different points are the basis for the implementation of an extrapolation method. Consequently, by means of an extrapolation, the temperature at the surface of the substrate is calculated.

In this chapter, the main components of the Surface Temperature Reference System will be described. Furthermore, the implementation of the extrapolation method (ordinary linear regression) and the results will be presented.
Priori the project start, some improvements have been suggested regarding the reference system in terms of the number of thermocouples, in which have been recommended an increment of at least one thermocouples.
Furthermore, the effect on the estimated uncertainty by the increment in the number of measurement points will be analysed. This evaluation will be conducted by comparing the estimated uncertainty from the extrapolation method of two different configuration conditions (3TC vs 4TC).

[1] Data Acquisition System and temperature controller are not shown.
[2] By performing a calibration procedure.

3.1 Main Components Description

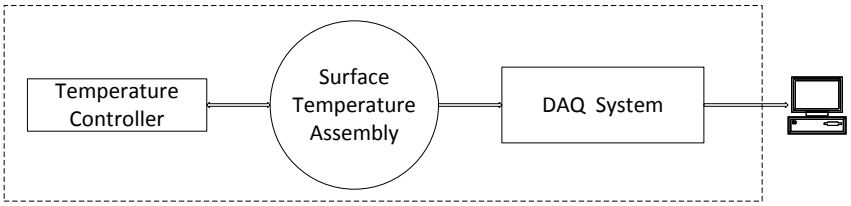

Figure 3.2: Surface Temperature Reference System (Diagram)

In figure 3.2 an illustration diagram of the "Surface Temperature Reference System" is shown. The components that will be described in the section will focus on the Surface Temperature Assembly.

3.1.1 Overview of the Surface Temperature Assembly

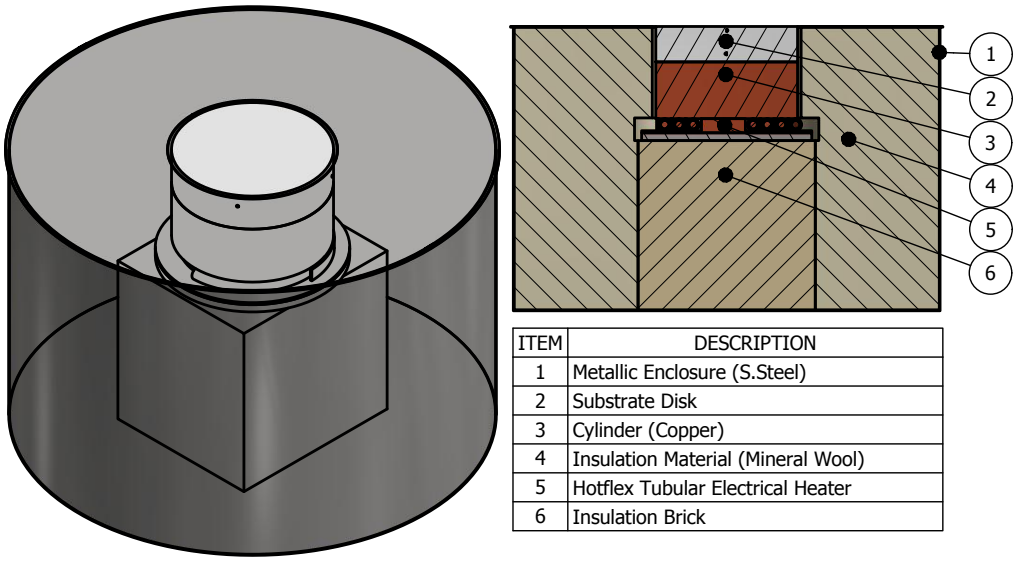

ITEM	DESCRIPTION
1	Metallic Enclosure (S.Steel)
2	Substrate Disk
3	Cylinder (Copper)
4	Insulation Material (Mineral Wool)
5	Hotflex Tubular Electrical Heater
6	Insulation Brick

Figure 3.3: Surface Temperature Assembly

The surface temperature assembly (see figure3.3) is divided into three subsystems according to the functionality of each of them, as follow: Metallic Enclosure and Insulation, Substrate, Heating Element and Copper Cylinder.
The metal enclosure is a cylindrical cover constructed of stainless steel sheet (1[mm]thickness), that provides mechanical protection and structural strength to the entire system.
The insulation material placed underneath of the electric heater is a refractory brick, that provides thermal insulation and support to the assembly. Moreover, electric heater, copper cylinder and substrate sides are surrounded by a mineral wool blanket, in order to ensure thermal stability and reduce the potential risk of thermal disturbance to other types of equipment.

3.1.2 Substrate and Heating Element

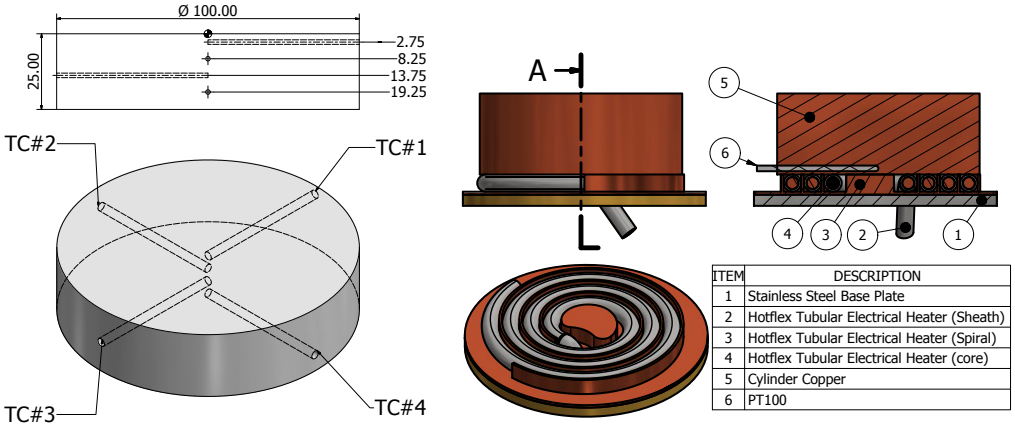

Figure 3.4: Substrate (Thermocouples Positioning) and Heating Element

The substrate dimensions and the positioning of the thermocouples are the relevant parameters of the component in order to obtain a well-defined surface temperature at the top substrate(see figure 3.4). As mentioned before, the surface temperature at the top of the substrate disk is estimated by extrapolation method. The extrapolation is a curve-fit evaluation based on the temperature measurements at four different points along the substrate disk vertical axis (z-direction). Those measurements are performed by means of four thermocouples (TC type N $\phi_{sheath} = 1.5$[mm]) that can operate continuously up to 1100 [°C] that are inserted at different high levels and a DAQ system.
Furthermore, the DAQ system is a Fluke 1586A (Precision Temperature Scanner), that provides a temperature measurement acquisition with a resolution 0.01 [°C](Medium Sample Rate 1s/Channel) with an accuracy of 0.17 [°C] for thermocouples Type N.

The substrate materials could be different depends on the calibration purpose Aluminium, Steel or other materials. The upper surface of the substrate it is exposed to the laboratory environment,that provides physical and visual access to the contact sensor (thermometer) or non-contact sensors such as IR sensor or phosphor Thermometry system. This access, it is required in order to perform a comparison against the reference system with a calibration purpose.

The electrical heating element,is a flexible tubular heater ($\phi_{outer} = 8.5$[mm]), that can operate up to 700 [°C]. The flexible heater is embedded into a copper spiral bed that ensure a good thermal contact and as much as possible uniform heat distribution with the bottom copper cylinder surface.
The copper provides a very good thermal conductivity, in order to avoid high-temperature gradients with respect to the aluminium substrate. The temperature at the bottom of the copper cylinder is measured by a PT100(Platinum resistance thermometer). The output of the thermometer is connected to the PID controller (Eurotherm 3216) which is also connected to the heater to achieve the regulation of the system temperature.

3.2 Substrate Surface Temperature Estimation

3.2.1 Overview of the Uncertainty Contribution Parameters

The estimation of the substrate surface temperature is subjected to several uncertainty sources, the main contribution parameters are shown in figure 3.5. The implemented methodology to identify the uncertainty of the measurements is based on the GUM("Guide to the Expression of Uncertainty in Measurement"[17]). The general procedure to quantify the uncertainty can be summarized in the five following steps:

1. Definition of the Measurand and input sources.
2. Mathematical Model.
3. Estimation of the Uncertainties of input sources.
4. Propagation of Uncertainties.
5. Evaluation of the Expanded Uncertainty.

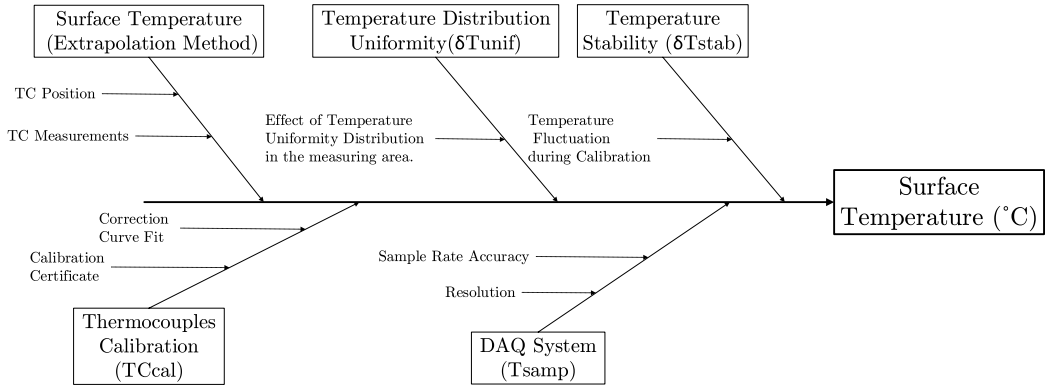

Figure 3.5: **Surface Temperature Estimation**(Main Uncertainty Components)

According to the GUM, the uncertainty contributors can be classified into two different types, Type A and Type B in function of the source. The Type A, are uncertainties contributions that are obtained empirically by a statistical analysis of the measurements, such as the standard deviation from a repeatability analysis. The Type B, are uncertainties contributions which are determined from any other source of information, such as a calibration certificate, reference books or obtained from limits deduced from personal experience.

Type A
Surface Temperature Extrapolation (T_{extr})
Substrate Surface Temperature Uniformity ($\delta_{T_{Unif}}$)[3]
Substrate Surface Temperature Stability ($\delta_{T_{Stab}}$)

Type B
Thermocouples Calibration (TC_{Calib})
DAQ System (T_{Samp})
- Sample Rate Accuracy
- Instrument Resolution

[3] **Remarks:**The Surface Temperature Uniformity $\delta_{T_{Unif}}$ it is still required to be quantified by IR camera or by other means.

3.2.2 Implemented Extrapolation Method (Ordinary Linear Regression)

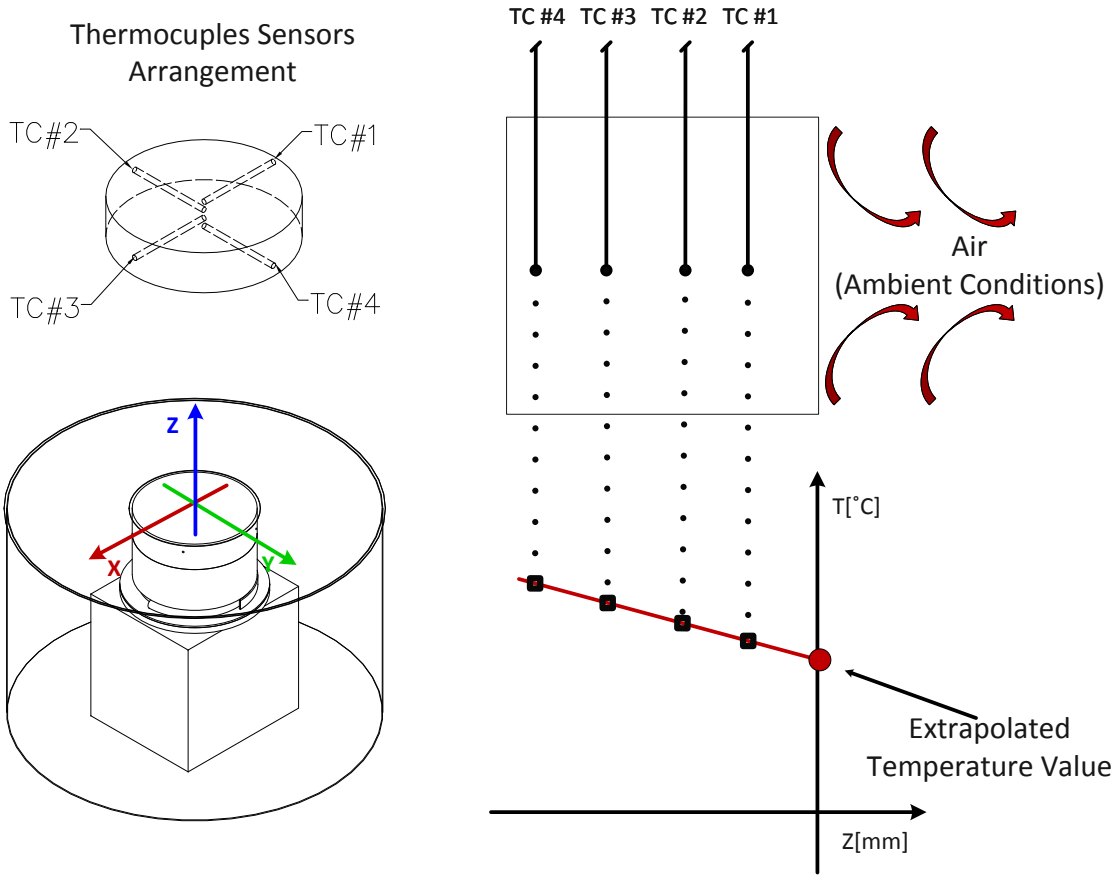

Figure 3.6: Extrapolation Method Diagram

In this subsection, it is discussed the implemented extrapolation method and the associated uncertainty to obtain the temperature at the surface of the substrate. The extrapolation method, which is one of the most precise ways to determine the surface temperature of solids, that rely on the principle shown in figure 3.6, where thin thermocouples are placed inside a solid body. Consequently, based on the measurement of the individual thermocouples(steady-state conditions), the surface temperature of the substrate can be determined, without perturbation of the original surface temperature distribution[9].

$$y_i = \beta_0 + \beta_1 x_i + \epsilon_i \quad i = 1, 2, \cdots, n \tag{3.1}$$

In this report, the extrapolation method is implemented by means of data fitting techniques, in which the main objective is to find the parameters of the model function that describe the connection between observations and conditions. The considered model function[4] (see eq. 3.1) that describe the temperature distribution in steady-state conditions along the z-axis of the substrate is assumed to be linear (straight line), based on the assumption of a constant thermal conductivity of the substrate material (Stainless Steel).

[4] Simple linear regression model, where β_0 (intercept),β_1 (slope) and ϵ_i is the random error term

The parameters estimation of the linear function is performed by an ordinary least squares (OLS) calculation(see Appendix A:"Matlab Implementation Codes").
The least squares method of solving for the slope(β_1) and intercept(β_0) for the "best fit" line is to calculate the sum of squared errors (residuals) between the line and the data and then minimize that value (vertical distance[5])(see eq. 3.2 [24]).

$$SS_E = \sum_{i=1}^{n} \epsilon_i^2 = \sum_{i=1}^{n} (y_i - (\beta_0 + \beta_1 x_i))^2 \tag{3.2}$$

In ordinary least squares, it is assumed that there are no errors in the x-values and the error (ϵ) is assumed random, normal distributed with mean zero and (unknown) variance (σ^2)($\epsilon \sim N(0, \sigma^2)$). Furthermore, the random errors corresponding to individual different observations are also assumed to be uncorrelated random variables.

The purpose of data fitting is not limited to the approximation of the data points. The data model in this case is used to predict which values of y (Temperature [°C]) would most likely be measured if other experimental conditions x_q ($z[mm]$ at the surface) were selected (known as a model prediction). Moreover, the interest focuses also in the estimation of the associated uncertainty of this model prediction.

$$\textbf{Prediction Interval} \quad y_q = (\hat{\beta}_0 + \hat{\beta}_1 x_q) \pm t_{\alpha/2,\nu} s_{y,x} \sqrt{1 + \frac{1}{n} + \frac{(x_q - \overline{x})^2}{SS_{xx}}} \tag{3.3}$$

Where:

x_q: new value of x in order to predict y.
$t_{\alpha/2,\nu}$: t-distribution with $\nu = n - p$ degrees of freedom ($p = 2$ number of fit parameters) and $\alpha = 0.05$ for a 95 % CI.

$s_{y,x}$: Standard deviation of y(x). $s_{y,x} = \sqrt{\frac{SS_E}{n-p}}$.

SS_{xx}: Sum squared error between the data x and the mean of the data $\overline{x}$.

Remarks:
The confidence interval of the predicted value represents only the linear regression (curve-fit) uncertainty and not any of the other uncertainties in the measurement, such as thermocouples calibration, data acquisition, etc.

In terms of the extrapolation some aspect it is required to take into account. The estimated linear regression relationships are valid only for values of the independent variable (x) within the range of the measured data, from where has been obtained.
However, in this case, the extrapolation is considered moderate since the distance moved beyond the range of x values is 50 % (2.75[mm]) of the distance between data points.
The results of the estimated surface temperature and the associated curve-fit uncertainty at different temperature ranges are presented in the following subsection.

[5] Ordinary linear regression by least squares fitting only minimizes the error in the dependent variable, the error in the independent variable is ignored.

3.2.3 Estimated Surface Temperature Results

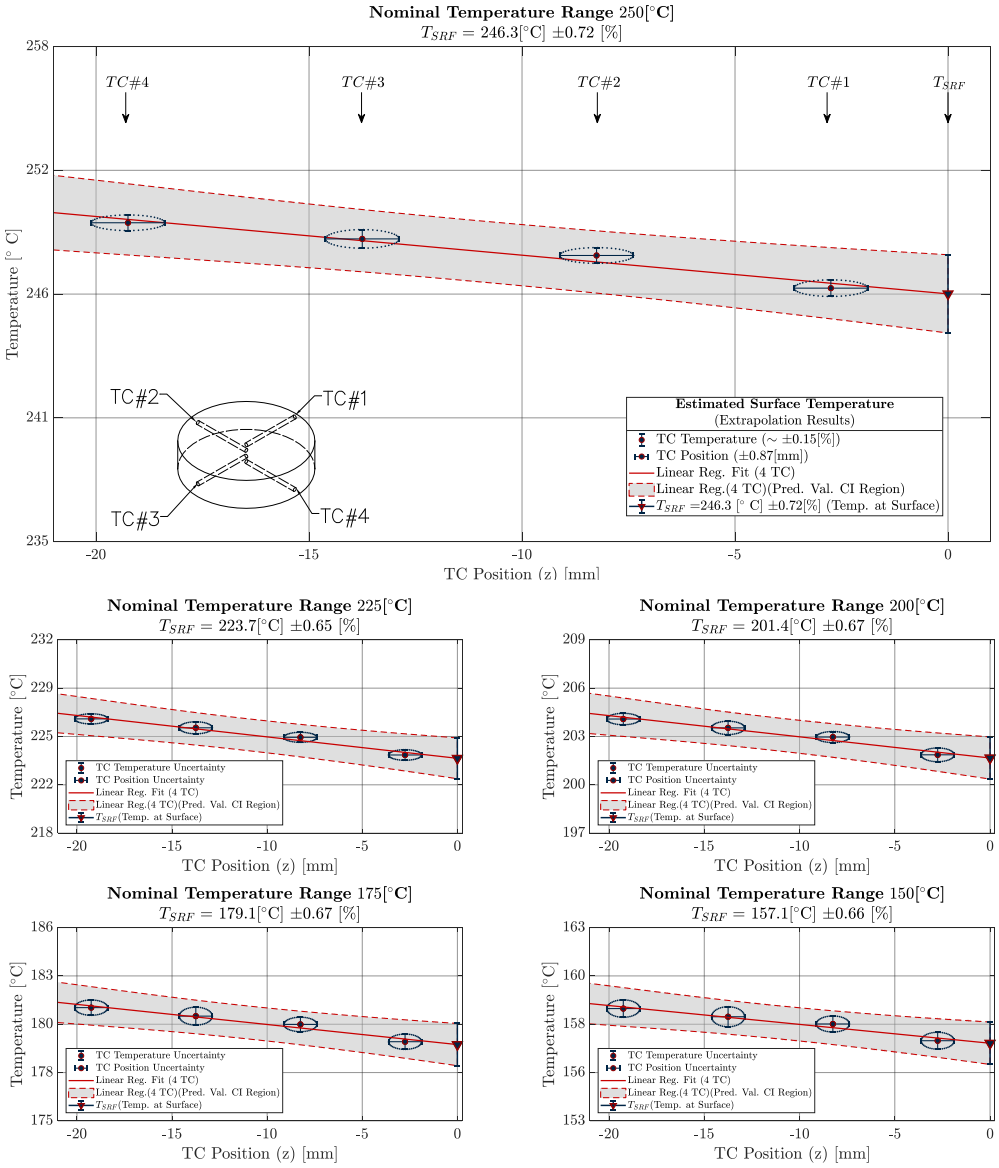

Figure 3.7: Estimated Surface Temperature and Associated Uncertainty

The quantification of the substrate surface temperature has been performed by experimental work at different temperatures from room temperature up to 250 [°C]. In figure 3.7 is shown the results of the measurements and the corresponding simple linear regression fit. It is observed that surface temperature relative uncertainties (from curve-fit) at different temperature are relatively close to each other with a maximum difference of 0.07%.
Furthermore, the relative uncertainty of the curve-fit (0.72%) is around 4.8 times than the estimated uncertainty of the individual thermocouples($\sim 0.15\%$) (for details on the uncertainty calculations of the individual thermocouples see Appendix A:"Matlab Implementation Codes"). Consequently, it is possible to assume that the uncertainty due to the curve-fit could be one the major contributors to the substrate surface temperature estimation.

3.2.4 Analysis of Increment on the Number of Thermocouples

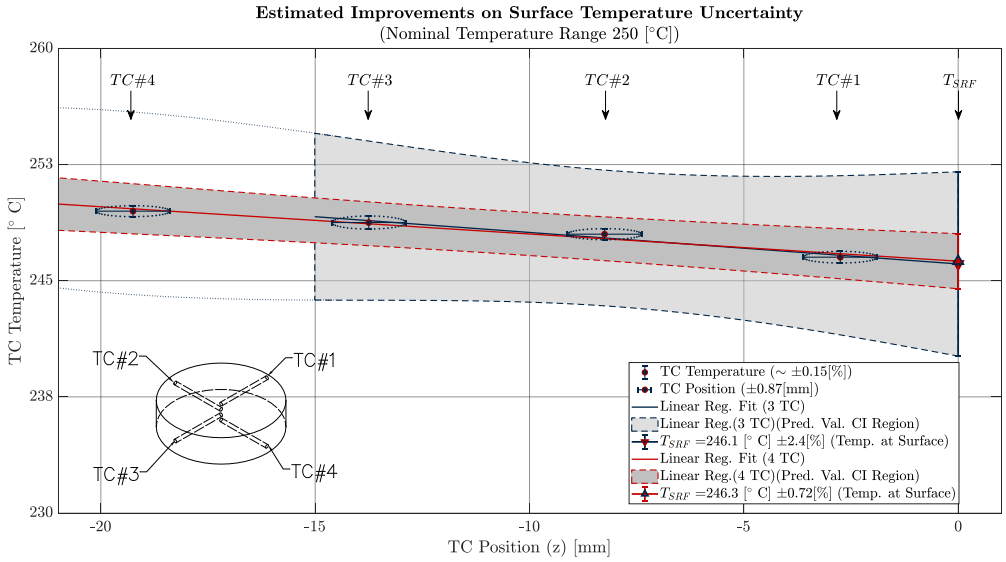

Figure 3.8: Estimated improvements on the surface temperature uncertainty

Previously to start the project, some improvements have been suggested regarding the reference system in terms of the number of thermocouples, which have been recommended an increment of at least one thermocouples. In figure 3.8 is shown the comparison of the estimated substrate surface temperature between two different configurations (3TC vs 4TC). It is observed a significant reduction of the uncertainty due to the extrapolation method by increasing the number of thermocouples. The relative uncertainty has been reduced from 2.4% to 0.72%, this reduction is a direct consequence of the increment on the degree of freedom.

3.3 Surface Temperature Reference System Summary

The main components of the "Surface Temperature Reference System" have been described. Furthermore, it is necessary to emphasise that this is one of the key systems in the development of a phosphor Thermometry system. The reference system provides a traceable well-defined surface temperature of a substrate, that will be correlated to the decay time (τ) measurement performed by the phosphor Thermometry system during a calibration procedure. The substrate surface temperature has been estimated by performing several measurements at different temperature ranges, from room temperature up to 250 [°C]. The uncertainty contribution due to the implemented extrapolation method, it is estimated to be in the order of 0.72% for a temperature of 246.3 [°C]. The resulting estimated uncertainty [6] does not include the contribution from the position of the thermocouples or other uncertainties in the measurement process. However, this component could be included in the final uncertainty budget as an extra contribution parameter[7]. The increment in the number of thermocouples from three to four has been shown a significant reduction in the uncertainty of the estimated substrate surface temperature(from 2.4% to 0.72%).

[6] Only the linear regression (curve-fit) uncertainty.
[7] by applying uncertainty propagation on the linear regression.

4

Development of a Phosphor Thermometry System

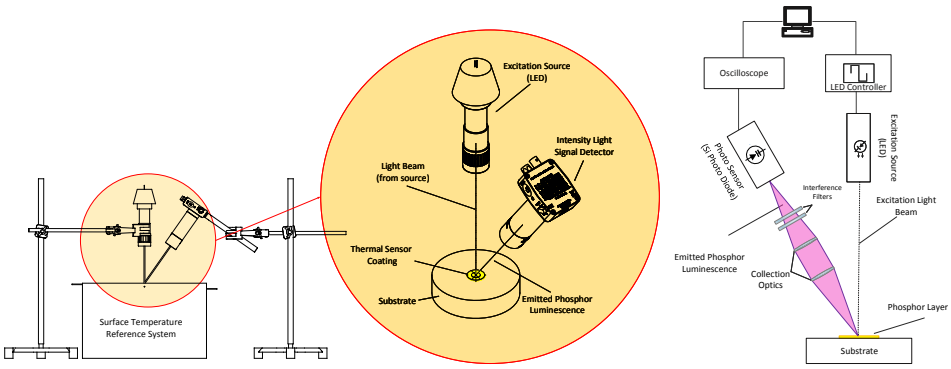

Figure 4.1: Phosphor Thermometry System

In this chapter the instrumentation, working principles of each individual component and selection criteria used in the development of a phosphor Thermometry is described. Additionally, the implemented algorithm that extract the information to estimate the decay time is detailed. In figure 4.1 is shown a diagram of the developed experimental set-up used in this project. The implementation of a decay time based phosphor Thermometry technique to a substrate under test requires an experimental setup composed primarily of a pulsed excitation light source (LED with a waveform controller), a phosphor layer sensor applied to the substrate surface(See chapter "Phosphor Layer Sensor Fabrication"), a photo-detector assembly[1], and a data acquisition system (oscilloscope).
The main steps involved in the decay time-based phosphor Thermometry procedure can be described as follow. A pulsed light source[2], it used to excite a thin layer of thermographic phosphor that has been deposited onto the substrate surface under test. The light is directed towards the target by means of adjustable magnifier that helps to focus the light on the phosphor layer sensor. After the excitation by the light source, the luminescence that it is emitted by the thermographic phosphor it collected by photo-sensor assembly. The optics(composed of a number of lenses) embedded in the photo-detector assembly concentrated the collected emitted luminescence onto the detector input window.
Furthermore, in order to select the spectral portion of the luminescence of interest, based on the expected spectral emitted luminescence of the characteristic phosphor, a set of interference filters is placed in front of the photo-sensor. The photo-sensor convert the input emitted luminescence signal into useful electric output signal(voltage) that it acquired by an oscilloscope and storage by software interface. The acquired data require a post-processing that involves the extraction of the information about the decay time and that it is associated to the specific temperature during the calibration.

[1] Composed by a photo-sensor(Photodiode), collection optics, and interference filters.
[2] Wavelength selected in function of the optical properties of the specific phosphor.

4.1 Phosphor Material Selection

4.1.1 Selection Criteria

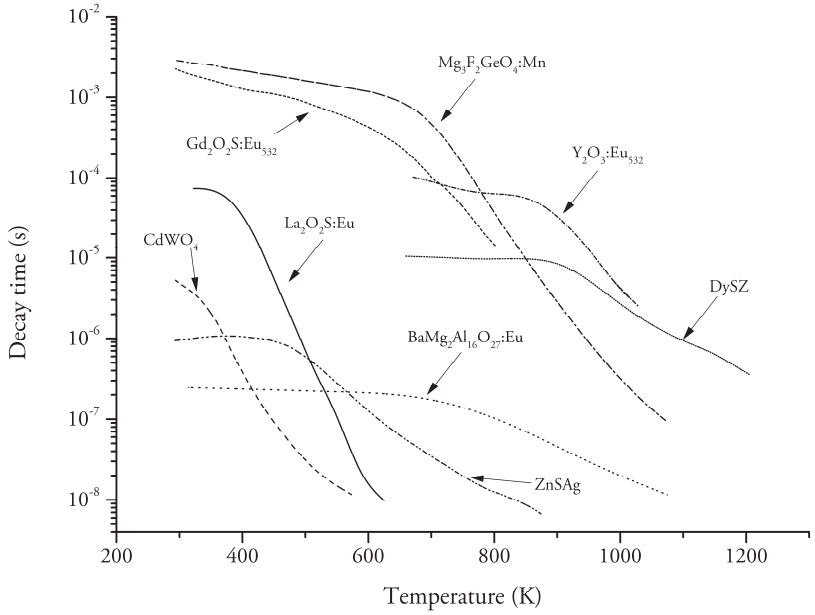

Figure 4.2: Decay Time (τ)of of Different Phosphors *(Adopted from [3])*

In this section, the factors that are required to take into account in order to select an appropriate thermographic phosphor for a specific temperature range are discussed. There are a large number of different thermographic phosphors that are available. In figure 4.2 is shown the decay time for different thermographic phosphors and temperatures. It is possible to observe that the decay time of the emitted luminescence becomes shorter with the increment in temperature and each thermographic phosphor has its own individual temperature sensitivity range and quenching temperature[3][3].

The selection criteria for the thermographic phosphors, in this particular application, is governed by the range of temperatures (Temperature-Sensitive Emission Range) at which it is expected to be exposed[4]. Additionally, in order to make a practical use of the decay time measurements as a temperature indicator, it is desirable for the decay time to have a linear dependence on temperature, within the temperature range of interest.

Other factors, that it is important to be aware when selecting thermographic phosphors and evaluate the results of decay time, are the excitation-energy dependence and thermal history effects. In terms of excitation-energy dependence, the excitation source can transfer heat to the phosphor layer sensor conducting to an increment of the surface temperature. Furthermore, increasing the energy of the excitation source results in a higher luminescence intensity, but an excess could produce the opposite effect, resulting in a reduced intensity and shorter luminescence decay time [6].

[3] Quenching temperature above which the decay time shows an increased sensitivity to temperature.
[4] Initially upto 500 [°C], however, the experimental work in this project has been performed up to 250 [°C] due to some technical issues with the heating element.

The thermal history effects, is related to a chemical or physical interaction within the phosphor, between phosphor and binder agent[5] or the substrate involved that can be enhanced at high temperature and inducing permanent change in the luminescence characteristics of a thermographic phosphor. The change in the luminescence characteristics could potentially introduce an error caused by thermal drifts in the estimated temperature using a phosphor Thermometry technique.
The main processes that could lead to an irreversible change of the luminescence properties of the thermographic phosphor are the following [6]:

- **Chemical Reactions**
  The host material (ceramic) that compose the thermographic phosphors usually are chemically inert. However, reactions of the phosphor layer sensor with substrates could be possible depending on the selected binder agent(some binder agents could react, for example with aluminium).

- **Diffusion**
  The diffusion rate between the substrate, phosphor and binder increase at high temperature and for long exposure times. The luminescence characteristics of phosphors could change showing a reduction in the decay time and the intensity. This effect has been observed by Brubach in $Mg_4FGeO_6 : Mn$ affected by the substrate (stainless steel) when the phosphor was heated to above 970 [K][21].

- **Annealing or Curing**
  In general, annealing or curing [6] allude to a form of heat treatment, that involve long-term exposure of a material to elevated temperatures, causing a which permanent alteration in the micro-structure of the material (in this case the phosphor layer sensor). The change in the micro-structure of the phosphor layer during the post-process of annealing conduct to the formation of a larger crystals, resulting in an improvement in the coupling of excitation energy to the electrons, that conduct to an increment of the luminescence intensity.

Remarks:

It is suggested in [6], that for phosphors that it is known to suffer for thermal history effects, to perform a curing process, prior to temperature calibration and measurements. However, the application of the heat post-process is not always possible (or very difficult). In such cases, it is recommended to use a phosphor layer sensor that does not change their luminescence characteristics as a result of annealing.

In order to detect the presence of thermal history effects, the calibration of the phosphor layer sensor can be performed by thermal cycling test (similar to detect hysteresis effect)[7]. If there is not a significant difference in the luminescence response (decay time) measured between the heating and the cooling phase of the calibration, the potential sources of possible errors from thermal history effects could be considered as negligible.

[5] Used in adhesive bonding techniques to fabricate a thermal sensor layer (see chapter "Phosphor Layer Sensor Fabrication").
[6] Annealing usually takes place during long-term exposure (several hours) to temperatures in excess of 800 [K] [38]
[7] Calibration is performed in the heating and the cooling phase.

4.1.2 Characteristics of Selected Phosphor Material

Magnesium fluorogermanate doped with manganese($Mg_4FGeO_6 : Mn$)

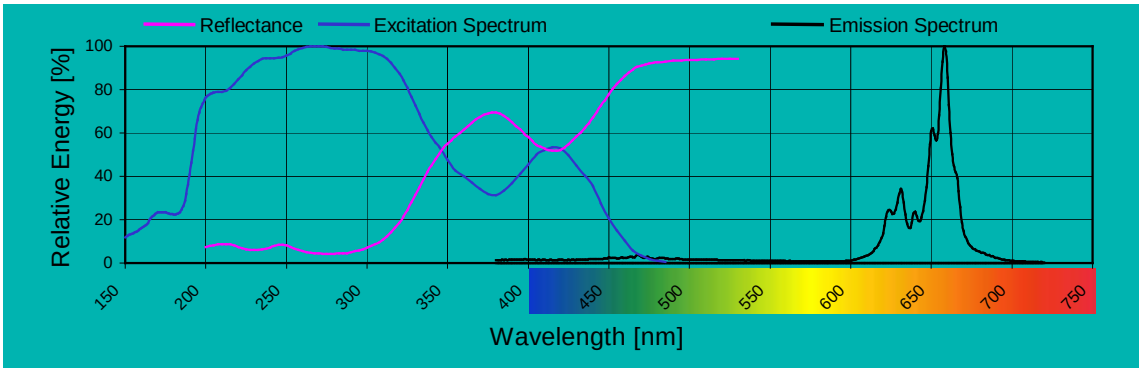

Figure 4.3: Optical Properties
($Mg_4FGeO_6 : Mn$)(see Appx. B)

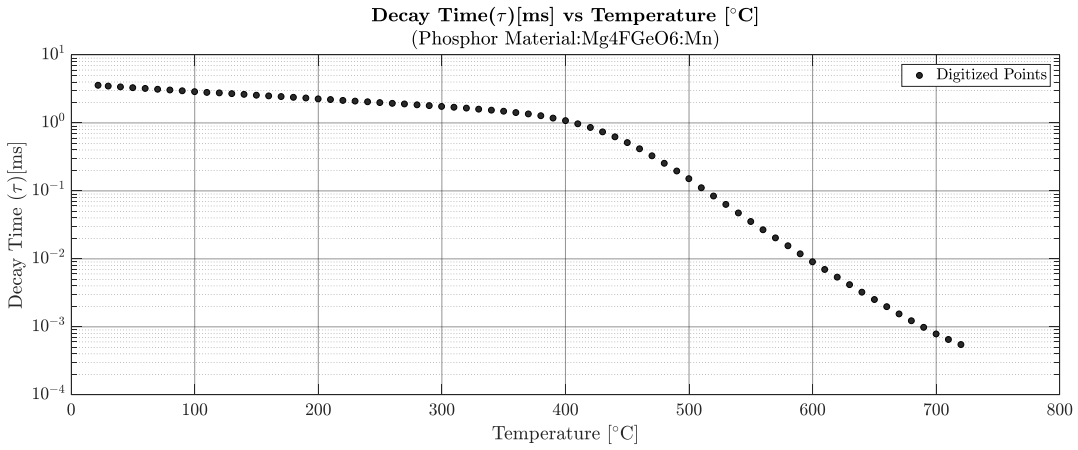

***Figure 4.4:* Characterization of Phosphor Material:$Mg_4FGeO_6 : Mn$**
Decay Time(τ) [ms] vs Temperature [°C]. Phosphor layer sensor: $thk < 10[\mu m]$. Substrate material: Stainless steel plate.(Digitized Data from original picture [21](original picture in [K] converted to [°C]),under authorization of Prof. J P Feist)

The selected phosphor for this project is $Mg_4FGeO_6 : Mn$[8]. In figure 4.3 is shown the optical properties of the phosphor material that will be relevant in the selection of the emitted light sensor and the excitation light source. The phosphor exhibits a quenching temperature in the vicinity of 425 [°C], that it is shown in figure 4.4 which is a characteristic curve that has been digitized from a picture extracted from "Characterization of manganese-activated magnesium fluorogermanate with regards to thermographic phosphor Thermometry" [21]. The digitization has been performed six times in a 71 measurement points to obtain the characteristic decay time in function of temperature curve. This curve will be used to compare the results of the experimental work in order to observe the presence of any significant difference in the linear trend of the decay time thermal dependency (up to 250 [°C]).

[8] Magnesium fluorogermanate doped with manganese

4.2 Photo-Sensor Selection

4.2.1 Selection Criteria

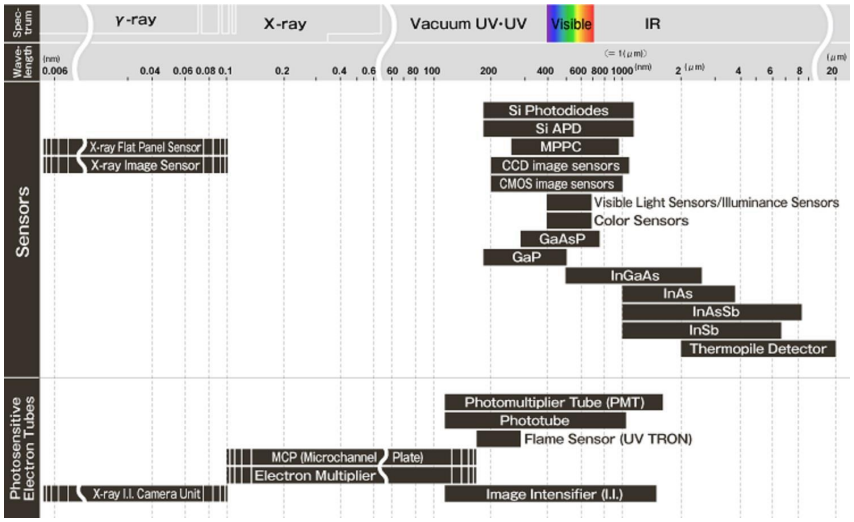

Figure 4.5: Light Emission Detector in Function of Wavelength*(source [35])*

The purpose of a photo-sensor is to convert incoming light from the phosphor layer sensor into a measurable electrical signal that it is proportional to the emitted light intensity. In figure 4.5 is presented the large variety of different equipment that could be potentially used depending on the emitted luminescence wavelength of the phosphor material and the application. The implemented criteria in order to select the appropriated photo-sensor and the required auxiliary devices(optics, filters) that combined will form the Photo-Sensor Assembly is based on the several factors detailed as follow:

- **Optical access to the substrate:** Optical access and distance to the substrate under study, in order to avoid a potential thermal disturbance from the substrate to the sensor.
- **Radiant responsivity:**[9] The sensor is selected based on the characteristic radiant responsivity, in order to ensure that it is as close as possible with respect to spectral range of the emitted luminescence wavelength.
- **Required Interference Filters:** Based on the radiant responsivity and the expected emitted luminescence wavelength, a set of shortpass filter and longpass filter has been selected.
- **Signal amplification capabilities:** This feature it is useful in case that the signal strength of the emitted luminescence decrease due to any thermal effect.
- **Future upgrades of the system:** Potential incorporation of fibre optics.

[9] Radiant responsivity([A/W] or [V/W]), is the ratio of the output photocurrent (or output voltage) divided by the incident radiant power at a given wavelength.[5]

4.2.2 Photo-Sensor Assembly

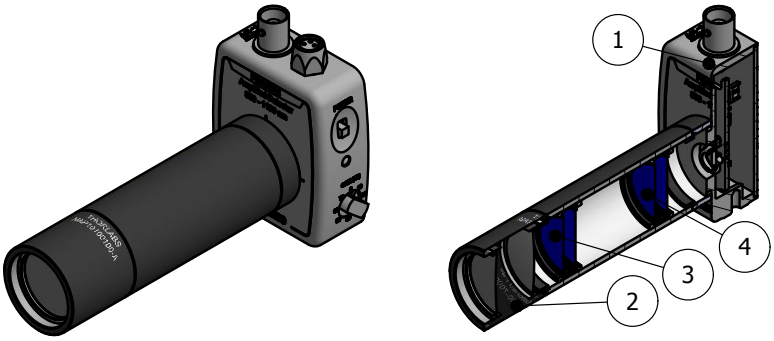

1	Si Free-Space Amplified Photodetectors
2	Visible Achromatic Doublet Pairs
3	Edgepass Filters Longpass (550 nm)
4	Edgepass Filters Shortpass (750 nm)

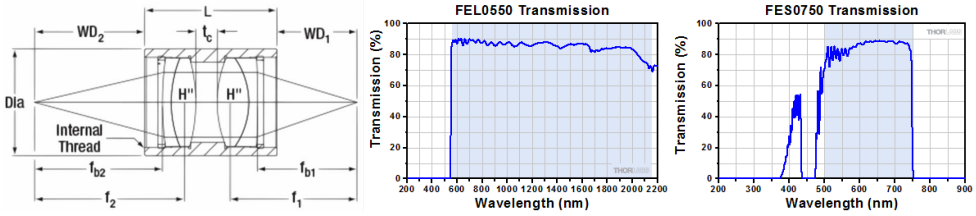

Figure 4.6: Photo-Sensor Assembly Diagram
(Photo-Sensor Assembly, optics diagram and selected long/shortpass filters)[39]

The selected photo-sensor, it is silicon (Si) a photo diode that is suitable for measuring both pulsed and CW light sources [6]. The model PDA36A2 incorporate a reverse-biased PIN photo diode and switchable gain amplifier. In figure 4.6 is shown the entire Photo-Sensor Assembly with the respective optics that concentrate the emitted light toward to the sensor and a set of filter(longpass(550nm) and shortpass (750nm)).

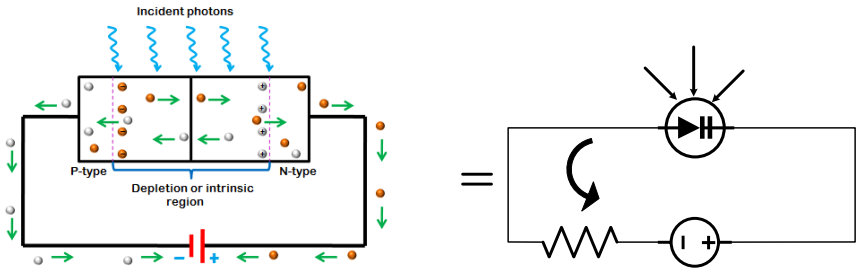

Figure 4.7: Photo Diode (PIN Type) Working Principle*(source [40])*

The working principle of the PIN diode is similar to a PN junction photodiode(see figure 4.7) except that the PIN photodiode is manufactured differently to improve its performance. The PIN diode comprises three regions, namely P-region, I-region and N-region.

4.3 Excitation Light Source Selection

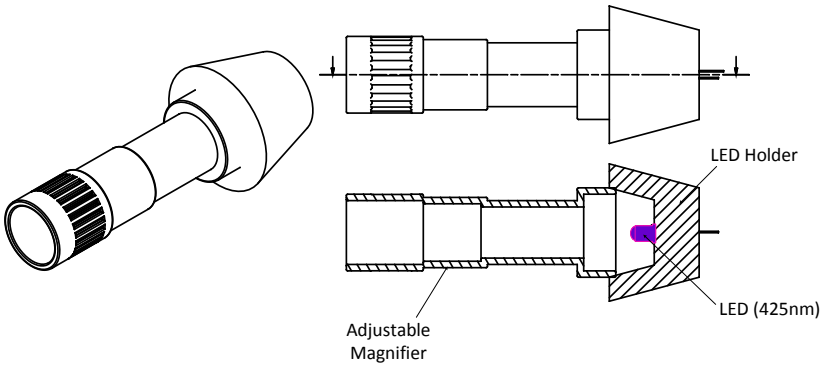

Figure 4.8: Excitation Light Source Assembly

The excitation light source is an LED with a peak emission wavelength of $\lambda_p = 425[\text{nm}]$. The selection is based on the optical properties of the phosphor material(see figure 4.3) where in the excitation spectrum shows a peak in this spectrum range. It is incorporated an adjustable magnifier in order to direct the light towards the phosphor layer sensor deposited on the substrate target(see figure 4.8).

4.3.1 Control System (Arduino Based)

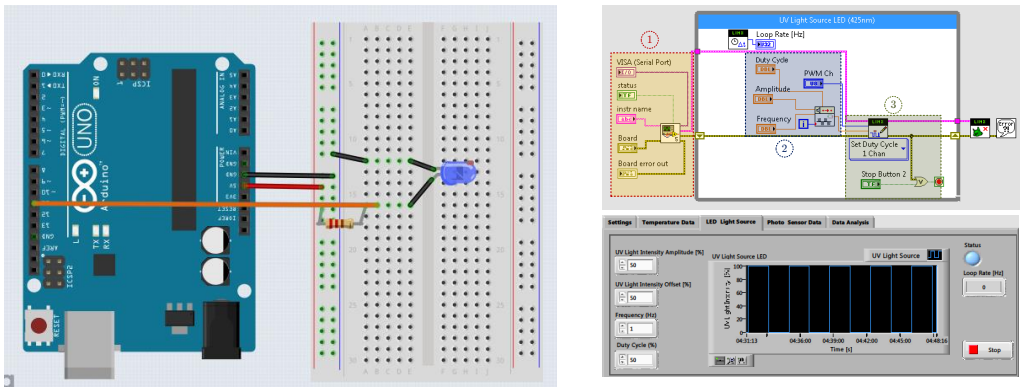

Figure 4.9: Arduino Based Controller and LabVIEW Implementation *(Block Diagram & User Interface)*

The developed controller is a very simple setup (see figure 4.9) in which the Arduino microcontroller by means of a LabVIEW implementation allows the user to controller different parameters on a pulsed waveform (square wave). The parameters that can be controlled are the frequency, duty-cycle[%] and amplitude. The LabVIEW implementation is based on a point-by-point that it is recommended for areal-time applications. The controller has been used during the experimental work to generate for pulsating signal of 10 Hz. However, the controller has some limitations on the waveform and the maximum frequency. It has been observed that the controller operates with a satisfactory performance for square waveform up to 25 Hz, in contrary for other types of waveform such sinusoidal start to behave slightly erratic.

4.3.2 LED Characterization (Estimations of switch-off lag time)

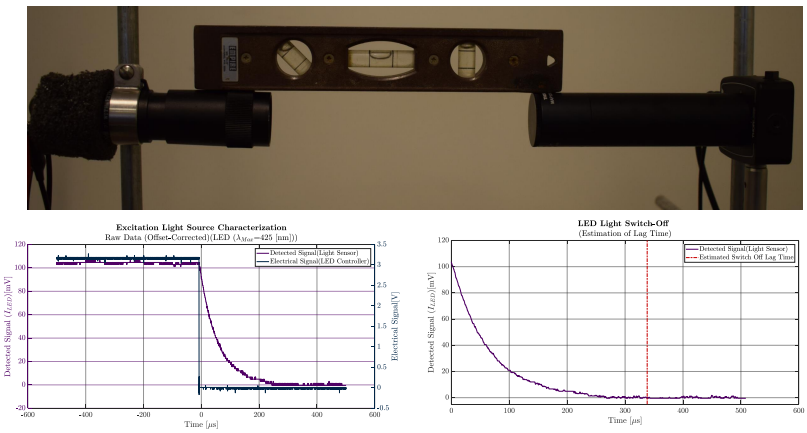

Figure 4.10: LED Characterization (Estimations of switch-off lag time)

The excitation source characterization is performed by measuring the detected light signal from the photo-sensor and comparing with electrical signal from the controller (see figure 4.10). The main idea behind this procedure is that in order to perform a decay-time based phosphor Thermometry it is required to ensure that the evaluation of the after-glow it is performed when the excitation source is completely off. Contrary to laser, an LED has longer lag-time between the electrical is turns-off and the emitted light. It is estimated that the LED switch-off lag time is 0.34[ms](estimation based on relation of five times the decay time of the signal ($5\tau_{LED}$)). This resulting switch-off lag time will be considered in the implemented algorithm to estimate the decay time.

4.4 Data Acquisition (Oscilloscope)

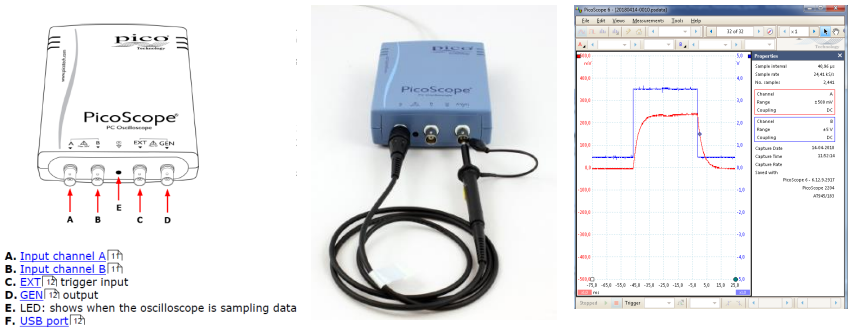

Figure 4.11: Data Acquisition (Oscilloscope)*(PicoScope 2204A)*

A PicoScope 2204A Oscilloscope and PicoScope 6 software (figure 4.11) are utilized to display and record the emitted luminescence decay curves. The sample rate of the oscilloscope is 24.41 kS/s and with a vertical resolution of 8 bits during the experimental work. The oscilloscope is equipped with two channels, one of them has been connected to LED controller electrical signal. The luminescence signal which is amplified by the photo-sensor it is connected with the other oscilloscope channel. The data is saved for later post-processing.

4.5 Implemented Method in Decay Time Estimation

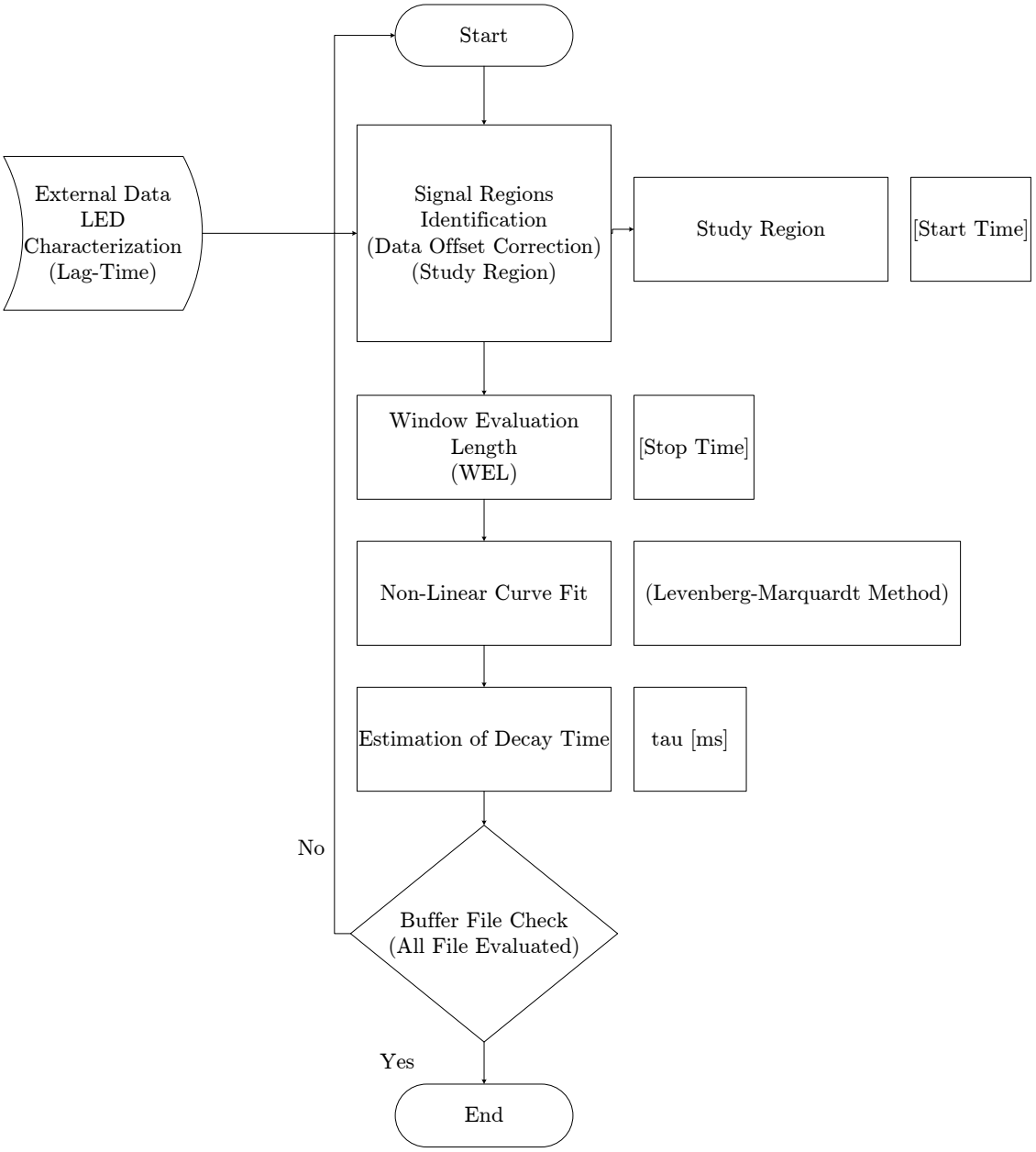

Figure 4.12: Decay Time Estimation Work-flow Diagram

The work-flow Diagram (figure 4.12) represents the implementation of the algorithm that has been developed for this project (inspired in several different sources [6] [21] [22] [23]) in order to estimate the mean decay time of the phosphor-emitted light(see Appendix A:Matlab Implementation Codes). The algorithm will be explained in detail in the following sub-sections.

4.5.1 Identification of the Different Regions on the Photo-Sensor Signal

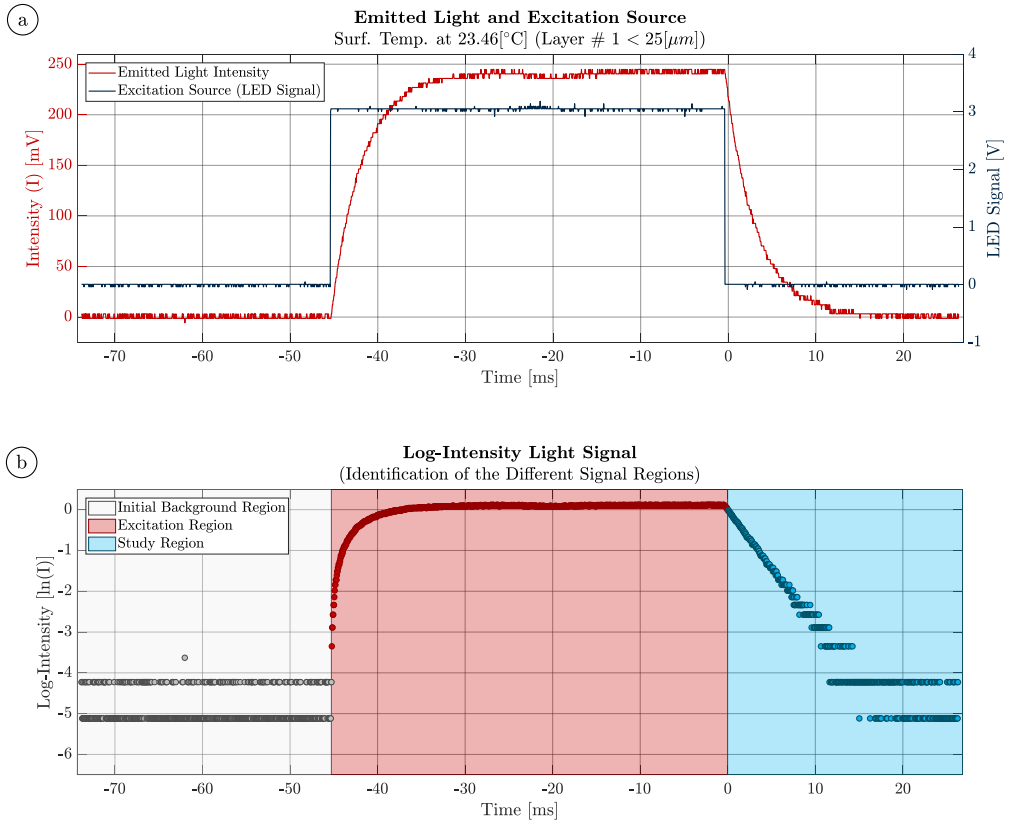

Figure 4.13: Identification of Different Regions on the Signal (at 23.46 [°C]) *(a) Phosphor emitted light signal and excitation light source(8 Bits resolution). (b) Transformed phosphor emitted light signal(ln(I) vs Time): The transformation helps to visualize the three main regions and with the particular interest on the region that decay mono-exponentially (study region).*

The first step is the identification of the different emitted light signal regions. This is performed by examining the electrical signal from the LED excitation source (see figure 4.13(a)). The LED signal will provide two temporal reference points (switch-on/switch-off) that define the excitation region (see figure 4.13(b) (red area)). The switch-on point of the LED signal will be used to determine the initial background noise detected by the Photo-Sensor. Accordingly, the signal detected by from the Photo-Sensor before the LED switch-on will be averaged and used as a signal offset correction parameter.
Subsequently, the offset of the signal(Photo-Sensor) is corrected and the starting point of the study region is located by looking at the instant in which the electrical signal switch-off. This starting point is adjusted due to the estimated LED switch-off lag time(0.34[ms] from the excitation light source characterization).
Thereafter, the evaluation process will lead to a well defined temporal starting point of the study region(Start Time)(see figure 4.13(b)). This method of establishing a fixed starting point will provide a higher window stability and enable the use of the emitted light signal parts which are still high above the background noise [23], in contrast with other methods that suggest the use of the curve fit results in order to determine the study region(start and stop time)[21].

4.5.2 Study Region: Observed Lack of Resolution

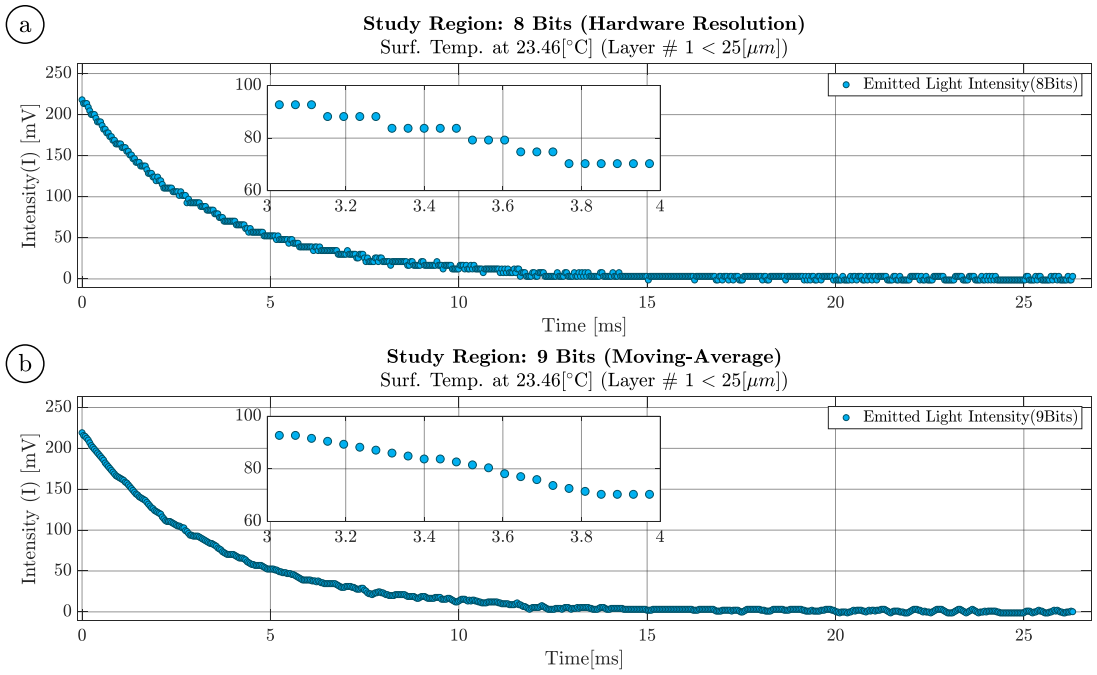

Figure 4.14: Potential Improvements by Resolution Enhancement (8 to 9 Bit) *(a) Study Region Data (8 Bits resolution): observed lack of resolution in the phosphor emitted light signal [mV] at 8 Bits. (b) Study Region Data (9 Bits resolution): signal resolution enhancement by moving-average of four samples.*

Before continuing with the explanation of the data analysis, it is required to emphasise the observed lack of resolution (see figure 4.14) due to a hardware oscilloscope(PicoScope 2204A). The above figure shows a data comparison between 8 Bit (0.4% of FS(full scale)[5]) resolution of the study region (raw data) with respect to an enhanced resolution estimated by a moving-average of four samples that correspond to a 9 Bit resolution (0.2% of FS [5]). Additionally, it is estimated that the resolution could be one of the major upgrades that need to be addressed in the future in order to improve the results.
Consequently, the upgrading of the oscilloscope, for example, PicoScope 5000 will improve the sample rate and the buffer capacity. This upgrade has a direct impact on the uncertainty of the results, by reducing the contribution from the decay time curve fit(repeatability).

4.5.3 Window Evaluation Length for Decay Time Estimation

Determining the windows evaluation length is a challenge and a very important step that could conduct to systematic errors in the estimation of the decay time (τ_μ). In order to minimize this potential systematic error contribution, it is required to pay special attention on the multi-exponential nature of the phosphor emitted light. The emission spectrum of the selected phosphor material: $Mg_4FGeO_6 : Mn$ is reported in the data sheet (see appendix D: Important Data Sheet).

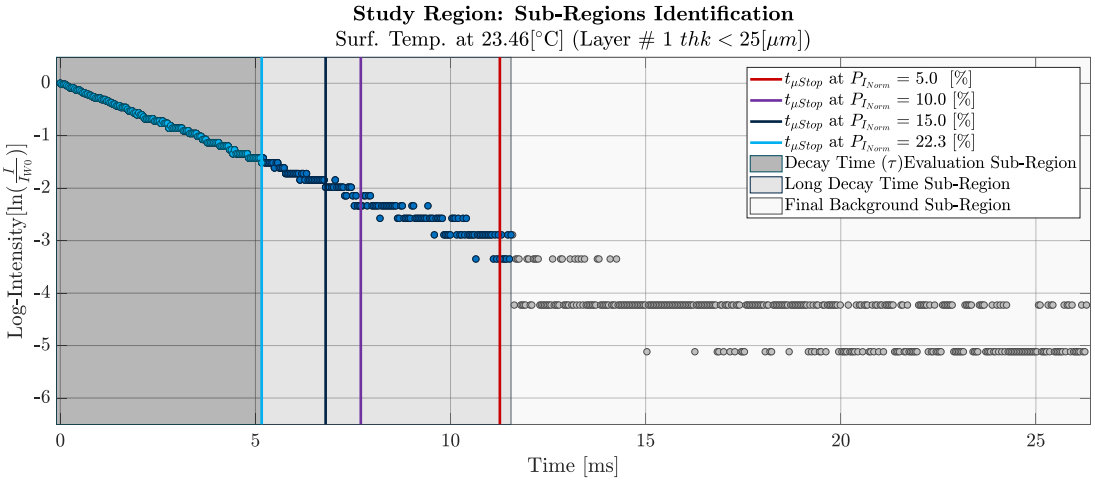

Figure 4.15: Determination of Window Evaluation Length (at 23.46 [°C]) *Log-Normalized Signal Intensity: identification of different sub-regions on the main study region in order to estimate the adequate window length.*

At this point, it is decided to investigate the different sub-regions that are present in the emitted light intensity under study. The procedure to identify the different sub-regions is implemented by a transformation of the emitted light intensity by normalizing and apply a natural logarithm (see figure: 4.15)(inspire by [22]). Three sub-regions have been identified: background noise, long-decay time (long-lived states from the phosphor-emitted light) and the evaluation sub-region which corresponds to a straight line(associated to a mono-exponential decay behaviour).

The different vertical lines in figure 4.15 represented by $P_{I_{Norm}}[\%]$ value. This value signifies the percentage of the normalized intensity at which the initial intensity has been reduced. The associated time to the $P_{I_{Norm}}$ value corresponds to the estimated time to stop t_{stop} the evaluation[10]. That defines the evaluation window length used to perform a mono-exponential curve fit in order to estimate the decay time(τ_μ). It is possible to observe that at $P_{I_{Norm}} = 15[\%]$(dark blue line) an estimation of the decay time by implementing a mono-exponential curve fit model could conduct to a reasonable result considering that

[10]Note: special algorithm has been implemented in order to determine the associated t_{stop}(see subsection:"Stop Time Estimation [t_{stop}]").

the influence of the background noise and the long-lived states (longer exponential decay signal) have not exhibited a strong influence.
In contrary, increasing the window evaluation in the tail direction of the curve means that longer decay time and background noise components will have more influence over the fitted function, and therefore results in longer mono-exponential decay times (potential induced systematic error).

However, it necessary to take into consideration that this corresponds to a single temperature of 23.46 [° C]. This means that there is a potential risk of inducing a systematic error if the same $P_{I_{Norm}}[\%]$ value it is used for the entire temperature range up to 250 [° C]. Therefore, in order to avoid a potential induced error and keep consistency in terms of the $P_{I_{Norm}}[\%]$ value for the entire temperature range, it is decided to reduce the window evaluation length to 22.3 [%].
The $P_{I_{Norm}}$ value of 22.3 [%] is not an arbitrary number, it has been estimated to be an optimum value in order to ensure at least 1.5 τ windows evaluation length for all the temperature that has been evaluated. In figure 4.16 it is illustrated the different windows evaluation length at the maximum temperature exposure of 246.3 [°C].
Furthermore, it is possible to observe that at $P_{I_{Norm}} = 15[\%]$ the influence of the longer-decay time has a relevant influence. This influence will conduct to potential error in the decay time estimation [11].

Study Region: Sub-Regions Identification (at 246.3 [°C])

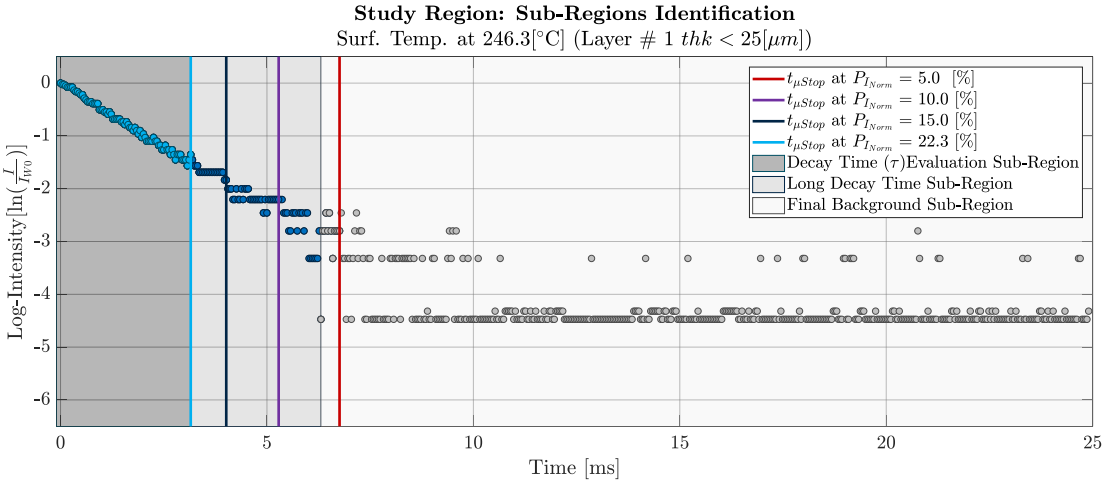

Figure 4.16: Determination of Window Evaluation Length (at 246.3 [° C])
Log-Normalized Signal Intensity: identification of different sub-regions on the main study region in order to estimate the adequate window length. The $P_{I_{Norm}}[\%]$ value represent the percentage of the normalized intensity at which the initial intensity has been decay. The associated time to the $P_{I_{Norm}}$ value correspond to the estimated time to stop t_{stop} the evaluation. That define the evaluation window length used to perform a mono-exponential curve fit (non-linear) in order to estimate the decay time(τ).

[11]Note: Further discussions about the induced error are explained in the following sections(see: section "Effect of Evaluation Windows Length in Decay Time Estimation").

Window Evaluation Length (Stop Time Estimation [t_{stop}])

The process of determining the window evaluation length finalize with the estimation of the Stop Time ([t_{stop}]). However, this is not a trivial process considering that selecting the correspondent time to the specific value of $P_{I_{Norm}} = 22.3[\%]$ could lead to a selection of an outlier. In order to overcome this situation, an algorithm has been implemented following the suggested method by [23] with same small adjustments in order to speed up the process (vectorization instead of a loop iteration).

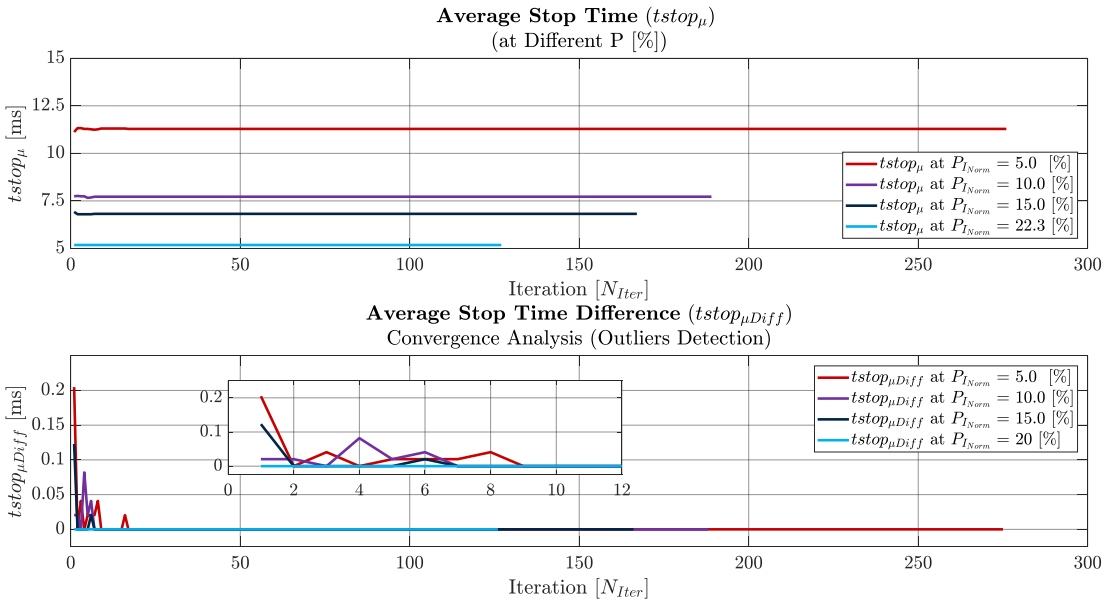

Figure 4.17: Stop Time Estimation [t_{stop}] (at 23.46 [°C])

The main idea behind the implemented algorithm that helps to determine the t_{stop} is to cluster the phosphor light intensity data into two vectors (above & below the $P_{I_{Norm}}$ threshold). Therefore,in order to obtain those vectors, the clustering of the data is performed by selecting all the light intensity points above and below the threshold of $P_{I_{Norm}} = 22.3[\%]$. Each of this vector has an associated time vector. The next step is to calculate the time average (t_{avg}) between the associated time from the last point above the threshold intensity and the associated time from the first point below the threshold intensity. The averaging process is repeated with the successive points.

The process terminates when the time difference between both data points in each iteration step has been converging to a minimum value(as was explained in [23]). The time difference convergence is illustrated in figure 4.17 for different $P_{I_{Norm}}$ values. The estimated value of t_{stop} is calculated from the average time value in the last iteration step. Furthermore, as mentioned in [23], it is expected that his method of establishing the window evaluation length will improve stability against the influence of the signal noise and outliers.

4.5.4 Decay Time Estimation (Non-Linear Curve Fit)

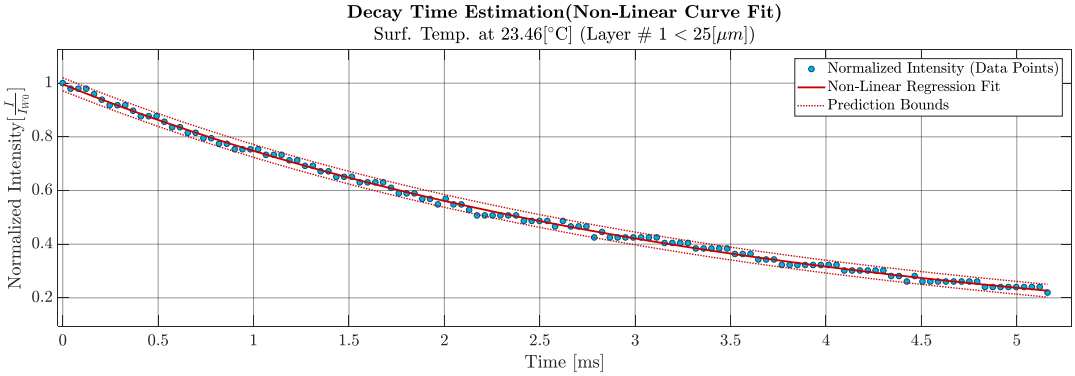

Figure 4.18: Non-Linear Curve Fit*(Mono-Exponential Model at 23.46 [°C])*

The mono-exponential fit (see equation 4.1 and figure 4.18) it is assumed to be suitable, considering that multi exponential fit could conduct to some level of ambiguity in terms of the attribution of the different exponential terms [21].

Furthermore, as mentioned before the offset of the phosphor luminescence intensity has been corrected by subtracting the background noise average before the LED switch-on. The curve fitting method used in this case is Levenberg–Marquardt optimization algorithm from Matlab [21][23]. In equation 4.1 the amplitude I_0 correspond to the initial intensity decay amplitude and τ the decay time.

$$I(t) = I_0 \cdot e^{\frac{-t}{\tau}} \tag{4.1}$$

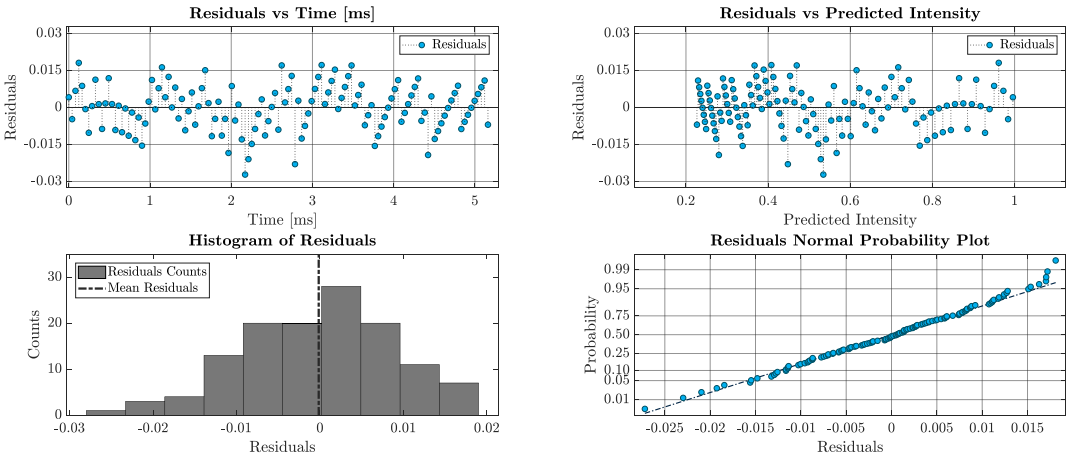

Figure 4.19: Non-Linear Curve Fit*(Residuals Analysis at 23.46 [°C])*

The analysis of the curve fit quality is performed by taking a close look at the residuals (figure 4.19). The curve fit model is considered good [27][28], if the residuals component behave like:

- **random drawings** (i.d., independent)
- **from a fixed distribution** (assumed that the fixed distribution is normal)
- **with fixed location** (assumed that the fixed location is zero)
- **with fixed variation** (good model the fixed variation should be as small as possible.)

In terms of normality and zero-location distribution, it is observed that the residuals fulfil those conditions. Based on the histogram and normal probability plot of residuals that are used to verify those assumptions on the residuals component. Regarding the magnitude of the variation is considered acceptable for this preliminary experimental work, since all the values are smaller than a 3 [%]. However, the randomness (independent) expected behaviour seems to be compromised. The randomness assumption is evaluated by inspecting the plots of the residuals versus the independent variable and the predicted values[12]. Furthermore, similar results have been observed for other temperatures, which means that this effect could be from a contribution that exert influence in a similar way to all the measurements, independently of the temperature. It is estimated that this contribution could be an effect of the lack of resolution.

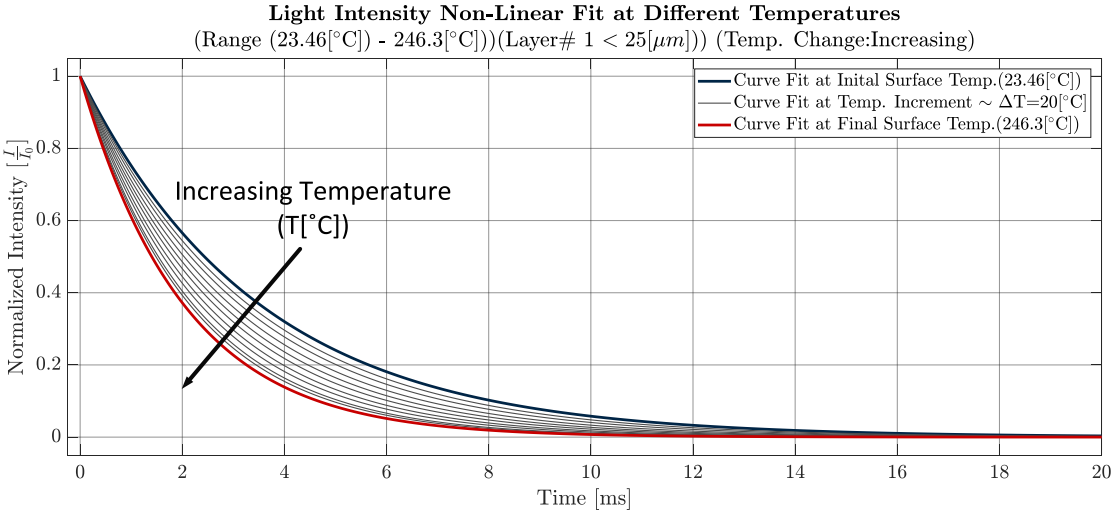

Figure 4.20: Non-Linear Curve Fit*(at Different Temperature)*

In figure 4.20 is shown the non-linear curve fit resulting from the data analysis at different temperatures(from 23.46 to 246.3 [°C])(in heating phase(Δ T increase))[13]. It is possible to observe, as it is expected, the reduction in the decay time (τ) as the temperature increase. The experimental results and the appropriated comparison will be discussed in the chapter "Phosphor Thermometry Experiments".

[12]Note: Residuals vs Predicted values are compared and not residuals vs observed values. This is based on that the residuals and observations are correlated, but the residuals and the predicted values are not[27].

[13]Phosphor Material:$Mg_4FGeO_6 : Mn$. Graphical representation of the data collected from the experimental work during the present thesis.

4.5.5 Effect of Evaluation Window Length in Decay Time Estimation

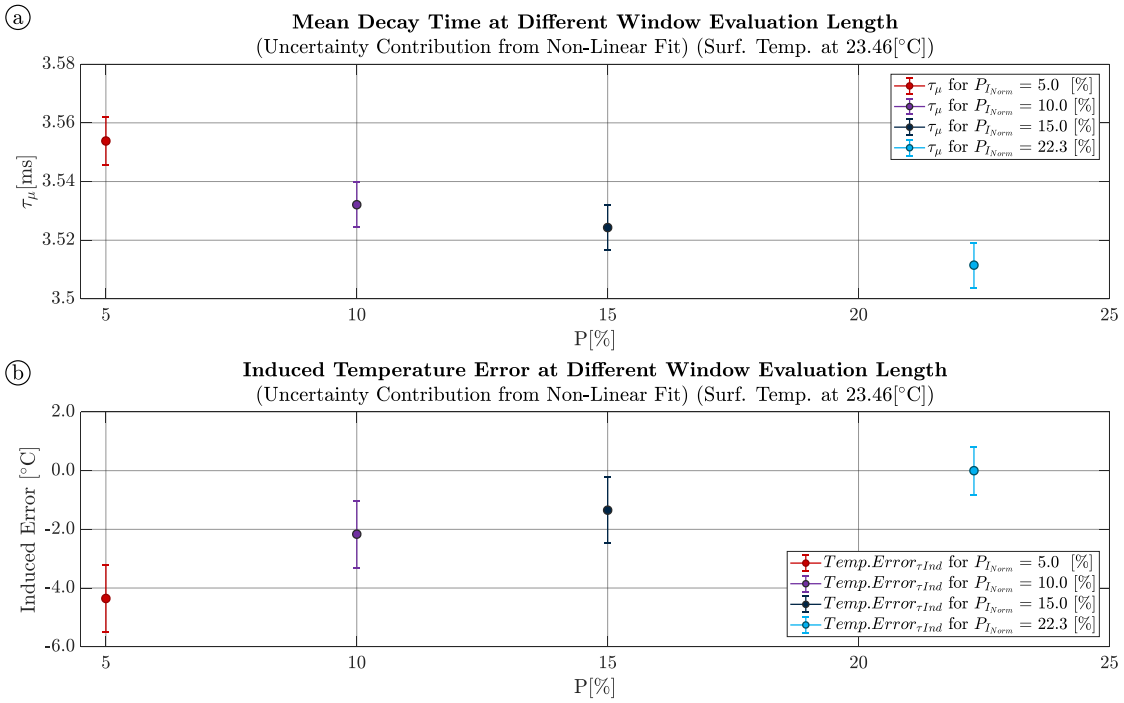

Figure 4.21: Estimated Potential Systematic Error (at 23.46 [°C])
ⓐ Decay Time at Different Window Evaluation Length. ⓑ Potential Induced Temperature Error.

The estimated mean decay time (τ_μ) for different window evaluation length is illustrated in figure 4.21(a). The reported uncertainty of the different values of τ_μ is based on the contribution from the repeatability of the curve fit. It is possible to observe that increasing the window evaluation length by reducing $P_{I_{Norm}}[\%]$ value, affects the estimate τ_μ results. Furthermore, the differences in τ_μ can be expressed in terms of temperature by assuming a linear relationship between two consecutive temperature measurements and estimate the sensitivity coefficient (c_i) (see figure 4.21(b) and equation 4.2).

$$\begin{aligned} T(\tau) &= m \cdot \tau + b \\ c_i &= \frac{dT(\tau)}{d\tau} = \frac{(T_i - T_{i-1})}{(\tau_i - \tau_{i-1})} \end{aligned} \tag{4.2}$$

In this case, for comparison purposes, the τ_μ estimated at $P_{I_{Norm}} = 22.3[\%]$ is considered error-free and used as a reference in order to evaluate the potential induced error.
The errors in temperature at 23.46 [°C] are estimated to be up to -4.3 ± 1.1[°C](for $P_{I_{Norm}} = 5[\%]$)(see figure 4.21(b)). However, for higher temperatures such for example 246.3[°C] the estimated induced errors has shown an increment up to -7.6 ± 3.3 [°C] (for $P_{I_{Norm}} = 5[\%]$)(see figure 4.22(b)).

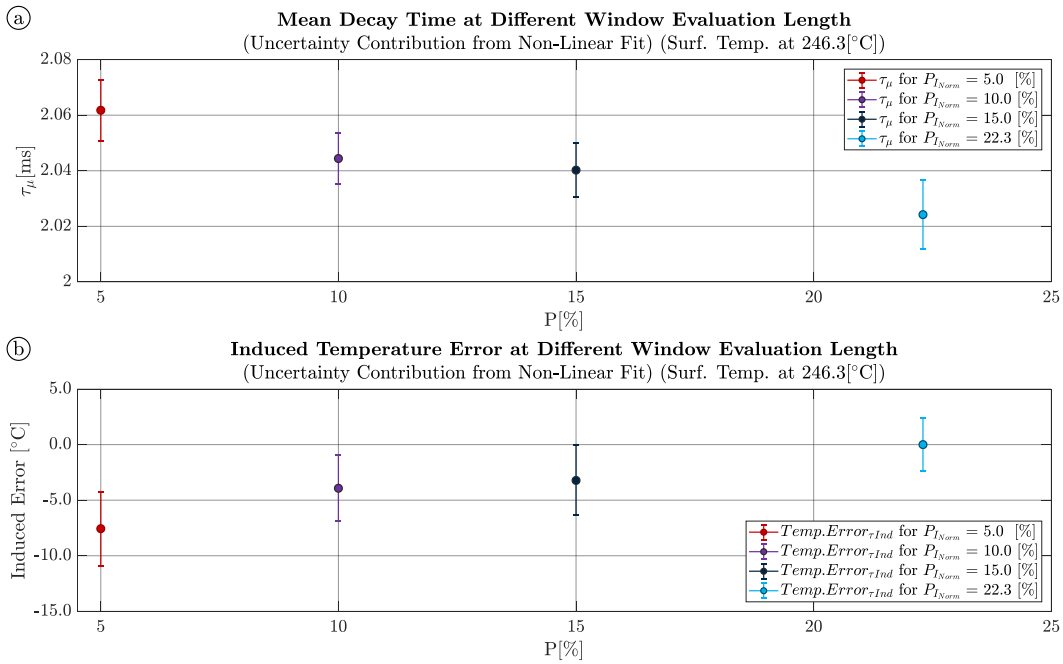

Figure 4.22: Estimated Potential Systematic Error (at 246.3[°C])
ⓐ Decay Time at Different Window Evaluation Length. ⓑ Potential Induced Temperature Error.

Remarks: Considering that there is only one temperature at which the signal was measured, these temperature changes can be interpreted as systematic errors [23].

4.6 Developed Phosphor Thermometry System Summary

In this chapter, the experimental set-up to develop a phosphor Thermometry system has been presented, followed by a discussion of the individual components and their relevant performance parameters those that affect the measurements.

The developed set-up still required further improvements. It is considered that the excitation source and the corresponding controller system could be improved by using a standard mounted LED system with a controller that could be used also in different modes (phase shifting decay estimation). This will provide flexibility to the phosphor Thermometry system and the opportunity to investigate different methods.
Furthermore, it is observed that there is a potential lack of the resolution (only 8 bit hardware) and buffer memory size, in the oscilloscope that can have an influence in the estimated uncertainty of the curve fit. The upgrading of the hardware resolution of the DAQ (oscilloscope) is suggested as a future improvement.

The implemented method to estimate the decay time of the phosphor luminescent, is based on a combination of different techniques that have been applied in a similar context ([6] [21] [22] [23]). Additionally, it is considered that combining the different approaches with a graphical representation is helpful in order to visualize the procedure. The effect of the window evaluation length over the decay time has been quantified, showing potential induced error, in the order of -4.3 ± 1.1[°C](for $P_{I_{Norm}} = 5[\%]$ at 23.46 [°C]) and -7.6 ± 3.3[°C](for $P_{I_{Norm}} = 5[\%]$ at 246.3 [°C]).

5

Phosphor Layer Sensor Fabrication

This chapter describes the main procedure implemented to fabricate the phosphor layer sensor. Furthermore, it is reported the estimated thickness layer including the associated sources of uncertainty.
As mentioned before, in the introduction, the thickness of the phosphor layer sensor is an important parameter that could conduct to a potential error in the estimation of the surface temperature of an object (potential error is due to thermal intrusion).
Furthermore, it is estimated that the major challenges in the fabrication of a phosphor layer sensor are the manufacture of a reproducible layer that it is thermally non-intrusive and the quantification of the thickness.
In summary, the fabrication process[1] should be able to provide a phosphor layer sensor that fulfils the following requirements for the suitable application of a phosphor Thermometry technique [6][19]:

- Reproducible thickness layer and negligible thermal intrusiveness [29] (thickness $\sim$ 20 [μm]).
- Resistant to the expected maximum operating temperature (500 [° C]).
- Inert and should not change the spectral (expected wavelength of the emitted light) and thermographic properties (e.g. emitted light decay time at specific temperature) of the phosphor.
- Provide good thermal contact(e.g. Sandblasting (creating microscopic teeth) the surface of the substrate prior to the application of the layer in order to increase the adhesion of the phosphor layer sensor.) and good thermal expansion relation with respect to the substrate in order to avoid cracks or flake off.
- Durable (withstand thermal shocks and vibrations (harsh environments)) and at the same time easy to remove(for this particular project).
- High degree of layer homogeneity in order to ensure equal emitted phosphorescence intensity and thickness throughout the phosphor layer surface.

[1] Bonding or adhering process of the phosphor layer sensor to the substrate surface.

5.1 Thermal Sensing Layer Adhering Method

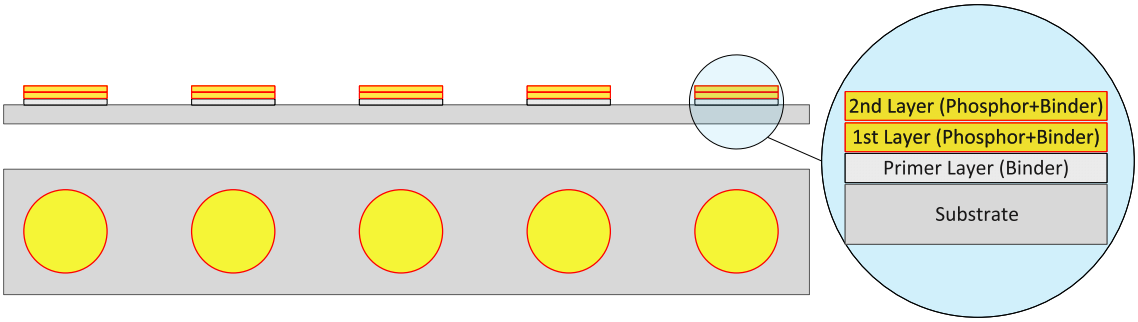

Figure 5.1: Thermal Sensing Layer (Deposition Overview)

There are different methods[2] available for adhering a phosphor layer sensor on the surface of the substrate.
In this thesis, the implemented method is the adhesive binder coatings. This process involves mixing powdered phosphor material ($Mg_4FGeO_6 : Mn$) with suspension agent/binder liquid (ZYP Coating BNSL Binder, see Appendix D: Important Data Sheet) to create a paint that can be applied by an airbrush onto a substrate surface.
In figure 5.1, is shown the layer deposition procedure, in which the first layer is a thin binder coating [3] that works as a primer. The reason for that is to avoid the previous mentioned sandblasting procedure (provide good thermal contact), that will cause an undesirable surface roughness change in the polished substrate. The next layers are applied in a similar manner as the primer layer with the phosphor added in the mixed paint.

The main advantage of the adhesive binder coating method is the flexibility in terms of the application on-site on almost any substrate surface size and geometry [6].
Furthermore, the required equipment does not represent a high-cost investment(compressor[4] and airbrush). During the application process, the phosphor particles remain unaltered and in general, there is no need for curing (annealing) process prior to their use in remote surface temperature measurements.

However, some disadvantages are present in the method, for example, the presence of the suspension binder that it is required to use in order to prepare the paint. The binder does not play any role in the phosphoresce phenomenon, but may absorb part of the excitation and phosphorescence emitted light. Consequently, this binder interaction usually produces a lower intensity emitted light that could represent a challenge in terms of the signal-noise ratio (SNR).
Additionally, other potential disadvantages are the low control of the phosphor layer sensor thickness and homogeneity distribution on the substrate surface. These factors, mainly depend on the skills of the operator.
Nevertheless, in the next section, a detailed procedure is described, as an attempt to minimize the contribution from the required skills of the operator.

[2] Adhesive Binder Coatings, Chemical Vapour Deposition (CVD), Physical Vapour Deposition (PVD)
[3] Highly diluted solution 15-20 vol.% mixed with solvent (acetone/ethanol(mix 50%/50%))
[4] The compressor should be oil-free in order to avoid an extra source of potential contamination.

5.2 Layer Preparation Materials

Figure 5.2: Layer Preparation Materials

The main materials that has been used in the preparation of the phosphor layer sensor can be summarized as follow (see figure 5.2):

- Phosphor Material ($Mg_4FGeO_6 : Mn$)
- Suspension agent/binder liquid (ZYP Coating BNSL Binder)
- Air-brush kit (oil-free compressor, airbrush)
- Acetone/Ethanol Solvent
- Masking Film (substrate surface preparation)
- Auxiliary Items (syringes(volumetric quantification purposes), scale, containers mixing)

The binder agent can withstand up to 1600 [° C]. However, besides that, the selection criteria are based on the versatility of the product that is not very reactive to the different substrate materials.
Furthermore, the BNSL binder which is solvent-based is recommended as a suspension agent for first trials due to its inertness to most powder additives that do not require a curing process (according to the manufacturer).(ZYP Coating BNSL Binder, see Appendix D: Important Data Sheet)

5.3 Layer Preparation Main Steps

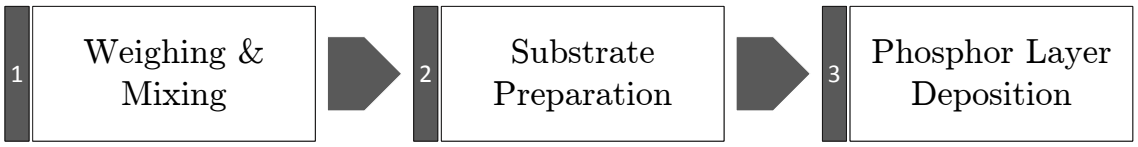

Figure 5.3: Thermal Sensing Layer Preparation (Main Steps)

In order to obtain an adhering procedure that can be reproduced, the implemented systematic process is divided into three main steps (see figure 5.3). The process involved in each steps are explained in the following sub-sections.

5.3.1 Weighing & Mixing

The steps of Weighing & Mixing involves several different sub-steps [5]. The weighing is related to the assessment of the adequate relation between the amount of phosphor powder and binder. Furthermore, this step has been turned out to be an iterative process in order to ensure not only an adequate thickness of the layer but also a suitable emitted intensity luminescence.

The relation that has been established as a suitable for this project is 1:5 (1 gr of phosphor powder with 5 gr of binder). The mixing step, it is required in order to establish the amount of solvent and the different sub-steps that are necessary to achieve a suitable pulverization by the airbrush. In this case, it has been observed the mixing ratio that suits the airbrush kit capability is the following:[6]

- Mix or combine 1 gr of phosphor material with 1 ml of a solvent mixture acetone/ethanol (50%/50%)(to avoid potential clogging of the airbrush nozzle)(Mix in a separate reservoir and agitate)
- Mix binder liquid (5gr) with 6 ml of a solvent mixture.(Mix in a separate reservoir and agitate)
- Combine the previous two mixture in the same reservoir and agitate.
- Agitate the mixture is recommended, even between the deposition of different layers considering that has been observed a fast precipitation of the phosphor.

The solvent mixture (50%/50%) is not a trivial decision, it is based on the observed effect of using only acetone. This has been shown a potential risk of the mixture drying in the way to the substrate, depending on the pulverization distance of the airbrush nozzle, which increases the difficulty of obtaining a homogeneous layer, due to the required operator skills.
Consequently, the solvent mixture allows a more flexible application in terms of distance to the substrate surface. Furthermore, the slower drying process of the phosphor layer sensor due to the presence of the ethanol provides the possibility of applying a subsequent layer before it is completely dry. The new layer will bond to the previous one, without showing any apparent delamination or flake off between layers.

[5] All specifics safety personal devices and working condition should be fulfilled.
[6] The reason for this detailed quantity is mainly for documentation purposes.

5.3.2 Substrate Preparation

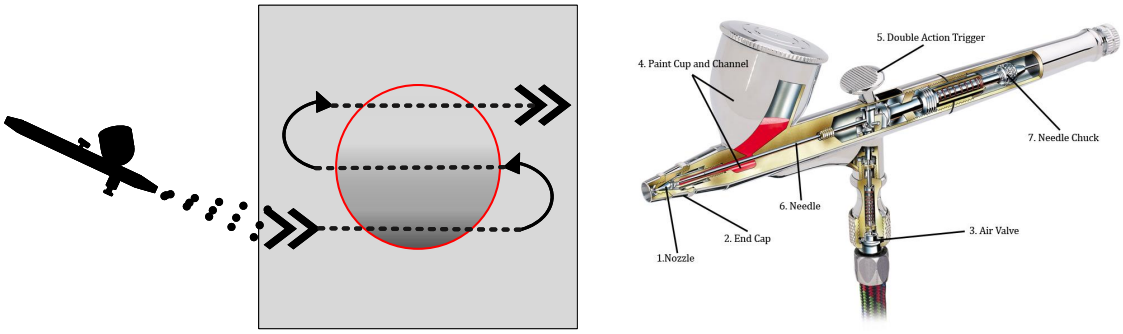

Figure 5.4: Primer Layer Deposition Procedure and Airbrush Components *(Airbrush components picture source:[33])*

The preparation of the substrate surface involves three main sub-steps: Cleaning, Masking Film Application and Deposition of a Primer Layer.
The cleaning of the substrate surface involves as a first step, the use of ethanol, after drying, cleaning with acetone. Moreover, the cleaning process has been performed from the centre of the area of interest toward the edges using a paper or cloth that does not leave any residual. It is also recommended to use powder-free gloves to avoid potential contamination. The reason for using the two different solvents is due to that each of them will remove contamination with different polarities.
The application of a masking film is to delimit an area (at the centre of the substrate surface) on which the phosphor layer sensor will be deposited.
In figure 5.4 is shown the procedure to apply the primer binder layer with highly dilute binder.

Additionally, it is necessary to emphasise the following aspects of the deposition procedure in order to maximize the homogeneity of the final resulting layer:

- Start the spraying outside of the area of interest to avoid uneven deposition.
- When the spraying process begin do not change the position of the double trigger action(see figure 5.4).
- Always keep a normal position of the airbrush nozzle with respect to the substrate surface (potential "Orange peel effect" (dusty texture)).
- Continuously phosphor spraying is recommended.(Avoid intermittent deposition.)
- In order to maximized the thickness homogeneity is recommended to avoid excessive layer overlapping.

5.3.3 Phosphor Layer Sensor Deposition (Spray Procedure)

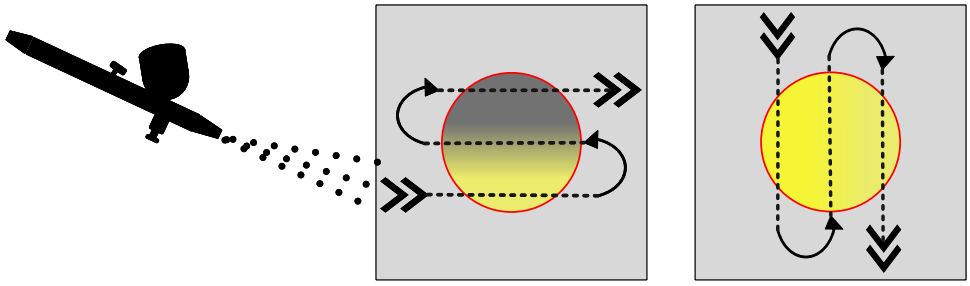

Figure 5.5: Spray Deposition Procedure

The procedure for the deposition of the phosphor layer sensor is similar to the previously explained method for the substrate surface preparation.
However, there are some details that need to be taken into account such as the orientation of each layer. In this project has been observed a positive effect by crossing the different layers, in order to achieve a homogeneous deposition. Furthermore, another factor that has been tested is the drying between different layers with a hot air gun, this did not show any beneficial effect. In contrary, cracks have been observed. Consequently, instead of completely dry every layer, the subsequent layer has been applied when the previous is still slightly wet.

5.3.4 Preparation Considerations

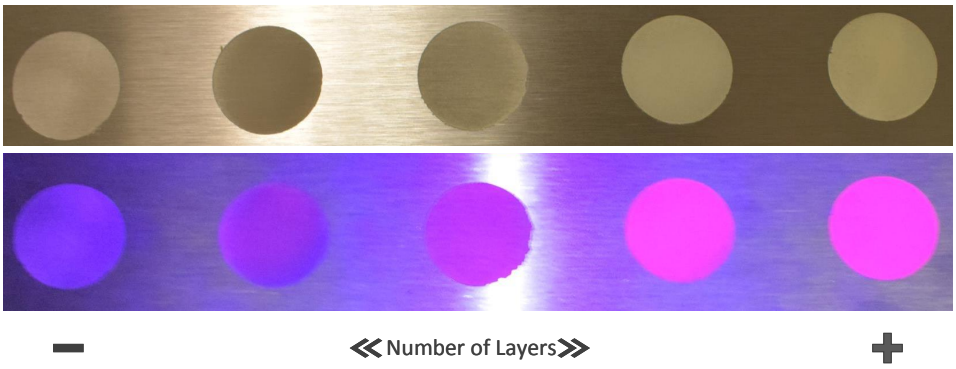

Figure 5.6: Observed Effect on Luminescence due to Number of Layers
(Phosphor Layers sensors are excited by an LED(λ_{peak} =425[nm]))

In figure 5.6 is observed one of the first trials of the phosphor layer sensor preparation. During this process, several sample phosphor sensors have been prepared in which each of them has a different number of phosphor layers deposited. The test has been shown that in the most transparent phosphor layer sensor (lower number of layers) the intensity of the emitted luminescence is lower and the excitation light (LED) is reflected in the substrate surface. Consequently, as the number of deposited layers increases the intensity of the emitted luminescence also increase.
As a consequence, the intensity of the emitted luminescence together with the thickness should be taken into account at the time of fabricate the phosphor layer sensor.

5.4 Phosphor Layer Thickness Quantification Procedure

5.4.1 Thickness-Meter Working Principle

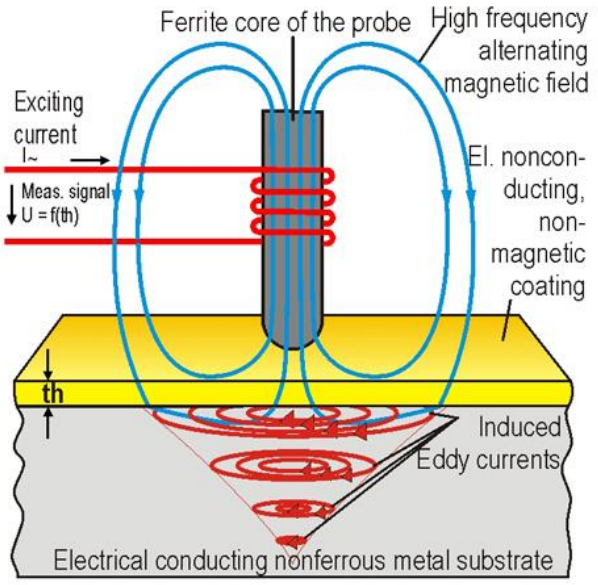

Figure 5.7: Schematic diagram of Eddy Current Method *(amplitude-sensitive)*(Picture Source:[30])

The selected instrument to quantify the thickness of the phosphor layer sensor is an Eddy-Current thickness-meter (see figure 5.7).
The instrument work on the principle that an alternating electromagnetic field generated at the probe will produce eddy-currents in the substrate material (metallic) beneath of the phosphor layer sensor on which the probe tip is placed.

The induced eddy-currents on the substrate generate a magnetic field that opposes the magnetic field from the sensor, causing a change in the last one. Therefore, the interaction between these magnetic fields, resulting in a change in the amplitude of the probe coil impedance. The density of the induced eddy-current depends on the distance between the generating coil and the substrate metallic surface.

In order to quantify the thickness of the phosphor layer sensor, the measure of the change in the coil impedance is used, by means of a calibration with respect to a reference standard. The sensor electronics measure the change in the coil impedance (magnetic fields interaction) and generate an output voltage that it is proportional to the thickness. Consequently, the measurement signal of the output voltage is converted in the instrument into the coating or layer thickness value.[30][32]

5.4.2 Thickness Measurements Procedure

Thickness Meter Performance

The assessment of the thickness-meter performance has been carried out, prior to any thickness measurements(see figure 5.8). This assessment has been performed on a well define substrate surface and with a set of reference plastic foil with different thickness provided by the manufacturer thickness range from 50 [μm]- 1020 [μm] $\pm$ 1 %. Furthermore, it is considered that the estimation of the thickness-meter performance[7]will be helpful in order to quantify the uncertainty contribution from the instrument under well-known conditions.
The main parameters considered in the estimated uncertainty of the instrument performance are the following:

- Resolution of the instrument at the specific range.
- Specified instrument accuracy (from manual).
- Reference plastic foils (uncertainty specified in the foils ($\pm$1%)).
- Repeatability of a set of measurements for the different reference plastic foils thickness.

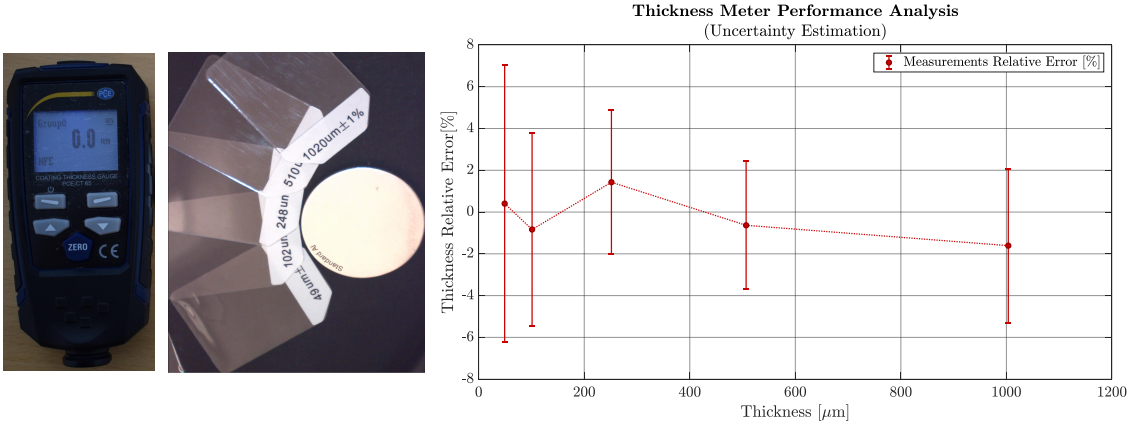

Figure 5.8: Thickness Meter Performance

The results of the thickness-meter test (see figure 5.8) shows that, for the reference plastic foils 49 [μm] thickness, the relative error is 0.4 $\pm$ 6.7 [%][8]. The relevant information extracted from this test is the associated relative uncertainty of a thickness range of 49 [μm], which is the closest to the required thickness of the phosphor layer sensor.
Consequently, it is possible to infer that the relative uncertainty of the phosphor layer thickness should be higher than 6.7 [%], due to the fact that the resolution and the associated accuracy of the instrument remain the same. Furthermore, this result highlights the potential limitation of the thickness quantification method due to the uncertainty from the instrument accuracy.

[7] All measurements have been performed on an aluminium substrate.
[8] Preliminary estimation, to validate the results it requires a calibration by a qualified laboratory.

Measurements Procedure

The reported phosphor layer thickness in this work (see section "Thickness Quantification Results") is the result of measuring directly on top of the phosphor layer sensor. The thickness has been checked by performing some measurements with a reference plastic foil (102 um) on top of the phosphor layer sensor[9](see figure 5.9), prior to the direct measurements.
However, the results did not show significant differences with respect to the direct measurements, due to the increment on the uncertainty contribution from the resolution and accuracy of the instrument. Although, it is estimated that this procedure has been beneficial in order to evaluate the presence of any potential significant indentation or plastic deformation in the phosphor layer sensor during the process, as well as an elastic deformation[10].

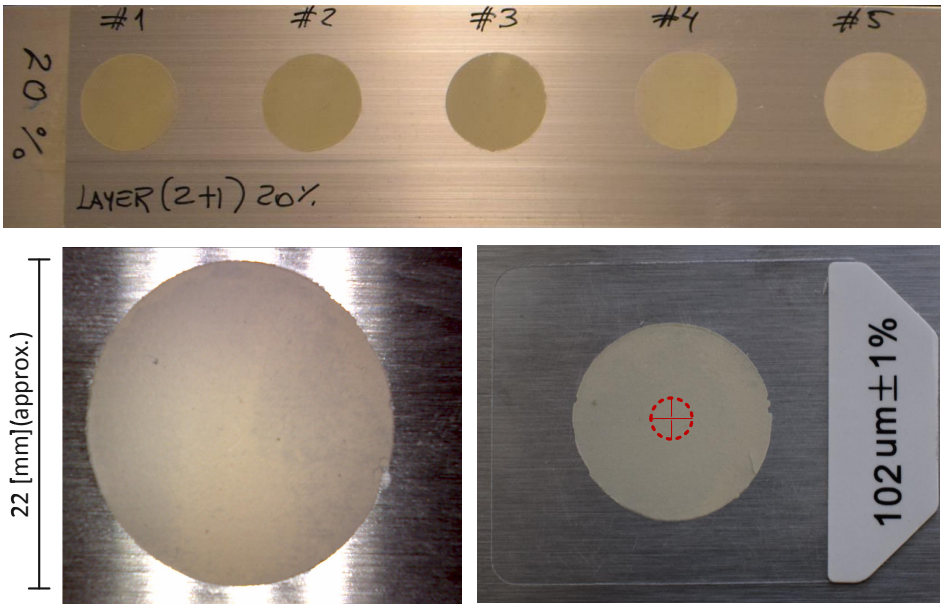

Figure 5.9: Phosphor Layer Sensor Thickness Quantification
Measurement zone (red crossed circle)

Furthermore, has not been observed[11] any potential indentation or plastic deformation in the phosphor layer sensor.
On the other hand, as a suggestion, in order to quantify a potential phosphor layer deformation, a non-contact thickness measurement method could be implemented, such as optical techniques that determine the thickness of the layer by measuring the interaction with light. However, this thickness quantification method, for a preliminary development, is considered out of the project scope due to the higher cost but could be taken into account as a further improvement.

[9] Subtracting later the well known extra thickness.
[10] Assuming non-significant elastic deformation in the reference plastic foil (102 um).
[11] By using a hand-held digital microscope.

5.4.3 Thickness Uncertainty Estimation

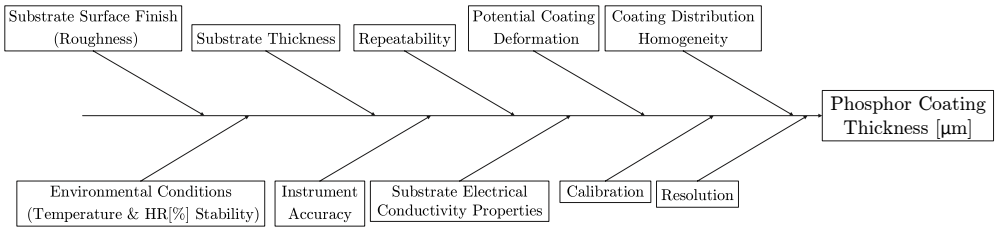

Figure 5.10: Ishikawa Diagram (Thickness Uncertainty Parameters)

The phosphor layer thickness quantification process is subjected to several uncertainty sources [31], the main parameters are shown in figure 5.10. The objective of this subsection, is to summarized the potential source of uncertainty in the quantification of the thickness. However, it is not possible to quantify all of the parameters during the project time frame. Additionally, it is assumed that the effect from some of them can be neglected, the main reasons are discussed as follow:

- **Substrate Surface Finish (Roughness).** Neglected due to polished substrate.
- **Substrate Thickness.** Neglected due to fulfil instruments requirements (min.0.3[mm]).
- **Environmental Conditions.** Neglected, due to stable Temperature & HR [%] laboratory conditions. Additionally, during the measurement process, the substrate and the phosphor layer sensor have not been in direct contact with the hands of the operator that could induce a geometrical change (thermal expansion) due to an increment in temperature.
- **Potential Layer Deformation (during measurement process).** It is not possible to quantify due to the inherent limitation of the measurements method (contact method). It is required other technique, such as optical method.
- **Layer Distribution Homogeneity.** It is not possible to quantify at the moment that the project was carried out. It is required other technique. such optical method.
- **Substrate Electrical Conductivity Properties.** Neglected, considering that the setting of the zero reference and the set of measurements are performed in the same substrate material.
- **Certified Calibration.** Not available during project time frame. Therefore, to validate the results, it is required a calibration by a qualified laboratory.

In summary, the main parameters considered in the reported estimated uncertainty of the phosphor sensor thickness are the following (details about calculations see Appendix A):

- **Resolution of the instrument at the specific range.**(0.1[μm]).
- **Specified instrument accuracy.** (from manual)($\pm$(2.5%+2[μm])).
- **Repeatability of a set of measurements.**

5.5 Thickness Quantification Results

5.5.1 Determination of the Optimum Phosphor Layer Sensor

The process to establish the optimum phosphor layer sensor in order to achieve a layer that it is as less as possible thermally intrusive ($\sim$ 20 [μm]), has been required several preparations. Furthermore, each of the different tests has been prepared with a different number of layers and percentage of phosphor, in order to determine the combination that ensures a suitable thickness and emitted luminescence intensity. Therefore, in order to keep the preparation process in a methodical manner, a designation code system has been implemented (see table 5.1) to identify the different preparations.

(N_{L1}+N_{L2} **Deposited Layers at** P_P [%])	
N_{L1}	Number of Mixing Layers (Phosphor + Binder)
N_{L2}	Number of Binder Layers (Primer)
P_P [%]	Percentage of phosphor mass with respect binder

Table 5.1: Implemented Designation Code in the Phosphor Layer Preparation

In figure 5.11, it shows the process to determine the optimum phosphor layer sensor[12]. This process has been narrowed down to three tests with different configurations in terms of the number of layers and percentage of the phosphor. Additionally, each of the tests involves the preparation by the same operator of several phosphor layer sensors (phosphor sample).

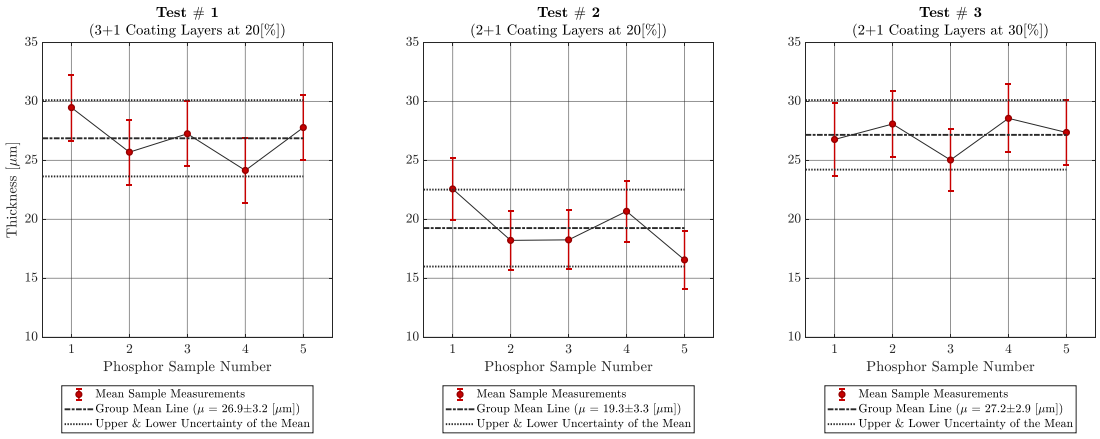

Figure 5.11: Determination of the Optimum Phosphor Layer Sensor

It is estimated that the optimum combination of the number of layers and percentage of the phosphor is the Test#2, in which has been possible to achieve an average of the prepared group of 19.3 $\pm$3.3[μm] and with phosphor layer samples that did not exceed a mean thickness value of $\sim$ 25[μm].
However, it has been observed during the preparation, that reproduce a phosphor layer sensor is a challenging process, considering the number of factors that are involved such as operator, compressor pressure, deposition distance. The quantification of the repeatability and reproducibility is discussed in the following subsection.

[12] Samples selected from several preparations, based on visual inspection of the homogeneity and luminescence intensity.

5.5.2 Thickness Repeatability and Reproducibility

The quantification of the repeatability and reproducibility has been assessed by preparing a set of five phosphor samples in which three different operators are involved.
The main objective is to evaluate the influence of the operators with different previous experience in the preparation of the phosphor layer sensor. The Operator #1 has a previous experience, while the Operators #2 and #3[13], it is the first time for them to be in contact with the preparation methodology and equipment. Furthermore, a brief explanation about how to prepare the layers has been given in the case of the Operators #2 and #3.

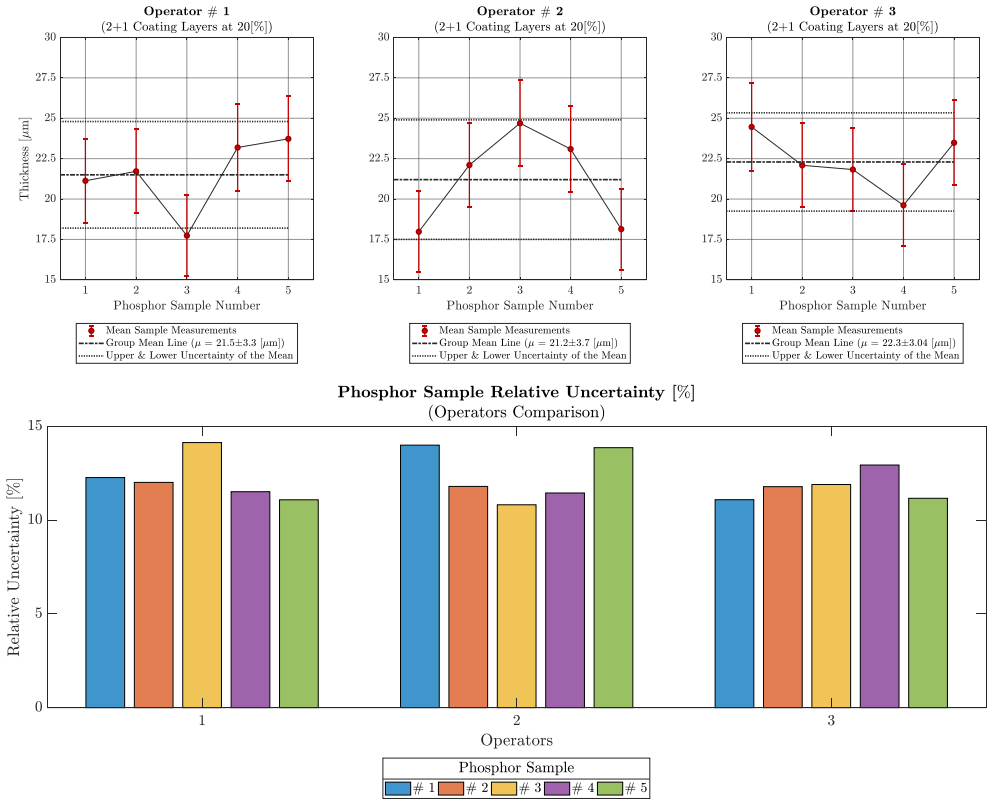

Figure 5.12: Thickness Repeatability & Reproducibility

The figure 5.12, presents the results of the five samples prepared by the different operators. The assessment of the repeatability has been performed based on the dispersion of the thickness measurements within the operator's samples. It is observed that the set of five samples prepared by Operator #2, shows a particular thickness deviation behaviour. It is assumed that this deviation is caused by an observed inconsistent angle and distance of the airbrush during the deposition process. However, the causes of the deviation in the thickness of the samples prepared by the other two operators are difficult to estimate, as mentioned before, due to the number of factors that are involved.

In this case, in terms of reproducibility, the main objective is to evaluate the non-thermal intrusiveness of the prepared samples. Consequently, the values of interest are the thick-

[13]The Operators #2 and #3 participate only in the deposition method (by airbrush) of the phosphor layer, not in the previous preparation of the material or mixing of compounds.

ness upper extreme values of the prepared phosphor layer. In figure 5.12, it is possible to observe that the three operators have been achieved a set of layers where the thickness mean values do not exceed 27.5 [μm].

The uncertainty of the phosphor samples prepared by each operator has been estimated, the results show values up to 14.1[%] of relative uncertainty(see figure 5.12). Furthermore, the main contribution to the estimated uncertainty is from the accuracy of the thickness meter. However, the use of the thickness-meter as a quantification method, it is still considered suitable compared to the method in which the thickness of the phosphor layer it is estimated by comparing the weight of coated and uncoated substrate [21]. Considering that, the weighing method involves the use of several instruments in order to determine the phosphor layer thickness $\left[thk = \frac{mass}{(Area.\rho)}\right]$ and an assumption about the density (density of the material in bulk and the thin layer is different.), which increase the number of potential source of uncertainty.

5.6 Limitations and Potential Improvements

The repeatability and reproducibility of the manufactured phosphor layer sensors still require further improvements. It is estimated that the incorporation of a manometer in the oil-free compressor set-up will be beneficial. The manometer will provide a quantification of the delivered air pressure during the process, that could help to improve the consistency of the deposited phosphor layer in order to obtain a thickness closes to $\sim$ 20 [μm].

The effect or influence of the previous experience in the phosphor samples prepared by each of the different operators does not exhibit clear impact, considering the Operators #1 and #3. However, as mentioned before, in the case of the phosphor samples prepared by the Operator #2 has been shown a systematic deviation behaviour in the deposition of the phosphor layer. Accordingly, the development of the operator's skills, that can be achieved by training in the deposition procedure could improve the repeatability and reproducibility of the process. Another potential improvement could be the incorporation of an automated system (robotic arm, 3D CNC router or similar concepts), in order to minimize the human interaction in the process. However, the automation of the process has pros and cons, that will require a benefit-cost analysis in order to evaluate if it is still a suitable deposition method or another process should be considered.

As mentioned before, the high relative uncertainty of the quantified thickness is a limitation, in particular, the contribution from the accuracy of the thickness-meter. Consequently, it requires further improvements in the thickness quantification. These improvements could be achieved using a more accurate device using the same measurement principle or by the use of another thickness measurement method [14] that can provide a higher accuracy, conducting to a reduction in the uncertainty of the measurements. Additionally, the quantification of the thickness dispersion effect on the decay time estimation (τ) it will be beneficial, considering that this could provide an estimation of the required level of accuracy in terms of the thickness. This quantification can be performed by estimating the decay time of several different phosphor layers and quantifying if the differences are significant.

[14] Optical techniques that determine the thickness of the coating or layer by measuring the interaction with light. No contact method that reduces potential phosphor layer deformation during the measurement procedure.

5.7 Phosphor Layer Sensor Fabrication Summary

In this chapter, based on a literature review and experimental work, it has been presented and discussed a method to fabricate a phosphor layer sensor for a Thermometry system. The implemented deposition method is the adhesive binder coatings, applied with an air-brush. Moreover, this method provides flexibility in terms of the application on-site on almost any substrate surface and the required equipment does not represent a high-cost investment.

The fabrication process should be able to provide a phosphor layer that fulfils several requirements for the suitable application of a phosphor Thermometry technique. In this case, it is estimated that with the airbrush deposition method, the most challenging requirement, is to fabricate a reproducible layer with a thickness in which the thermal intrusiveness is negligible($\sim$ 20 [μm]).
Consequently, in order to quantify the thickness of the prepared phosphor layer, thickness measurements have been performed by a contact sensor (Thickness-meter). The sensor measures the thickness of a non-conductive layer by using the working principle of eddy currents on a conductive and non-magnetic substrate.

The quantification of the phosphor layer thickness has been performed on several different phosphor samples. In the preparation of the samples, three operators have been involved. Moreover, the different operators have achieved a set of layers with a thickness mean value that do not exceed 27.5 [μm].

However, the repeatability and reproducibility of the manufactured phosphor layers still require further improvements. The incorporation of a manometer in the compressor set-up could be beneficial, by providing a quantification of the delivered air pressure during the process, that could help to improve the consistency of the deposited phosphor layer.

Furthermore, the estimated uncertainty of the thickness quantification process is relatively high (values up to 14.1[%]), where the major contribution is estimated to be the accuracy of the thickness meter.
The uncertainty could be improved by using a more accurate device that works under the same measurement principle or by the utilization of an optical thickness measurement method that can provide a higher accuracy without introducing potential error due to the deformation of the phosphor layer under test. Nevertheless, the implemented thickness quantification method, it is still considered suitable compared to the method in which the thickness of the phosphor layer it is estimated by comparing the weight of coated and uncoated substrate.

6

Phosphor Thermometry Experiments

The objective of the experimental work as mentioned in the introduction is to estimate the mean decay time (τ_μ) of the emitted luminescence from the phosphor layer sensor after the excitation light source has been switched-off(after-glow). The experiments have been carried out on two different phosphor layer sensors ($\sim thk < 25[\mu m]$) exposed to a temperature range from approximately room temperature up to 250 [°C] (substrate material: stainless steel).
During the thermal exposure cycles, the intensity of the emitted luminescence from the phosphor layer sensor is detected by the photo-sensor. The signal is acquired and storage by the oscilloscope in order to estimate the decay time(τ_μ) in a post-processing step.
It is expected that the results could contribute to a preliminary characterization of the Phosphor Thermometry System in order to estimate the surface temperature of an object by means of the luminescence decay time.

6.1 Experiments Overview

Layer	**Test**	**Cycle**	**ΔT [°C]**	**Meas. Pt #**	**t[hr]**	**thk [μm]**	**Range [°C]**
# **1**	1	Up	∼ 20	11	8	<25	23-250
		Down	∼ 20	11	8		
	2	Up	∼ 50	6	4.5		
		Down	∼ 50	6	4.5		
# **2**	1	Up	∼ 50	6	4.5		
		Down	∼ 50	6	4.5		
	2	Up	∼ 50	6	4.5		
		Down	∼ 50	6	4.5		

Table 6.1: Experiments Plan Table

The table 6.1 provides an overview of the entire "Phosphor Thermometry" experimental work that has been performed during this project. The number of points (Meas.Pt#) reported in the above table corresponds to a thermal cycle exposure.
This means that for example, 11 measurements points with a "Cycle Up"(heating phase) and a ΔT of 20 [°C] correspond to a thermal cycle exposure in which the temperature increase from 23 [°C] with an increment of 20 [°C] up to 250 [°C] and in the other way around for a "Cycle Down"(cooling phase). The intention behind this cyclic experimental procedure is to determine the presence of thermal history effects and also quantify the repeatability[1]/reproducibility[2] of the implemented measurement process.

[1] Results comparison within a phosphor layer
[2] Results comparison between phosphor layers

6.2 Experimental Set-Up

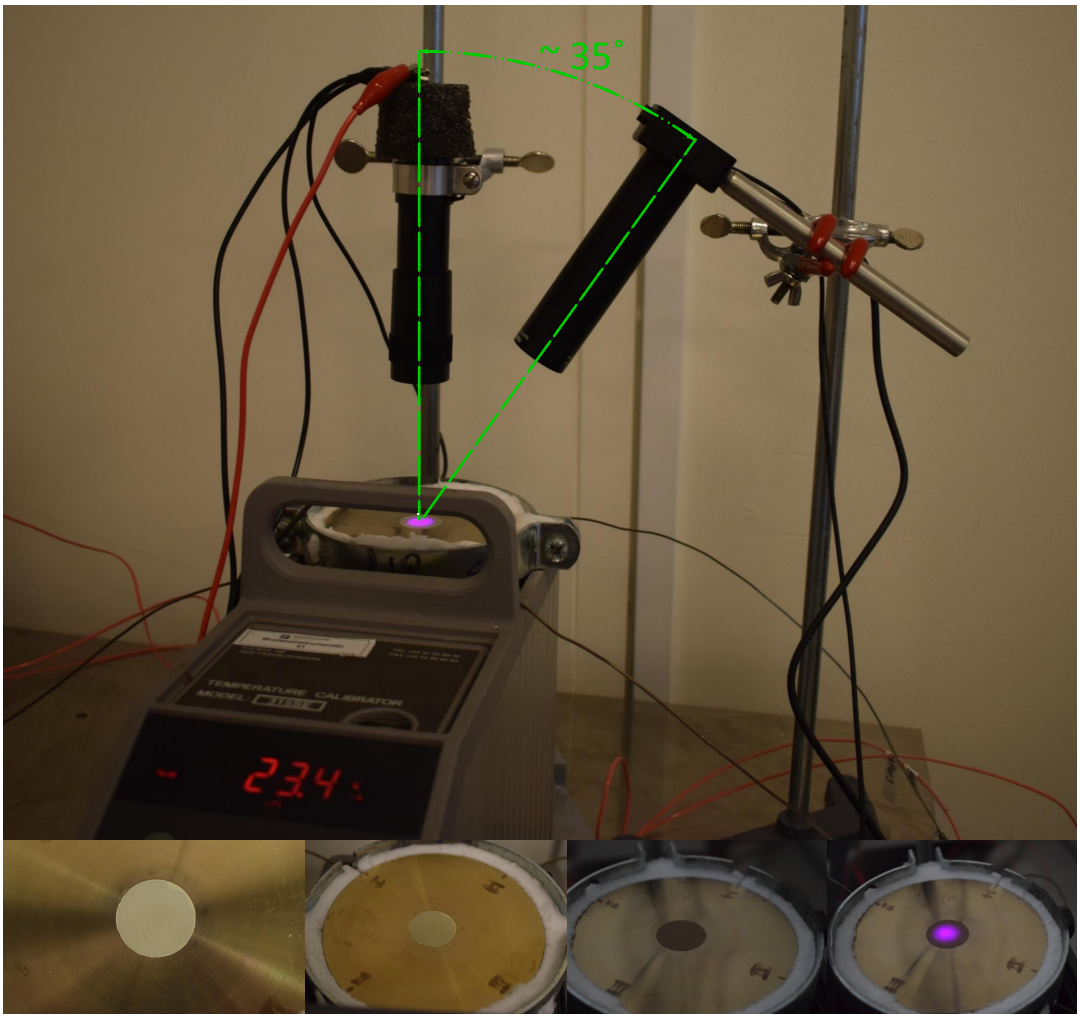

Figure 6.1: Developed Phosphor Thermometry System
Set-Up and the observed effect on the thermal sensing layer (change in color on the phosphor layer sensor due to thermal exposure)

In figure 6.1 the developed Phosphor Thermometry System is shown, with all the main components that has been described in section "Development of a Phosphor Thermometry System". It is required to mention that due to some technical issues and the lack of a cooling system[3] of the surface temperature assembly (see section "Surface Temperature Reference System") some minor changes in the heating element have been done. However, those changes do not affect the traceability of the measurement due to the fact that the substrate and thermocouples remain the same.
As a preliminary approach, it is observed a change in color on the phosphor layer sensor after the first the thermal exposure. This raises some questions about the effect on the emitted luminescence properties (intensity and decay time), that will be discussed in further sections.

[3] The cooling system feature, is beneficial in terms of time saving of the experiments, especially in the thermal cycling test

6.3 Estimated Decay Time Results Analysis (Layer#1)

The Layer#1 is deposited on top of a stainless steel substrate with an estimated thickness < 25 [μm]. The phosphor layer sensor (Layer#1) has been exposed to a temperature range from 23 [°C] up to 250 [°C] in a cyclic manner as mentioned in the experiments overview.

6.3.1 Decay Time at Different Temperatures

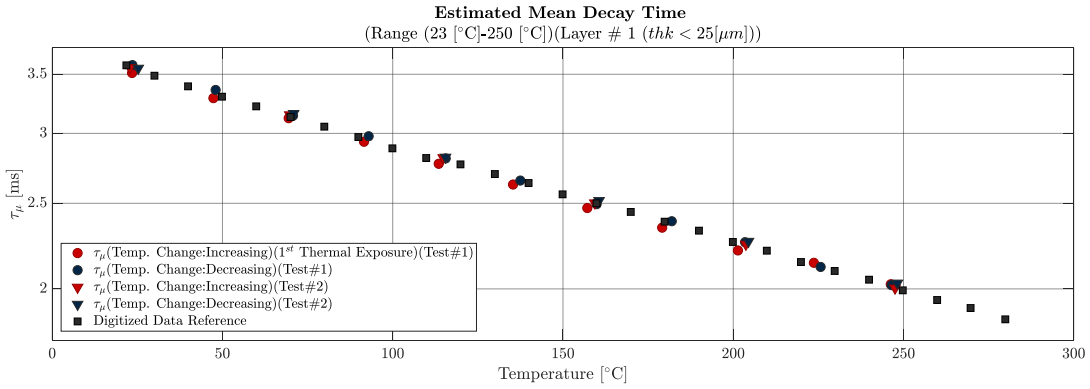

Figure 6.2: Mean Decay Time(Layer#1)

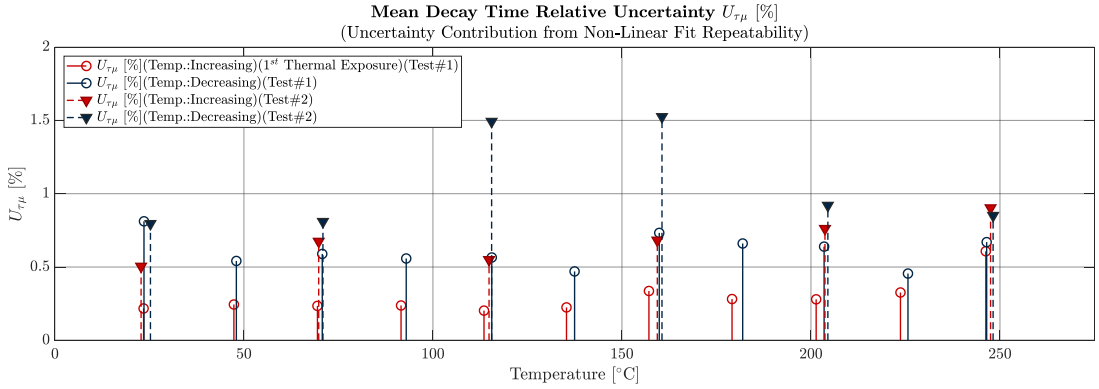

Figure 6.3: Mean Decay Time Associated Uncertainty (Layer#1)

The results of the decay time and the associated uncertainty are shown in figure 6.2 and figure 6.3 respectively. It is observed that the decay time results exhibit an apparent linear relationship with respect to the temperature similar to the digitized data reference(see figure 6.2). However, the first thermal exposure shows a slight deviation (below reference) compared to the other measurements. The associated uncertainty (figure 6.3) due to the repeatability revels a clear increment after the first thermal exposure of the phosphor layer sensor. It is estimated that the nature of these differences with respect to the first thermal exposure, could be due to an apparent irreversible change in the phosphor layer sensor due to thermal exposure. These observations will be discussed again, but in the context that investigates the changes in the initial intensity and the direct effect on the Signal to Noise Ratio. It is assumed that this different approach could lead to a potentially reasonable explanation of the nature of this behaviour.

6.3.2 Decay Time Comparison with to Respect Digitized Data

In figures 6.4 and 6.5 are shown, the comparison and relative difference between the estimated decay time (τ_μ) with respect to the digitized data reference. In order to compare the results a simple linear regression of the transformed [4] digitized data has been obtained. The main objective of this comparison is to obtain a quantification of the relative difference between the experiments and the digitized data. However, it is relevant to mention that the uncertainty of the digitized data it is an unknown. Consequently, caution should be taken at the time to make any inference about the differences that could lead to a biased interpretation.

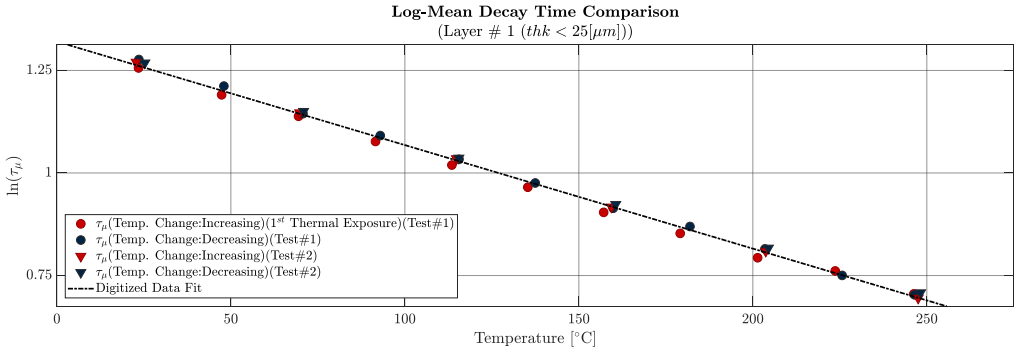

Figure 6.4: Layer#1 Decay Time Comparison*(with respect to digitized data.)*

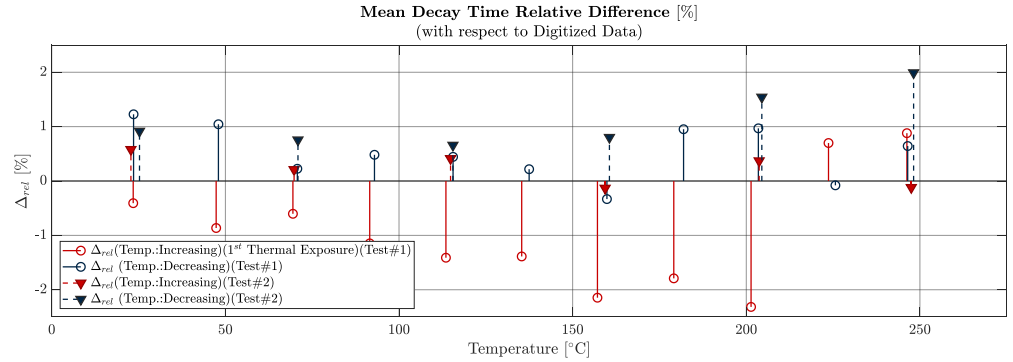

Figure 6.5: Layer#1 Decay Time Relative Difference*(with respect to digitized data)*

The results from the experiments as well as the digitized data shown a similar linear relationship with respect to the temperature. Furthermore, it is observed that the relative difference of the first thermal exposure of the phosphor layer sensor exhibits a different trend with respect to the subsequent tests. This is noticeable until $\sim 200[°C]$, apparently something happens at this temperature. In this case, an interesting study could be done by a Scanning Electron Microscopy in order to observe if there is any change in the micro-structure of the phosphor layer sensor. As a preliminary conclusion that can drawn from this comparison is that, it is required to keep track of the decay time behaviour in the vicinity of $200[°C]$ in order to evaluate if it is a consistence pattern. This could be done by approaching from another perceptive and look at the initial intensity and the SNR (Signal to Noise Ratio) as was mentioned in the previous discussion about the associated uncertainty.

[4] The natural logarithm transformation has shown a better fit, than without transformation.

6.3.3 Initial Emitted Light Intensity and SNR

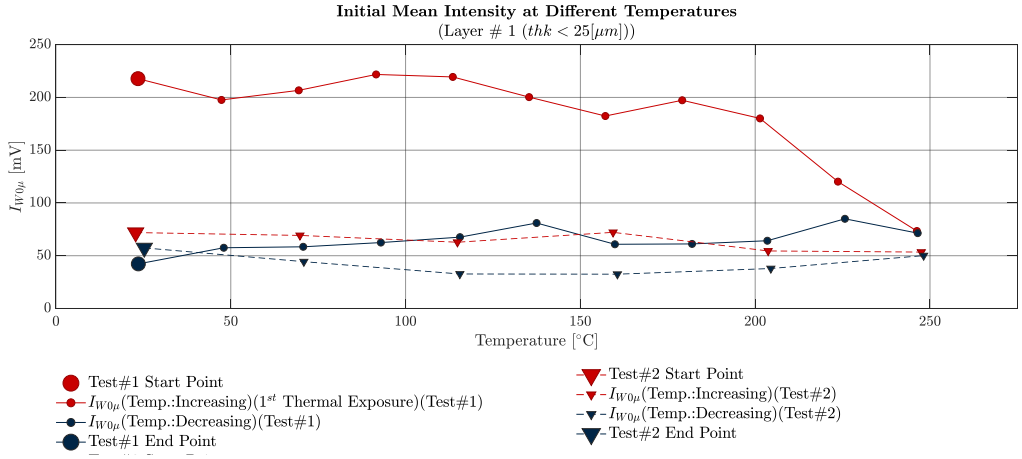

Figure 6.6: Layer#1 Initial Emitted Light Intensity

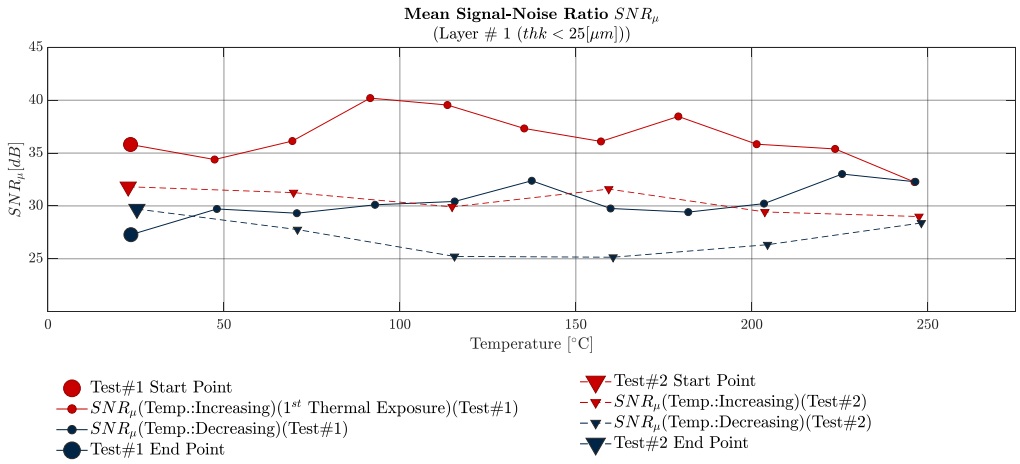

Figure 6.7: Layer#1 Mean SNR (Signal to Noise Ratio)

In figure 6.6 is shown the initial mean intensity of each different temperatures. It is observed that the first thermal exposure exhibit a clear much higher initial intensity. Additionally, the mean SNR that it is shown in figure 6.7 presents similar trend but not as pronounced as the initial intensity.
In the associated uncertainty (due to the repeatability from curve fit) of the experiments (from the previous section), it has been noticed an increment after the first thermal exposure of the coating layer. A potential explanation of the increment in uncertainty could be that the SNR of the experiments has been reduced and contribute directly in the curve fit due to the noisier data. In terms of the point ($\sim 200[°C]$) that was found of interest, a plausible explanation could be drawn from the figure (6.6) in which it is observed that at this temperature the initial intensity decrease noticeably.

6.4 Estimated Decay Time Results Analysis (Layer#2)

The Layer#2 has been prepared by applying the same methodology as for the Layer#1. The phosphor layer sensor (Layer#2) has been exposed to a temperature range from 23 [°C] up to 250 [°C] in a cyclic manner. However, due to the time consuming of the experiments, the number of measurement points has been reduced to almost half of it (6 points, with a Δ T $\sim$ 20 [°C]). Furthermore, it is considered that the number of measurement points has a relevance form the point of view of the temporal thermal exposure. This means that at the time to infer any potential conclusion, this parameter should be taken into account, in particular when the Layer#1 and Layer#2 will be compared.

6.4.1 Decay Time at Different Temperatures

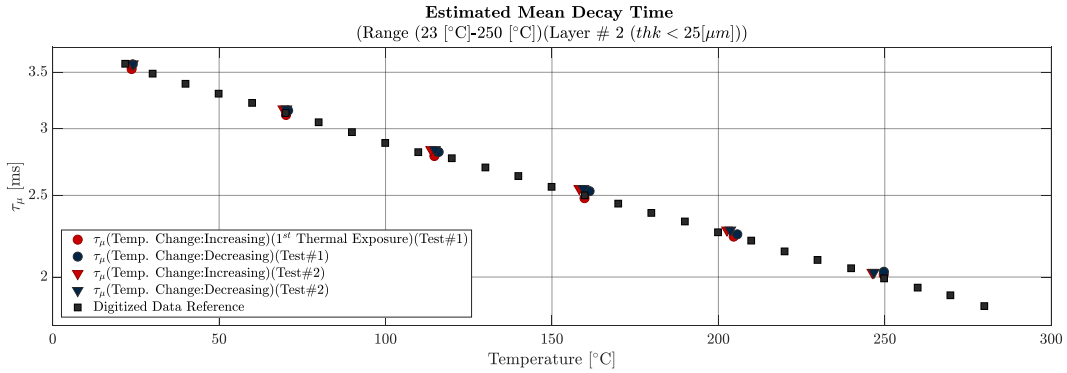

Figure 6.8: Mean Decay Time (Layer#2)

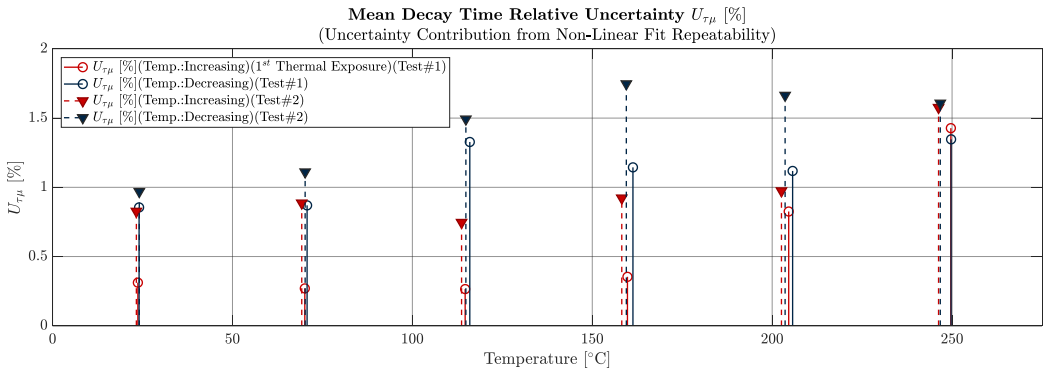

Figure 6.9: Mean Decay Time Associated Uncertainty (Layer#2)

The results of the decay time and the associated uncertainty are shown in figure 6.8 and figure 6.9 respectively. It is observed similar linear relationship with respect to the temperature as the Layer#1(see figure 6.8). However, the first thermal exposure has not shown noticeable deviation as in the Layer#1. The associated uncertainty (figure 6.9) due to the repeatability revels a clear increment after the first thermal exposure of the phosphor layer sensor similar to the other layer(Layer#1). However, in the Layer#1 during the first thermal exposure the uncertainty values remain relatively stable below 0.5 %, while for the Layer#2 it is noticed a clear increment in the vicinity of 200 [°C]. These observations will be discussed again, but in the context intensity and SNR.

6.4.2 Decay Time Comparison with Respect to Digitized Data

In figures 6.10 and 6.11 are shown , the comparison and relative difference between the estimated decay time (τ_μ) with respect to the digitized data reference (performed on the same type of phosphor) similarly as in the Layer#1.

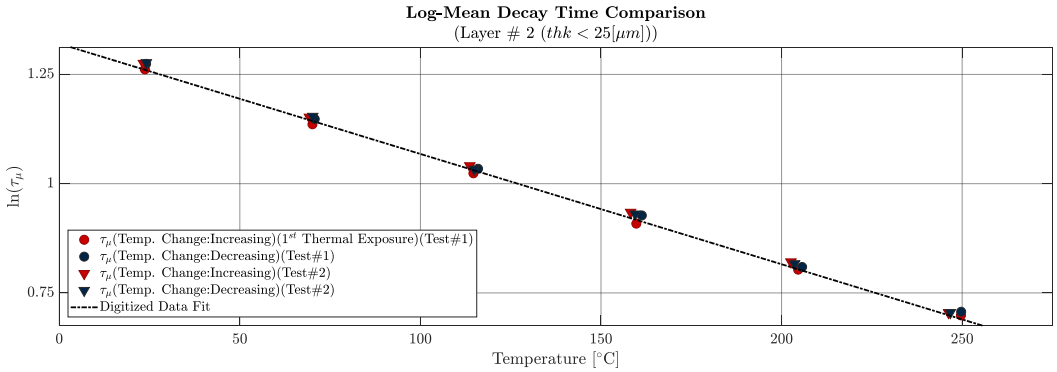

Figure 6.10: Layer#2 Decay Time Comparison *(with respect to digitized data.)*

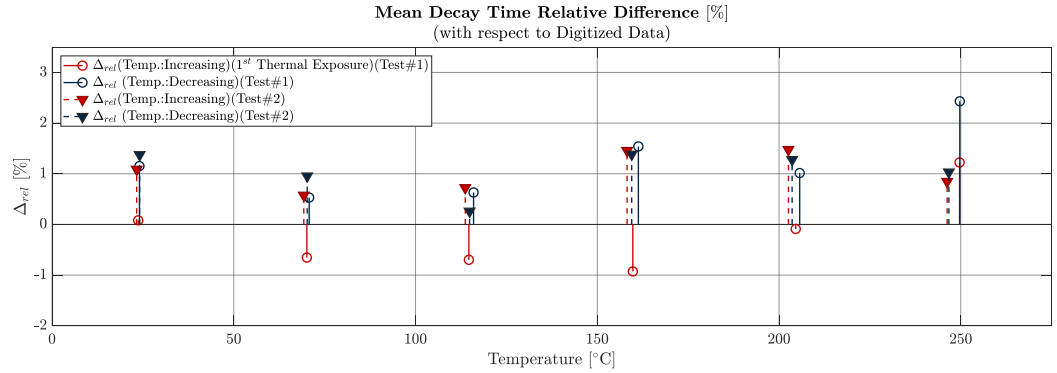

Figure 6.11: Layer#2 Decay Time Relative Difference
(with respect to digitized data.)

The results from the experiments as well as the digitized data shown a similar linear relationship with respect to the temperature. Furthermore, it is observed that the relative difference of the first thermal exposure of the phosphor layer sensor exhibits a different trend with respect to the subsequent tests. This is noticeable until $\sim 160[°C]$, apparently, something happens at this temperature (similar to Layer#1).
These observations are very similar as in the Layer#1 except that the drift shifting happens earlier. It is necessary to remember that in the Layer#1 the first thermal exposure has been done in smaller temperature increments, that increase the temporal thermal exposure, compared to the Layer#2, this could be plausible reason for this earlier transition. However, in order to estimate a clear transition temperature point, multiple experiments will be required.

6.4.3 Initial Emitted Light Intensity and SNR

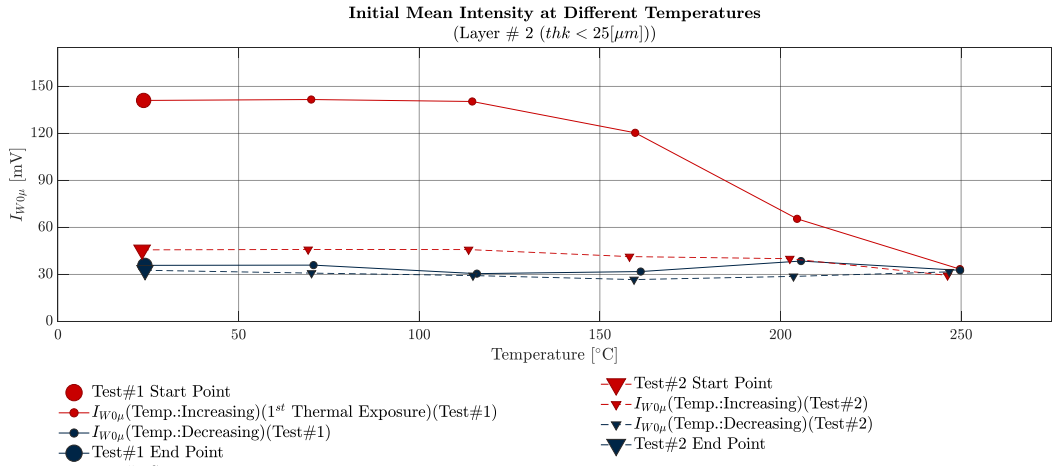

Figure 6.12: Layer#2 Initial Emitted Light Intensity

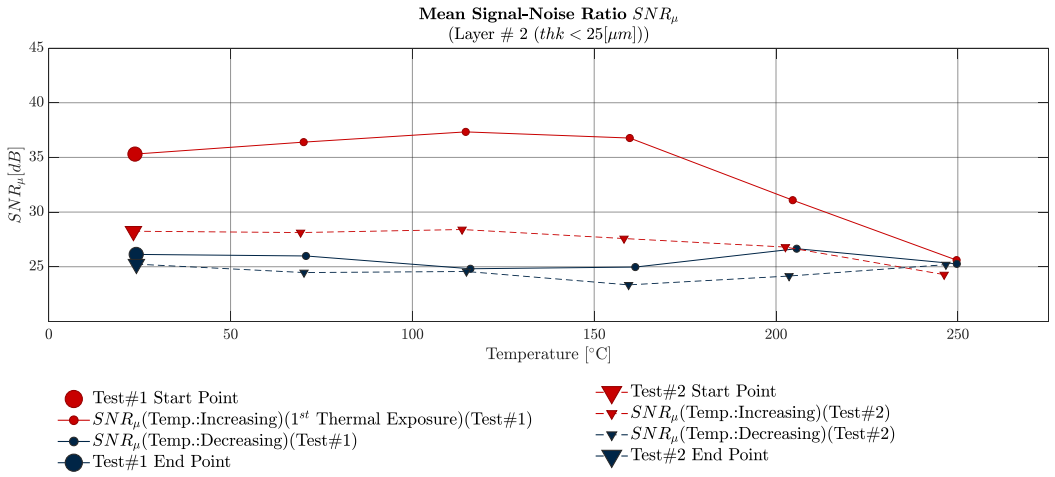

Figure 6.13: Layer#2 Mean SNR(Signal to Noise Ratio)

In figure 6.12 is shown the initial mean of each different temperatures. It is observed that the first thermal exposure exhibit a clear much higher initial intensity until approximately 160 [°C] where start to decreasing.
The mean SNR remain in a approximately similar range as in the Layer#1, between 25 to 40 [dB] (see figure 6.13). In the associated uncertainty the highest value corresponds to the lowest value of SNR, that could pointed out a relation between the two parameters since happens on both phosphor layer sensors.

6.5 Statistical Comparison Methods

In this section, is described the statistical methods that will be implemented in further sections in order to compare the different results. The comparisons is aiming to determine if there is an statistically significant difference between linear regressions coefficients estimated from the decay time at different temperatures cycle(heating and cooling phase) and phosphor layers. The implemented methods are the t-test(Welch's)([24])[5] and the Normalized Error(E_n) comparison [25].

6.5.1 Performed Statistical t-test (Welch's t-test)

Assumptions

The assumptions in the t-test(Welch's) are that the two compared values (slope or intercept in this case) comes from a population that are normal distributed and with unequal variances($\sigma_1^2 \neq \sigma_1^2$).

Calculations

Statistic t formula:

$$t = \frac{\overline{X}_1 - \overline{X}_2}{\sqrt{\frac{s_1^2}{N_1} + \frac{s_2^2}{N_2}}} \tag{6.1}$$

Degree of freedom (ν)(Welch–Satterthwaite equation):

$$\nu \approx \frac{\left(\frac{s_1^2}{N_1} + \frac{s_2^2}{N_2}\right)^2}{\frac{s_1^4}{N_1^2\nu_1} + \frac{s_2^4}{N_2^2\nu_2}} \tag{6.2}$$

Confidence Interval of the Difference:

$$(\overline{X}_1 - \overline{X}_2) - t_{\alpha/2,\nu} \cdot \sqrt{\frac{s_1^2}{N_1} + \frac{s_2^2}{N_2}} \leq (\mu_1 - \mu_2) \leq (\overline{X}_1 - \overline{X}_2) + t_{\alpha/2,\nu} \cdot \sqrt{\frac{s_1^2}{N_1} + \frac{s_2^2}{N_2}} \tag{6.3}$$

Where:

- i Index 1 or 2.
- X_i Values under test, in this case could m(slope) or b(intercept).
- N_i Sample size from where the values under test has been draw.
- ν Degree of freedom(DOF). If ν is not an integer, should be round down to the nearest integer.
- s_i Standard deviation of values under test.
- $\nu_i = N_i - 1$ DOF associated with the corresponding variance.
- α Significance level.
- μ_i Population mean value for the corresponding values under test.

[5] Recommended in [26] instead of the t-test due to the robustness of the method since in the Student t-test if the equal variance assumption fail, alters the Type I Error (Rejecting the null hypothesis H_0 when it is true).

The t and the ν values are computed and used to calculate the P-Values[6] from a t-distribution (using two-tailed test), the significance level ($\alpha = 0.005$) is set to 5 %. The P-Values are reported together with the 95 % confidence interval(CI) of the population difference, for example Δ_m(difference in slope) or Δ_b(difference in intercept). The rejection criteria of the null hypothesis (for example $H_0 : m_1 - m_2 = 0$) it is when the P-Values are smaller than α. This means that there is strong evidence against the null hypothesis (H_0). However, since the P-Values are reported with the 95 % CI, it also possible to visualize the rejection or failing of rejecting the H_0 by taking a look of the 95 % CI . If the zero it is included in the interval there is not enough evidence to reject the null hypothesis. In contrary, if it is not included the $H_0 : m_1 - m_2 = 0$, it is rejected at 5 % significance level.

6.5.2 Normalized Error (E_n) Estimation

The estimation of the Normalized Error (E_n) is a procedure that it is implemented in inter-laboratory measurements comparison (see equation 6.4). In this case the uncertainty component (U_i) it is estimated from the confidence interval of the coefficients (m and b respectively) obtained from the linear regression.
Normalized Error (E_n) Formula:

$$E_n = \left| \frac{((\overline{X}_1 - \overline{X}_2)}{\sqrt{(U_1^2 + U_2^2)}} \right| \tag{6.4}$$

This is a pass or not pass a test, in which the rejection it is stated as $E_n < 1$ pass. This means that if $E_n < 1$ the difference between the two compared values is smaller than the combined uncertainty of the values under test. Furthermore, in the results tables in the next sections the 95 % CI it is also reported as in the t-test in order to have a clear comparison between the two different methods.

6.5.3 Decay Time Regressions Comparison Overview

The analysis that is presented in further sections is divided in three main comparisons by implementing the regressions comparison methods, that has been described before, on the estimated decay time linear regression:

Analysis of Phosphor Layer Irreversible Change: In this first analysis, is expected that the statistical comparison will provide extra information about the observed change in the emitted light intensity after the first thermal exposure. The objective, is to determine if there is a significant difference in the decay time of the emitted luminescence during the first thermal cycle (between heating (ΔT Increasing) and cooling (ΔT Deceasing) phase).

Repeatability Analysis (Thermal History Effect): This analysis is oriented to investigate the occurrence of the thermal history effect by comparing results (within the same layer) between heating (ΔT Increasing) and cooling (ΔT Deceasing) phase) after the first thermal cycle.

Reproducibility Analysis: The reproducibility analysis involves the comparison of the linear regression between the two different layers in heating (ΔT Increasing) phase after the first thermal cycle.

[6] P-Values can be interpreted as probability evidences about the null hypothesis. Where the value of 1 is the maximum, meaning that there is weak evidences against the null hypothesis.

6.6 Analysis of Phosphor Layer Irreversible Change

6.6.1 Layer#1 (1^{st}Thermal Exposure)

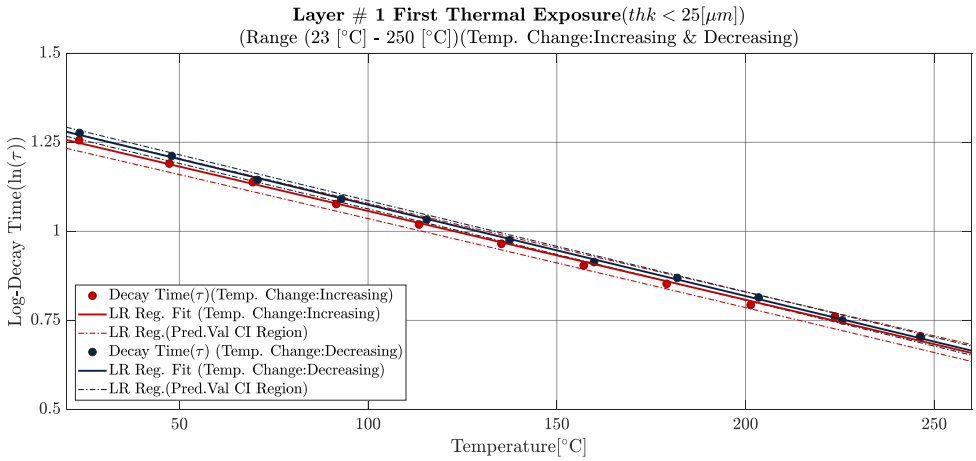

Figure 6.14: Layer#1 Irreversible Change Thermal Effect Analysis

	Simple Linear Regression Results	
Δ T	**m** [$°C^{-1}$] **CI (95 %)**	**b CI (95 %)**
Incr.	m_1=-0.0025 ± 0.0001	b_1=1.307 ± 0.013
Decr.	m_2=-0.0026 ± 0.0001	b_2=1.331 ± 0.007

	Statistical Study Results		
	(Difference in Slope Comparison)		
	$H_0 : \Delta_m = 0$	Δ_m **CI (95 %)**	**Rejected ?**
P_{Value}	0.0001	$-0.0001 \leq \Delta_m \leq -0.00004$	Yes
E_n	0.69	$-0.0002 \leq \Delta_m \leq 0.00003$	No
	(Difference in Intercept Comparison)		
	$H_0 : \Delta_b = 0$	Δ_b **CI (95 %)**	**Rejected ?**
P_{Value}	4.1e-09	$-0.03 \leq \Delta_b \leq -0.02$	Yes
E_n	1.6	$0.01 \leq \Delta_b \leq 0.04$	Yes

Table 6.2: Layer#1 Irreversible Change Thermal Effect Analysis

In figure 6.14, it is shown the 1^{st} thermal exposure cycle to which the Layer#1 has been exposed. The t-test (see table 6.2), shows clear agreement in the rejection of the null hypothesis for the differences between the regression coefficients (zero it is not included in the CI of both tests). On the other hand, the results from the normalized error show a disagreement in terms of the rejection of the different coefficients. It is interesting to notice that the E_n fails in the intercept [7], while passing the test for the slope. This observation pointed out the existence of a vertical shift between regressions.

[7] This constant coefficient, in this case, do not have any meaningful physical implications more than reflecting a vertical shifting. This due to the fact that the behaviour of the sensing phosphor it is unknown at this temperature

6.6.2 Layer#2 (1^{st}Thermal Exposure)

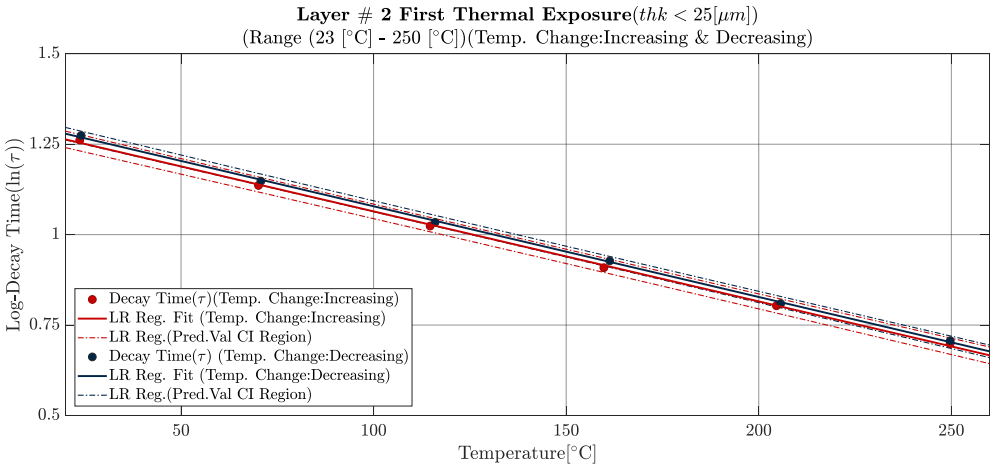

Figure 6.15: Layer#2 Irreversible Change Thermal Effect Analysis

	Simple Linear Regression Results	
Δ T	**m [$°C^{-1}$] CI (95 %)**	**b CI (95 %)**
Incr.	m_1=-0.0025 ± 0.0001	b_1=1.313 ± 0.015
Decr.	m_2=-0.0025 ± 0.0001	b_2=1.329 ± 0.012

	Statistical Study Results		
	(Difference in Slope Comparison)		
	$H_0 : \Delta_m = 0$	Δ_m **CI (95 %)**	**Rejected ?**
P_{Value}	0.3	$-0.00006 \leq \Delta_m \leq 0.00002$	No
E_n	0.16	$-0.0001 \leq \Delta_m \leq 0.0001$	No
	(Difference in Intercept Comparison)		
	$H_0 : \Delta_b = 0$	Δ_b **CI (95 %)**	**Rejected ?**
P_{Value}	0.00029	$-0.02 \leq \Delta_b \leq -0.01$	Yes
E_n	0.84	$-0.04 \leq \Delta_b \leq 0.003$	No

Table 6.3: Layer#2 Irreversible Change Thermal Effect Analysis

The results from the estimate decay time and the linear regression coefficients are shown in figure 6.15 and table 6.3 respectively. In this case, the normalized error agrees in that the differences between both regressions are not statistically significant. However, the t-test agrees only in that the slope difference are not significant.
The differences between the two regression in not conclusive in terms of statistical significance. However, this difference could be introduced as the uncertainty contribution of the Phosphor Thermometry System in the calibration curve.

6.7 Repeatability Analysis (Thermal History Effect)

6.7.1 Layer#1 (Thermal History Effect)

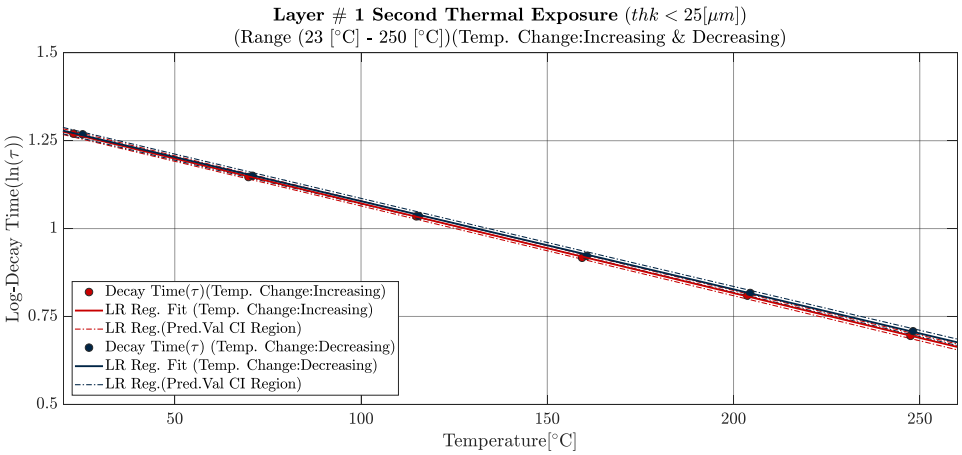

Figure 6.16: Layer#1 Thermal History Effect Analysis *(Graphical Representation)*

	Simple Linear Regression Results	
Δ T	**m** [$°C^{-1}$] **CI (95 %)**	**b CI (95 %)**
Incr.	m_1=-0.0026 ± 0.00004	b_1=1.327 ± 0.006
Decr.	m_2=-0.0025 ± 0.00004	b_2=1.329 ± 0.006

	Statistical Study Results		
	(Difference in Slope Comparison)		
	$H_0 : \Delta_m = 0$	Δ_m **CI (95 %)**	**Rejected ?**
P_{Value}	0.00026	$0.00003 \leq \Delta_m \leq 0.00006$	Yes
E_n	0.81	$-0.00001 \leq \Delta_m \leq 0.0001$	No
	(Difference in Intercept Comparison)		
	$H_0 : \Delta_b = 0$	Δ_b **CI (95 %)**	**Rejected ?**
P_{Value}	0.12	$-0.005 \leq \Delta_b \leq 0.001$	No
E_n	0.25	$-0.01 \leq \Delta_b \leq 0.01$	No

Table 6.4: Layer#1 Thermal History Effect Analysis *(Regressions Comparison Heating (ΔT Increasing) vs Cooling (ΔT Deceasing) phase)*

In this case, for the Layer#1, the results (see table 6.4) of the normalized error are in agreement that the differences in the two regression coefficients are not significant. It is not the case for the t-test. However, this can be compensated by the introduction of a repeatability component in the uncertainty budget of the Phosphor Thermometry System. Additionally, it is observed that the analysis of the normalized errors seems to be a more flexible method if it is considered the confidence interval.

6.7.2 Layer#2 (Thermal History Effect)

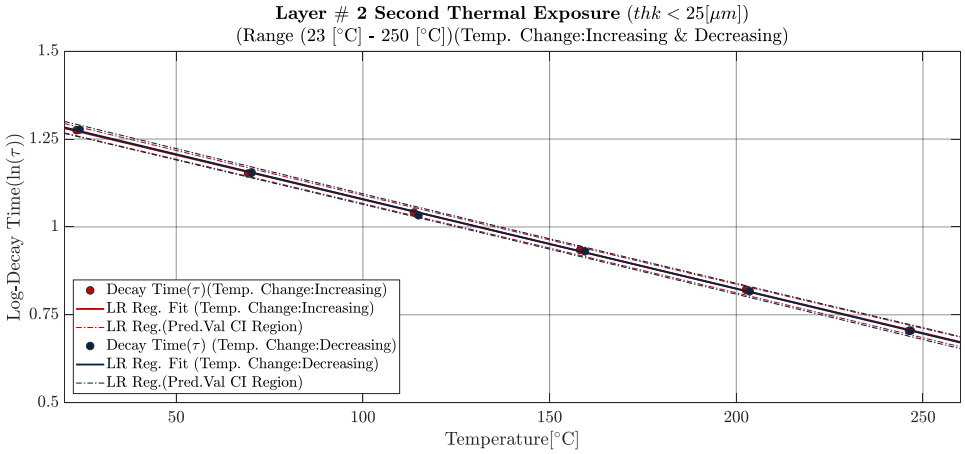

Figure 6.17: Layer#2 Thermal History Effect Analysis
(Graphical Representation)

	Simple Linear Regression Results	
Δ T	**m [$°C^{-1}$] CI (95 %)**	**b CI (95 %)**
Incr.	m_1=-0.0025 ± 0.00005	b_1=1.3317 ± 0.009
Decr.	m_2=-0.0026 ± 0.00007	b_2=1.3343 ± 0.012

	Statistical Study Results		
	(Difference in Slope Comparison)		
	$H_0 : \Delta_m = 0$	Δ_m **CI (95 %)**	**Rejected ?**
P_{Value}	0.26	$-0.0001 \leq \Delta_m \leq 0.00001$	No
E_n	0.18	$-0.0001 \leq \Delta_m \leq 0.0001$	No
	(Difference in Intercept Comparison)		
	$H_0 : \Delta_b = 0$	Δ_b **CI (95 %)**	**Rejected ?**
P_{Value}	0.25	$-0.007 \leq \Delta_b \leq 0.002$	No
E_n	0.18	$-0.02 \leq \Delta_b \leq 0.01$	No

Table 6.5: Layer#2 Thermal History Effect Analysis
(Regressions Comparison Heating (ΔT Increasing) vs Cooling (ΔT Deceasing) phase)

The results of the statistical comparison for the Layer#2 are shown in table 6.5. The two different methods, in this case, are in complete agreement on the absence of a significant difference between the two different regressions. Therefore, it possible to assume that there is not any sign of a potential thermal history effect in the estimated decay time at different temperatures from the heating and the cooling phase.

6.8 Reproducibility Analysis

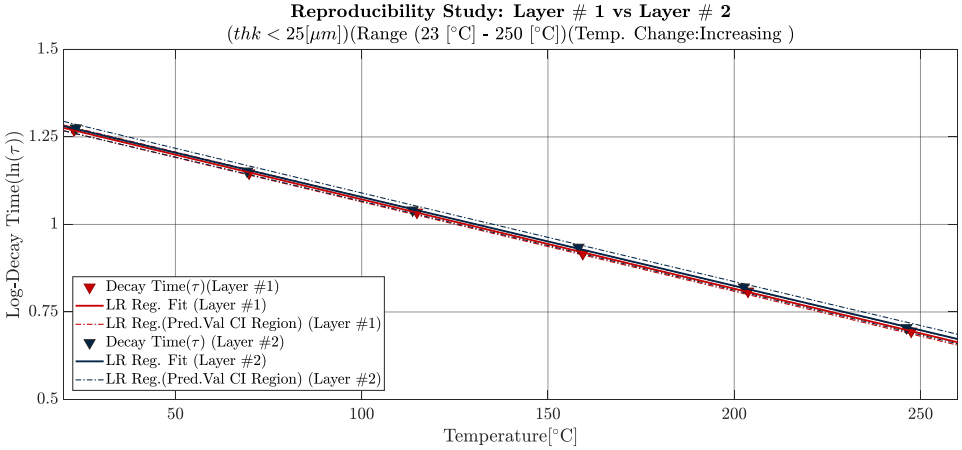

Figure 6.18: Reproducibility Analysis (Layer#1 vs Layer#2)

	Simple Linear Regression Results	
Δ T	**m [$°C^{-1}$] CI (95 %)**	**b CI (95 %)**
Incr.	m_1=-0.0026 ± 0.00004	b_1=1.3268 ± 0.006
Incr.	m_2=-0.0025 ± 0.00006	b_2=1.3317 ± 0.009

	Statistical Study Results		
	(Difference in Slope Comparison)		
	$H_0 : \Delta_m = 0$	Δ_m **CI (95 %)**	**Rejected ?**
P_{Value}	0.13	$-0.00001 \leq \Delta_m \leq 0.00004$	No
E_n	0.25	$-0.0001 \leq \Delta_m \leq 0.0001$	No
	(Difference in Intercept Comparison)		
	$H_0 : \Delta_b = 0$	Δ_b **CI (95 %)**	**Rejected ?**
P_{Value}	0.013	$-0.0085 \leq \Delta_b \leq -0.0013$	Yes
E_n	0.47	$-0.02 \leq \Delta_b \leq 0.01$	No

Table 6.6: Reproducibility Analysis*(Regression Comparison Layer#1 vs Layer#2) (both layers in Heating (Δ T Increasing) phase)*

In figure 6.18 is shown the graphical presentation of the log-decay time data in function of temperature with the respective linear regressions for the Layer#1 and Layer#2 (both in heating phase.). The results of the t-test and the normalized error are shown in table 6.6. The examination of the normalized errors results for the slope(m) and the intercepts(b), shows that they are in agreement. This means that the differences between the estimated decay time between the two experiments are not statistically significant. In other words, the experiment has been reproduced.
In contrary, the results from the t-test that has been shown to be more restrictive, reject the null hypotheses of the intercept coefficient.

6.9 Phosphor Thermometry Experiments Summary

The Layer#1 and Layer#2 have been prepared on top of a stainless steel substrate with an estimated thickness < 25 [μm]. The phosphor layer sensors has been exposed to a temperature range from 23 [°C] up to 250 [°C] in a cyclic manner("Cycle Up"(heating phase) and "Cycle Down"(cooling phase)). The experimental results can summarized as follow:

Estimated Decay Time Results Analysis (Layer#1 & #2)

It is observed that the decay time results in both phosphor sensor layers exhibit a linear relationship with respect to the temperature, similar to the digitized data reference.
The associated uncertainty due to the repeatability (curve fit) in the estimated decay time revels a clear increment after the first thermal exposure of the phosphor layer sensors. The plausible explanation for this uncertainty increment could be that, after the thermal exposure, the emitted luminescence intensity has shown a significant reduction that consequently affect the SNR (signal-noise ratio).
The reduction in the emitted luminescence intensity could be due to a micro structure change in the phosphor layer sensors that affect the luminescence properties. Furthermore, a change in the original color of the phosphor layers is observed after the first thermal exposure.
In contrary, after the first thermal exposure of the phosphor layer sensors, the consecutive measurements do not show a significant reduction in the emitted intensity, but neither a recover to the original state, that could conduct to assume that is a permanent change in the structure of the phosphor layer.

Analysis of Phosphor Layer Irreversible Change

The preliminary conclusion from the results, it is that the Layer#1 has been shown a change in the decay time estimated from the emitted light at different temperatures after the first thermal exposure. In terms of the irreversibility factor, the initial emitted light intensity of the Layer#1 has been shown a clear reduction after the first thermal exposure. Additionally, this amplitude reduction remains at a lower level and did not show any signal of potential recovery to an initial amplitude state. Consequently, this can be interpreted as a permanent change due to the thermal exposure.

In the case of the Layer#2, the results are inconclusive due to the disagreement between the two different methods[8]. However, the difference in the estimated decay time could be introduced as an uncertainty contribution to the Phosphor Thermometry System, in order to take into account this mismatch at the time to characterize a calibration curve. Another option in order to overcome this irreversible change in the luminescence could be to perform curing process before calibration or temperature measurements.

[8] Another factor that required to be taken into account is the resolution of the oscilloscope, considering the fact that the resolution is not optimum. Therefore, this could conduct to a biased inference about the results.

Repeatability Analysis (Thermal History Effect)

The results of the statistical comparison for the Layer#2, shows that the two different methods, in this case, are in complete agreement on the absence of a significant difference between the two different regressions. Therefore, there is not any sign of a potential thermal history effect in the estimated decay time at different temperatures from the heating and the cooling phase.

Reproducibility Analysis

The examination of the normalized errors results shows that they are in agreement. This means that the differences between the estimated decay time between the two experiments are not statistically significant(experiment has been reproduced). In contrary, the results of the t-test that has been shown to be more restrictive, reject the null hypotheses of the intercept coefficient.
Based on that, since there is not an agreement between methods, it is estimated that further experiments will be required in order to validate the performance of the Phosphor Thermometry System, as was expected from the beginning.

7
Discussion and Conclusion

7.1 Surface Temperature Reference System

The surface temperature reference system provides a traceable well-defined surface temperature of a substrate in order to perform a calibration of the phosphor Thermometry system. The substrate surface temperature has been estimated by performing several measurements at different temperature ranges, from room temperature up to 250 [°C]. The uncertainty contribution due to the implemented extrapolation method, is estimated to be in the order of 0.72% for a temperature of 246.3 [°C]. The resulting estimated uncertainty [1] does not include the contribution from the position of the thermocouples or other uncertainties in the measurement process. However, this component could be included in the final uncertainty budget as an extra contribution parameter[2].
The increment in the number of thermocouples from three to four has been shown a significant reduction in the uncertainty of the estimated substrate surface temperature(from 2.4% to 0.72%).

7.2 Development of a Phosphor Thermometry System

The developed set-up still required further improvements. It is considered that the excitation source and the corresponding controller system could be improved by using a standard mounted LED system with a controller. This will provide flexibility to the phosphor Thermometry system and the opportunity to investigate different methods, for example, phase shifting decay estimation.
There is a potential lack of the resolution (only 8 bit hardware) and data storage capacity (buffer memory size) in the oscilloscope that can have an influence in the estimated uncertainty of the curve fit. Consequently, it is suggested an upgrading of the oscilloscope. An automation of the entire process, that unify the Surface Temperature Reference System and the Phosphor Thermometry System, could be also a potential improvement that will speed-up the process.
In terms of the implemented decay time based method, the effect of the window evaluation length over the decay time has been quantified, showing potential induced error, in the order of -4.3 ± 1.1[°C](for $P_{I_{Norm}} = 5$[%] at 23.46 [°C]) and -7.6 ± 3.3[°C](for $P_{I_{Norm}} = 5$[%] at 246.3 [°C]). Therefore, as it pointed out in [23], special caution should be taken in terms of the evaluation window length in order to avoid the induction of a systematic errors in the decay time estimation(τ).

[1] Only the linear regression (curve-fit) uncertainty.
[2] by applying uncertainty propagation on the linear regression.

7.3 Phosphor Layer Sensor Fabrication

The implemented method to fabricate a phosphor layer sensor, involves the deposition by an airbrush of the phosphor material mixed with an adhesive binder. This method provides flexibility in terms of the application on-site on almost any substrate surface and the required equipment does not represent a high-cost investment. It is estimated that with the airbrush deposition method, the most challenging requirement, is to fabricate a reproducible layer with a thickness in which the thermal intrusiveness is negligible (~ 20 [μm]).

Consequently, the quantification of the phosphor layer thickness (by contact sensor) has been performed on several different phosphor samples. In the preparation of the samples, three operators have been involved. Moreover, the different operators have achieved a set of layers with a thickness mean value that do not exceed 27.5 [μm].

The estimated uncertainty of the thickness quantification process is relatively high (values up to 14.1[%]), where the major contribution is estimated to be the accuracy of the thickness meter. It is still required to perform several measurements in order to estimate if this variation in the thickness of the fabricated phosphor layer have any significant impact in the estimated decay time.
The uncertainty could be improved by using a more accurate device that works under the same measurement principle or by the utilization of an optical thickness measurement method that can provide a higher accuracy without introducing potential error due to the deformation of the phosphor layer under test.
However, the implemented thickness quantification method, it is still considered suitable compared to the method[3] in which the thickness of the phosphor layer it is estimated by comparing the weight of coated and uncoated substrate.

The fabrication process still requires further improvements in terms of the repeatability, reproducibility and also a reduction in the thickness of the phosphor layer sensor. The incorporation of a manometer in the compressor set-up could be beneficial, by providing a quantification of the delivered air pressure during the process, that could help to improve the consistency of the deposited phosphor layer.

[3] This method involves several instruments and an assumption about the density of the phosphor layer sensor.

7.4 Phosphor Thermometry Experiments

In the experiential work, the Layer#1 and Layer#2 has been prepared on top of a stainless steel substrate with an estimated thickness < 25 [μm]. The phosphor layer sensors have been exposed to a temperature range from 23 [°C] up to 250 [°C] in a cyclic manner("Cycle Up"(heating phase) and "Cycle Down"(cooling phase)).
It is observed that the decay time results in both phosphor sensor layers exhibit a linear relationship with respect to the temperature, similar to the digitized data reference.

The associated uncertainty due to the repeatability (curve fit) in the estimated decay time revels a clear increment after the first thermal exposure of the phosphor layer sensors. An explanation for this uncertainty increment could be that, after the thermal exposure, the emitted luminescence intensity has shown a significant reduction that consequently affect the SNR (signal-noise ratio).
The reduction in the emitted luminescence intensity could be due to a micro structure change in the phosphor layer sensors that affect the luminescence properties. Furthermore, a change in the original color of the phosphor layers is observed after the first thermal exposure.

In contrary, after the first thermal exposure of the phosphor layer sensors, the consecutive measurements do not show a significant reduction in the emitted intensity, but neither a recover to the original state, that could conduct to assume that is a permanent change in the structure of the phosphor layer.

In terms of repeatability (Thermal History Effect), for the Layer#1, the results of the comparison of the two different methods are not in agreement. Therefore, it is not a conclusive comparison.
However, the results of the statistical comparison for the Layer#2, shows that the two different methods, in this case, are in complete agreement on the absence of a significant difference between the two different regressions. Therefore, there is not any sign of a potential thermal history effect in the estimated decay time at different temperatures from the heating and the cooling phase.

Considering the reproducibility, the results from the experiments of the two different phosphor layers sensors(Layer#1 and Layer#2) has shown a similar linear behaviour. However, the difference is statistically significant depending on the comparison approach, besides the inconclusive results is necessary to mention that in order to obtain a calibration curve that characterize the system this difference could introduced as an uncertainty contribution factor.

8

Future Work

8.1 Automation of the Entire Process

There are several improvements in different aspects of the developed Phosphor Thermometry System, the automation of the entire process could be one of them. The objective is to automate the process and unify the two main systems involved (Surface Temperature Reference and the Phosphor Thermometry System) that could reduce the calibration time and also reduce the associated uncertainty of acquiring the temperature measurements manually.

8.2 Effect of Different Binders

The fabricated phosphor layer sensor in this project makes use of an acetone-alcohol based binder. However, there are other types that, for example are water-based. The investigation on the effect of the different binders in the luminescence properties could be an interesting future work to perform, which does not require a high investment.

Bibliography

[1] EMPRESS Project Website ,University of Strathclyde Glasgow-UK.url:https://www.strath.ac.uk/afrc/projects

[2] Pearce, J.V.and Edler, F. and Elliott, C.J.and Rosso, L. and Sutton, G. and Zante, R and Machin, G., A European project to enhance process efficiency through improved temperature measurement: EMPRESS. 17th International Congress of Metrology (2015)url:https://doi.org/10.1051/metrology/20150008001

[3] Abou Nada, Fahed. (2016) *"Phosphor Thermometry: Advances in Technique Development and Applications."*Doctoral Dissertation.Division of Combustion Physics,Department of Physics,Lund University - Sweden.(ch.2). url:http://lup.lub.lu.se/record/d1326fed-8ead-4e29-bd6c-b5c531c15f67

[4] Holman,J.P. *"Experimental Methods for Engineers"*(8ed)(2012)McGraw-Hill Series in Mechanical Engineering.(ch.8)

[5] Fraden,Jacob. *"Handbook of Modern Sensors",(Physics, Designs, and Applications)*(5ed)(2016)Springer[page 228].url:http://www.springer.com/la/book/9783319193021

[6] Knappe, Christoph. (2013) *"Phosphor Thermometry on Surfaces - A Study of its Methodology and its Practical Applications."*Doctoral Thesis.Division of Combustion Physics,Department of Physics,Lund University - Sweden.(ch.2).url:http://lup.lub.lu.se/record/4022201

[7] Fraden,Jacob. *"Manual on the use of the Thermocouples in Temperature Measurements"*(4ed)(1993)Sponsored by ASTM Committee E20 on Temperature Measurement (ch.2 and ch.7)

[8] AMETEK Thermocouples Assembly url:http://www.ametekcalibration.com/products/temperature/industrial-temperature-sensors/1500-and-1600-series-industrial-temperature-sensors

[9] L. Michalski, K. Eckersdorf, J. Kucharski, J. McGhee. *"Temperature Measurement"*(2ed)(2001)John Wiley & Sons Ltd(ch.16)

[10] Material Total Emissivity Table:https://www.omega.com/temperature/Z/pdf/z088-089.pdf

[11] Insulation Material Referencehttp://www.goodfellow-ceramics.com/

[12] Frank P. Incropera,David P. Dewitt *"Fundamentals of Heat and Mass Transfer"*(7ed)(2003) John Wiley & Sons(ch.2,ch.3)

[13] Kulakowski, Bohdan T. and Gardner, John F. and Shearer, J. Lowen *"Dynamic Modeling and Control of Engineering Systems"*(3ed)(2007) Cambridge University Press(ch.8)

[14] Dr.Derek Rowell *"State-Space Representation of LTI Systems"*(2002) MIT University http://web.mit.edu/2.14/www/Handouts/StateSpace.pdf

[15] Richard C.Dorf,Robert H.Bishop *"Modern Control Systems"*(12ed)(2011) Prentice Hall

[16] (JCGM 104:2009)Evaluation of measurement data — An introduction to the "Guide to the expression of uncertainty in measurement" and related documents .url:https://www.bipm.org/utils/common/documents/jcgm/JCGM_104_2009_E.pdf

[17] (JCGM 100:2008) Evaluation of measurement data — Guide to the expression of uncertainty in measurement url:https://www.bipm.org/utils/common/documents/jcgm/JCGM_100_2008_E.pdf

[18] (JCGM 200:2012) International vocabulary of metrology – Basic and general concepts and associated terms(VIM) url:https://www.bipm.org/utils/common/documents/jcgm/JCGM_200_2012.pdf

[19] Khalid, Ashiq Hussain and Kontis, Konstantinos (2008) "Thermographic Phosphors for High Temperature Measurements: Principles, Current State of the Art and Recent Applications" url:http://www.mdpi.com/1424-8220/8/9/5673

[20] Christoph Knappe,Martin Algotsson,Peter Andersson,Mattias Richter,Martin Tunér,Bengt Johansson,Marcus Aldén (2013) *"Thickness dependent variations in surface phosphor thermometry during transient combustion in an HCCI engine"*(Elsevier) url:http://dx.doi.org/10.1016/j.combustflame.2013.02.023

[21] J Bruubach, J P Feist and A Dreizler (2007) *"Characterization of manganese-activated magnesium fluorogermanate with regards to thermographic phosphor thermometry"*(IOP PUBLISHING) url:http://iopscience.iop.org/article/10.1088/0957-0233/19/2/025602/meta

[22] Dr. James E. Parks(2013) *"Temperature Dependent Lifetime Measurements of Fluorescence from a Phosphor"*(Special Edition for 2013 AAPT Summer Meeting Workshop) url:http://www.phys.utk.edu/labs/modphys

[23] Christoph Knappe,Kristin Pfeiffer,Mattias Richter,Marcus Aldén (2013) *"A library-based algorithm for evaluation of luminescent decay curves by shape recognition in time domain phosphor thermometry"*(Elsevier) url:https://link-springer-com.ez.statsbiblioteket.dk:12048/content/pdf/10.10072Fs10973-013-3337-3.pdf

[24] Douglas C. Montgomery *"Applied Statistics and Probability for Engineers"(5ed)*(2011)(John Wiley & Sons, Inc)[page 365/405]

[25] NIST: National Institute of Standards and Technology url:https://www.nist.gov/document/pt-ilc-report-terminology-guidance-8-4-2011-2doc

[26] Donald W. Zimmerman *"A note on preliminary tests of equality of variances"* url:https://onlinelibrary.wiley.com/doi/pdf/10.1348/000711004849222

[27] Edmund S. Scanlon *"Residuals and Influence in Regression"* url:https://www.casact.org/pubs/proceed/proceed94/94123.pdf

[28] *"NIST/SEMATECH e-Handbook of Statistical Methods"* url:https://www.itl.nist.gov/div898/handbook/eda/section3/6plot.htm

[29] C. Knappe, M. Algotsson, P. Andersson, M. Richter, M. Tunér, B. Johansson,(2013) *"Thickness dependent variations in surface phosphor thermometry during transient combustion in an HCCI engine"*Division of Combustion Physics,Department of Physics,Lund University - Sweden.url:http://lup.lub.lu.se/record/3920815

[30] *"Eddy current test method, (amplitude sensitive)"* according to the standards ISO 2360, ASTM 7091.url:http://www.fischer-technology.com/en/united-states/knowledge/methods/coating-thickness-measurement/eddy-current-method-amplitude-sensitive/

[31] I.C.Sellars (Available online 21 April 2000) *"The dangers of single-point calibration for electronic coating thickness gauges"* Elcometer Instruments Ltd., Droylsden, Manchester, England.url:https://www-sciencedirect-com.ez.statsbiblioteket.dk:12048/science/article/pii/0026057695913079?_rdoc=1&_fmt=high&_origin=gateway&_docanchor=&md5=b8429449ccfc9c30159a5f9aeaa92ffb&ccp=y

[32] *"Non-conductive coatings on non-magnetic electrically conductive base metals – Measurement of coating thickness – Amplitude-sensitive eddy-current method"* ISO 2360:2017.url:https://www.iso.org/obp/ui/#iso:std:iso:2360:ed-4:v1:en

[33] *"Airbrush Components"* url:https://www.reddit.com/r/minipainting/comments/3a1ihn/rminipaintings_official_airbrush_guide/

[34] Focus Eye Health url:https://www.focuseyehealth.com

[35] Hamamatsu url:https://www.hamamatsu.com/jp/en/product/wave/index.html

[36] Edited by Leah Bergman, Jeanne L. McHale (2012) *"Handbook of Luminescent Semiconductor"* ISO 2360:2017.url:https://www.iso.org/obp/ui/#iso:std:iso:2360:ed-4:v1:en

[37] Encyclopædia Britannica *"Selection rule. Atomic Physics"*url:https://www.britannica.com/science/selection-rule

[38] R M Ranson†, C B Thomas and M R Craven (1998) *"A thin film coating for phosphor thermography"* Department of Electrical and Electronic Engineering, Nottingham Trent University. url:http://iopscience.iop.org.ez.statsbiblioteket.dk:2048/article/10.1088/0957-0233/9/12/003/pdf

[39] ThorLabs url:https://www.thorlabs.com/newgrouppage9.cfm?objectgroup_id=3257

[40] Physics and radio-electronics website url:http://www.physics-and-radio-electronics.com/electronic-devices-and-circuits/semiconductor-diodes/photodiodesymboltypes.html

A

Appendix A: Matlab Implementation Codes

Thermocouples Measurement Uncertainty Estimation

Thermocouples Position Associated Uncertainty

```
%% TC Position
k=2;%Coverage Factor (95% CI)
TC_Pos=[-2.75;-8.25;-13.75;-19.25];
TC_Pos_sd=1.5/(2*sqrt(3));
U_TC_Pos=k*TC_Pos_sd;
```

Thermocouples Temperature Uncertainty

Calibration Uncertainty Certificate

```
%% Uncertainty TC (k=2 95% CI)
%% 1_Calibration Uncertainty Certificate (Linear Interpolation)(simplified method)
method='linear';
x=[49.9;300.30];%from Certificate
v=[0.042;0.18];%from Certificate
xq=max(TC_Temp_Corr_Layer_1_UP_dt20(1:11,4));
U_Cert_Calib=interp1(x,v,xq,method);
u_Cert_Calib=U_Cert_Calib/2;
```

Repeatability Contribution

```
%% 2_Repeatability(Norm. Dist)
N_rep=20;
%sd
TC_Temp_Corr_Layer_1_UP_dt20_sd=(vec2mat(Temp_Layer_1_UP_dt20(:,2),4));
%standard uncertainty
u_TC_rep_Layer_1_UP_dt20=TC_Temp_Corr_Layer_1_UP_dt20_sd'./sqrt(N_rep);
```

Correction Fit Contribution

```
%% 3_Correction Fit
u_TC_fit_Layer_1_UP_dt20=abs((abs(TC_Temp_Corr_UB_Layer_1_UP_dt20)...
-abs(TC_Corr_Layer_1_UP_dt20))./2);
u_TC_fit_Layer_1_UP_dt20=(vec2mat(u_TC_fit_Layer_1_UP_dt20,4))';
```

DAQ Resolution Contribution

```
%% 4_DAQ Resolution(Unif. Dist)(Medium Sample Rate)
resol_DAQ=0.01;
%standard uncertainty
u_resol_DAQ=0.01/(2*sqrt(3));
```

DAQ Accuracy Contribution

```
%% 5_DAQ Accuracy(Norm. Dist)(for TYPE N TC)(INTERN CJC)
method='linear';
x=[0;500];
v=[0.34;0.24];%(from FLuke Manual)
xq=max(TC_Temp_Corr_Layer_1_UP_dt20(11,4));
U_DAQ_Accuracy=interp1(x,v,xq,method);
%standard uncertainty
u_DAQ_Accuracy=U_DAQ_Accuracy/2;
```

Temperature Stability Contribution

```
%% 6_Temp.Stability(Norm. Dist)
Temp_stab_sd=0.01;
%standard uncertainty
u_Temp_stab=Temp_stab_sd/sqrt(N_rep);
```

Expanded and Relative Thermocouples Uncertainty

```
%% Expanded Uncertainty of TC
k=2;
U_TC_Layer_1_UP_dt20=(sqrt(u_Cert_Calib^2+u_TC_rep_Layer_1_UP_dt20.^2+...
u_TC_fit_Layer_1_UP_dt20.^2+u_resol_DAQ^2+u_DAQ_Accuracy^2+u_Temp_stab^2)).*k;
%% Relative Expanded Uncertainty of TC
U_Rel_TC_Layer_1_UP_dt20=(U_TC_Layer_1_UP_dt20./TC_Temp_Corr_Layer_1_UP_dt20')*100;
```

Linear Regression

Formulas Summary

$$\textbf{DOF}(\nu) \quad \nu = n - p \tag{1}$$

$$\textbf{Total sum of squares} \quad SS_T = SS_{yy} \equiv \sum_{i=1}^{N} (y_i - \overline{y})^2 \tag{2}$$

$$SS_{xx} \equiv \sum_{i=1}^{N} (x_i - \overline{x})^2 \tag{3}$$

$$SS_{xy} \equiv \sum_{i=1}^{N} (x_i - \overline{x})(y_i - \overline{y}) \tag{4}$$

$$\textbf{Model} \quad \hat{y} = \hat{m}x + \hat{b} \tag{5}$$

$$\textbf{Slope} \quad \hat{m} = \frac{SS_{xy}}{SS_{xx}} \tag{6}$$

$$\textbf{Intercept} \quad \hat{b} = \overline{y} - \hat{m}\overline{x} \tag{7}$$

$$\textbf{Error Sum of Squares} \quad SS_E \equiv \sum_{i=1}^{N} (y_i - \hat{y})^2 \tag{8}$$

$$\textbf{Standard deviation of y(x)} \quad s_{y,x} = \sqrt{\frac{SS_E}{\nu}} \tag{9}$$

$$\textbf{Standard deviation of } \hat{m} \quad s_{\hat{m}} = \sqrt{\frac{s_{y,x}^2}{SS_{xx}}} \tag{10}$$

$$\textbf{95\% CI}(\alpha = 0.05) \textbf{ of } \hat{m} \quad \hat{m} \pm t_{\alpha/2,\nu} s_{\hat{m}} \tag{11}$$

$$\textbf{Standard deviation of } \hat{b} \quad s_{\hat{b}} = \sqrt{s_{y,x}^2 \left(\frac{1}{n} + \frac{\overline{x}^2}{SS_{xx}} \right)} \tag{12}$$

$$\textbf{95\% CI}(\alpha = 0.05) \textbf{ of } \hat{b} \quad \hat{b} \pm t_{\alpha/2,\nu} s_{\hat{b}} \tag{13}$$

$$\textbf{Prediction interval(new value of } y \textbf{ at } x_p) \quad (\hat{m}x_p + \hat{b}) \pm t_{\alpha/2,\nu} s_{y,x} \sqrt{1 + \frac{1}{n} + \frac{(x_p - \overline{x})^2}{SS_{xx}}} \tag{14}$$

All formulas are extracted from [24](page 405).

Linear Regression (Main Assumptions)

```
function [beta_LR,statistics_LR] = SLR(x,y,alpha)
%% Linear Regression
%% Assumptions

%% 1. Linearity

% Linear regression models the straight-line relationship between Y and X. Any curvilinear
%relationship is ignored.
% This assumption is most easily evaluated by using a scatter plot. This should be done
%early on in your analysis.
% Nonlinear patterns can also show up in residual plot. A lack of fit test is also provided.

%% 2. Constant Variance

% The variance of the residuals is assumed to be constant for all values of X.
%This assumption can be detected by plotting the residuals versus the independent variable.
%If these residual plots show a rectangular shape, we can
% assume constant variance. On the other hand, if a residual plot shows an
%increasing or decreasing wedge or bowtie  shape, nonconstant variance (heteroscedasticity)
%exists and must be corrected.
% The corrective action for nonconstant variance is to use weighted linear
%regression or to transform either Y or X in
% such a way that variance is more nearly constant. %
%The most popular variance stabilizing transformation is the to
% take the logarithm of Y.

%% 3.Special Causes

% It is assumed that all special causes, outliers due to one-time
%situations, have been removed from the data. If not,
% they may cause non-constant variance, , or other
%problems with the regression model. The existence
% of outliers is detected by considering scatter plots of Y and X as
%well as the residuals versus X. Outliers show up as
% points that do not follow the general pattern.

%% 4.Normality

% When hypothesis tests and confidence limits are to be used,
%the residuals are assumed to follow the normal distribution

%% 5. Independence

% The residuals are assumed to be uncorrelated with one another,
%which implies that the  Y  s  are also uncorrelated.
%This assumption can be violated in two ways: model misspecification or time-sequenced data.

%% Reference
%(NCSS Software)
%(Obtaining Uncertainty Measures on Slope and Intercept of a Least Squares Fit)
%http://pages.mtu.edu/~fmorriso/cm3215/UncertaintySlopeInterceptOfLeastSquaresFit.pdf
%% Douglas C. Montgomery
%"Applied Statistics and Probability for Engineers"(5ed)}(2011)[page405]
```

Linear Regression (Matlab Implementation)

```
%% Model
%   Y=beta_LR_0+beta_LR_1*X+epsilon
Model=@(x,m,b)  m.*x+b;
%% Variables
N= length(x);                   % Number of elements
x_mean= mean(x);                % Mean value of x
x_dev=x-x_mean;                 % Deviation of x
y_mean= mean(y);                % Mean value of y
y_dev=y-y_mean;                 % Deviation of y
p=2;                            % Number of Regression Parameters

%% Coefficient Estimates
SSxx=sumsqr(x_dev);
SSxy=sum(x_dev.*y_dev);
%Slope
m=SSxy/SSxx;
%Intercept
b=y_mean-m*x_mean;
beta_LR=[b;m];
%% Predicted Values of the Dependet Variable (Y_hat)
Y_hat=Model(x,m,b);
% DOF
nu=N-p;
%% Estimated Standard Deviations
% Syx Standard deviation of y(x)
e=y-Y_hat;
SSE=sumsqr(e);
Syx=sqrt(SSE/nu);
% Sm Standard deviation of slope m
Sm=sqrt(Syx^2/SSxx);
% Sb Standard deviation of intercept b
Sb=sqrt(Syx^2*((1/N)+(x_mean^2/SSxx)));
%% Confidence Intervals of the Intercept and Slope
statistics_LR.t_c_LR    = tinv(1-alpha/2,nu);
m_ci_UB=m+statistics_LR.t_c_LR*Sm;
m_ci_LB=m-statistics_LR.t_c_LR*Sm;
b_ci_UB=b+statistics_LR.t_c_LR*Sb;
b_ci_LB=b-statistics_LR.t_c_LR*Sb;
statistics_LR.coeff_ci_LR   =[b_ci_LB,b_ci_UB;m_ci_LB,m_ci_UB];
%% Pred Values
statistics_LR.Pred_Val=Model(xp,m,b);
%% CI(confidence intervals) Predicted Values
statistics_LR.predval_ci_UB_LR=statistics_LR.Pred_Val+ ...
statistics_LR.t_c_LR*Syx*sqrt(1+(1/N)+((xp-x_mean).^2/SSxx));
statistics_LR.predval_ci_LB_LR=statistics_LR.Pred_Val- ...
statistics_LR.t_c_LR*Syx*sqrt(1+(1/N)+((xp-x_mean).^2/SSxx));
```

Uncertainty Estimation of Coating Thickness

Uncertainty Components

Repeatability ($u_{Rep.}$)

$$u_{Rep.} = \frac{sd_{thk}}{\sqrt{N}} \tag{15}$$

Where:
sd_{thk}: thickness standard deviation of a set of measurements.
N: number of of measurements.
Associated PDF: Normal Distribution

Resolution ($u_{Resol.}$)

$$u_{Resol.} = \frac{Resol.}{2.\sqrt{3}} \tag{16}$$

Where:
Resol.: Instruments Resolution for an specific range (in this case 0.1 [μm])
Associated PDF: Uniform Distribution

Thickness Meter Specification Accuracy ($u_{Acc.}$)

$$u_{Acc.} = \left(\frac{\mu_{thk}.Spec_{Acc.} + Spec_{Acc.Floor}}{2} \right) \tag{17}$$

Where:
μ_{thk}: thickness mean value of a set of measurements.
$Spec_{Acc.}$: Instrument accuracy 2.5 % for the corresponding thickness range.(from manual)
$Spec_{Acc.Floor}$: Assigned floor value (in this case 2 [μm])for the corresponding thickness range.
Associated PDF: Normal Distribution

Standard Uncertainty

$$u_{thk} = \sqrt{u_{Rep.}^2 + u_{Resol.}^2 + u_{Acc.}^2} \tag{18}$$

Expanded Uncertainty (95 % CI)

$$U_{thk} = k.u_{thk} \tag{19}$$

Implemented Calculations Example(Operator#1)

```
%% Uncertainty Estimation of Coating Thickness
%Thickness Meter Specification Accuracy (from manual)
TM_Spec_Acc=2.5/100; % 2.5[%] of the reading.
TM_Spec_Acc_Floor=2; % Fixed floor value 2 [um]
%Individual Layer Meassurements
OP_1_mean=mean(OP_1);
OP_1_sd=std(OP_1);
%% Standard Uncertainty
%Repeatability
N=length(OP_1(:,1));%N=30; Number of Measurements
u_rep_OP_1=(OP_1_sd/sqrt(N));
%Resolution
u_resol=0.1/(2*sqrt(3));
%Thickness Meter Specification Accuracy
u_spec_acc_OP_1=(OP_1_mean*TM_Spec_Acc+TM_Spec_Acc_Floor)/2;
%Combined Uncertainty
for i=1:length(OP_1(1,:))
u_OP_1(i,1)=rssq([u_rep_OP_1(i);u_resol;u_spec_acc_OP_1(i)]);
end
%Expanded Uncertainty & Relative Expanded Uncertainty
k=2; %Coverage Factor (95 % CI)
U_OP_1=k.*u_OP_1; U_Rel_OP_1=(U_OP_1'./OP_1_mean).*100;
```

Mean Decay Time (τ_μ) Estimation Algorithm

```
%% WORKSPACE PREPARATION %%
close all                                          % Close figures
clc                                                % Clear screen
clear                                              % Clear all variables in memory
format compact                                     % Number Format
%% Layer#1 20um dT 20 Data Analysis
%% Data Up
tic
%% memory preallocation
Iw0=zeros(32,11);
I_stop=zeros(32,11);
I_0_NLF=zeros(32,11);
tau_NLF=zeros(32,11);
SNR=zeros(32,11);
Time=zeros(2445,32,11);
Emitted_Corrected=zeros(2445,32,11);
Excitation_Corrected=zeros(2445,32,11);
u_tau_Fit=zeros(32,11);
load('t_Off_Lag_mean_UV_LED')
t_Off_Lag_mean_UV_LED=t_Off_Lag_mean_UV_LED/1000;
```

```
for k=1:11
for j=1:32
%%  Sample Rate
Time(:,j,k)=Data(:,1,j);%[ms]
Emitted=Data(:,2,j);%[mV]
Excitation=Data(:,3,j);%[V]
Sample_Int=diff(Time(:,j,k));%Sample Interval[ms]
Sample_Int_mean=mean(Sample_Int);
Sample_Int_std=std(Sample_Int);
u_Sample_Int=Sample_Int_std/sqrt(length(Sample_Int));
Sample_Rate_msec=1./(Sample_Int_mean);%Sample Rate[Samples/s]
Sample_Rate_sec=1./(Sample_Int_mean./1000);%Sample Rate[Samples/s]
```

```
%% LED Electrical Signal
%Determine t_On (where tOn is the moment of LED On(Electrical Signal))
mask_on_off=Excitation>Excitation(1)*5;
t=1:length(Time);
t=t(mask_on_off);
t_On_Pos=t(1);
%Determine tOff (where tOff is the moment of LED Off(Electrical Signal))
t_Off_Pos=t(end)+1;
```

```
%% Light Intensity Offset Correction
Emitted_Offset=mean(Emitted(1:t_On_Pos-1));
Excitation_Offset=mean(Excitation(1:t_On_Pos-1));
Emitted_Corrected(:,j,k)=Emitted-Emitted_Offset;
Excitation_Corrected(:,j,k)=Excitation-Excitation_Offset;
```

```
%% Fitting Window
%LED Characterization
t_Off_Lag=t_Off_Lag_mean_UV_LED; %300 [us]from LED Characterization
tOff_Lag_Pos=ceil(t_Off_Lag/Sample_Int_mean);
```

```
%Start Time
t_start_Pos=t_Off_Pos+tOff_Lag_Pos;
Iw0(j,k)=Emitted_Corrected(t_start_Pos,j,k);
Emitted_Corrected_Clean=Emitted_Corrected(t_start_Pos:end,j,k);
Time_Clean=[0;(1:1:length(Time(t_start_Pos:end-1,j,k)))'].*Sample_Int_mean;
```

```
%Stop Time
p=22.3;% percentage of the iniital intensity
I_stop(j,k)=(p/100)*Iw0(j,k);%stop criteria
```

```
% Intensity above %p
mask_above=Emitted_Corrected_Clean>I_stop(j,k);
t_above=(1:length(Emitted_Corrected_Clean))';
t_above_p_Pos=flipud(t_above(mask_above));
t_above_p=Time_Clean(t_above_p_Pos);
```

```
% Intensity below %p
mask_below=¬mask_above;
t_below=(1:length(Emitted_Corrected_Clean))';
t_below_p_Pos=t_below(mask_below);
t_below_p=Time_Clean(t_below_p_Pos);
range=min([length(t_above_p) length(t_below_p)]);
```

```
% t_stop from t_avg
t_avg=mean([t_below_p(1:range) t_above_p(1:range)],2);
t_diff=abs(diff(t_avg));
t_stop_Pos=find(Time_Clean<t_avg(end-1));
t_stop_Pos=t_stop_Pos(end);
```

```
%Fitting Windows Range
FWL=(t_stop_Pos);%Fitting Window Length
Fit_Range=1:t_stop_Pos;
Time_Fit=(0:1:FWL-1)'.*Sample_Int_mean;
Emitted_Corrected_Fit=Emitted_Corrected_Clean(Fit_Range);
```

```

%% Curve Fitting
%% Non-Linear Fit
% Set up fittype and options.
ft = fittype( 'I_0*exp(-t/tau)', 'independent', 't', 'dependent', 'I' );
opts = fitoptions( 'Method', 'NonlinearLeastSquares' );
opts.Algorithm = 'Levenberg-Marquardt';
opts.Display = 'Off';
opts.MaxFunEvals = 1000;
opts.MaxIter = 1000;
% opts.Robust = 'Off';
%opts.Robust = 'LAR';
opts.Robust = 'Bisquare';
opts.StartPoint = [Iw0(j,k) 3];
% Fit model to data.
[fitresult_NLF, gof] = fit(Time_Fit, Emitted_Corrected_Fit, ft, opts );
coeffvals_NLF = coeffvalues(fitresult_NLF);
ci = confint(fitresult_NLF,0.95);
u_tau_Fit(j,k)=(coeffvals_NLF(2)-ci(1,2))/2;%standard uncertainty due to curve fit
R_2_NLF(j,k)=gof.rsquare;
I_0_NLF(j,k)=coeffvals_NLF(1);%Amplitude Non-Linear Fit
tau_NLF(j,k)=coeffvals_NLF(2);%Tau Non-Linear Fit

%% SNR (Signal-to-noise ratio)
x_signal=Emitted_Corrected_Fit;%Signal
y_noise=Emitted_Corrected(1:length(Fit_Range),j,k);%Noise
SNR(j,k) = snr(x_signal,y_noise);
end
end
```

```
%% Results
N=32;

%% Removing Faulty Buffer File (T6 UP 30)
for i=1:11
tau_NLF_w_Faulty{:,i}=tau_NLF(:,i);
I_0_NLF_w_Faulty{:,i}=I_0_NLF(:,i);
end

%% Tau
tau_NLF_w_Faulty{1,6}(30)=[];
tau_NLF= tau_NLF_w_Faulty;
%% I_0
I_0_NLF_w_Faulty{1,6}(30)=[];
I_0_NLF= I_0_NLF_w_Faulty;

%% Mean Results
for i=1:11
%% log
tau_NLF_log{:,i}=log(tau_NLF{:,i});
tau_NLF_mean_log(:,i)=mean(tau_NLF_log{:,i});
tau_NLF_sd_log(:,i)=std(tau_NLF_log{:,i});

tau_NLF_mean(:,i)=mean(tau_NLF{:,i});
tau_NLF_sd(:,i)=std(tau_NLF{:,i});
%%
I_0_NLF_mean(:,i)=mean(I_0_NLF{:,i});
end
%% Tau Standard Uncertainty
for i=1:11
    if i==6
        u_tau_NLF(:,i)=tau_NLF_sd(i)./sqrt(N-1);
        u_tau_NLF_log(:,i)=tau_NLF_sd_log(i)./sqrt(N-1);
    else
        u_tau_NLF(:,i)=tau_NLF_sd(i)./sqrt(N);
        u_tau_NLF_log(:,i)=tau_NLF_sd_log(i)./sqrt(N);
    end
end
```

B

Appendix B: Important Data Sheet

High CRI Phosphors

Phosphor SV 067N

Code: 464 0251

International Name	-
Chemical Composition	Magnesiumfluorogermanate: Mn
Chemical Symbol	$Mg_4FGeO_{5,5}$: Mn

Optical Properties

Emission Color*	Dark Red
Wavelength at Peak	λ_{max} = 659 nm
CIE Color Coordinates*	x = 0,544
	y = 0,284
Correlated Color Temperature*	-

(* incl. Hg-Radiation as determined in L 36 W / T8)

Physical Properties

Density	ρ = 3,9 g/cm^3
Body Color	Yellowish
Particle Size Distribution (CILAS 1064)	d_{50} = 6,5 - 10,5 µm
	b_{80} = $(d_{90} - d_{10})/d_{50} < 2,1$

Excitation

UV-Radiation, X-Rays, Cathode Rays

Typical Application

Low pressure mercury lamps (CFL; TFL) for high CRI applications; water and organic based suspension

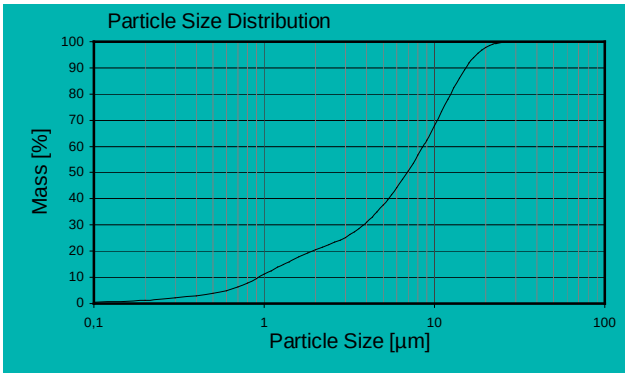

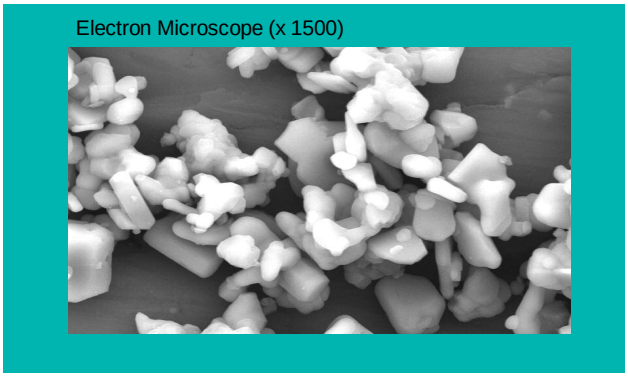

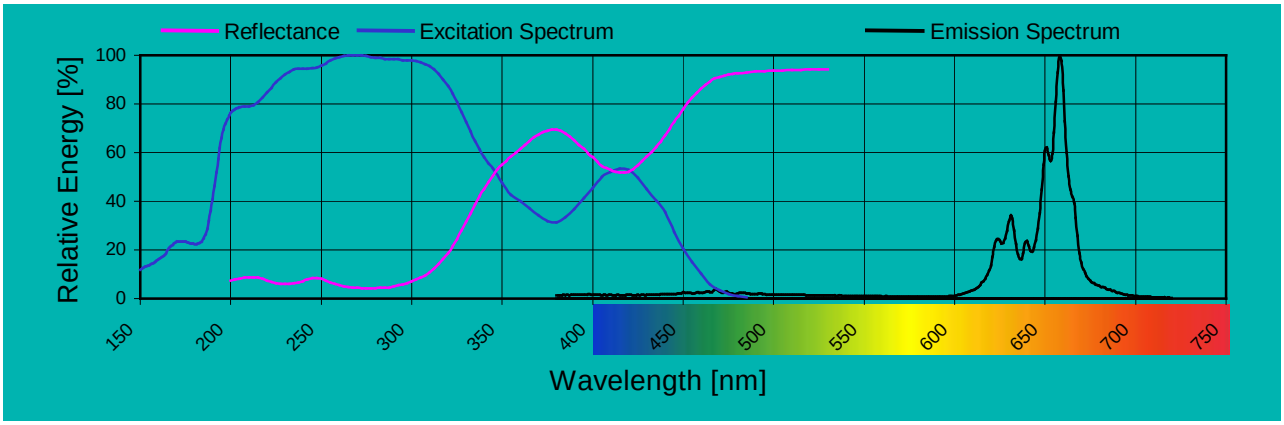

Note: (1) This reference is for general product specification purposes only. It does not cover a liable determination of the given data.
We reserve the right to alter the data at any time. Therefore, before you process this product we recommend to contact us.
(2) We are not able to warrant that you will not infringe third party intellectual property rights in case you process this product or employ it in other products.

Issue: 11/01

120 Valley Court
Oak Ridge, TN 37830
Ph: 865-482-5717
FAX: 865-482-1281
zypcoatings.com

BNSL Binder

Solvent-based Binder Liquid For Creating Your Own Paint

BNSL Binder is one of our most versatile suspension agent/binder liquids. With an alcohol-acetone based vehicle, it is the binder for our mainline aerosol sprays. The binder also has a medium ability to suspend solids and generally produces low to medium viscosity coatings with most refractory powders. With its non-aqueous binder liquid, BNSL not very reactive to materials. Most any powder can be used with it. It has a long shelf life and flash point of 15 F. BNSL Binder is often a preferred binder for first trials due to its utility in air environments and inertness to most powder additives.

Key Attributes

- Moderate water-resistance on ambient drying
- Moderate suspendability of 'filler' powders
- Forms moderate-hardness coatings
- Good in all atmospheres, including air
- Minimal outgassing (H_2O, CO_x)—mostly complete by 150 C
- Dilutable with Ethanol for slower drying or Acetone for faster drying or any combination of these
- Safe, easy-to-use
- No cure needed

Ideal Uses

- Binder/Suspender
- Infiltrant

Possible Fillers

- Compatible with most everything
- Ideal for water-sensitive/reactive materials
- Consider eutectics that form low-melting situations

Use Notes

1. Add refractory 'filler' (<10 microns preferred)
2. Start at 50wt.% powder. Mix by rolling/shaking.
3. If too thick, add water; if too thin, add powder.
4. Re-mix by rolling or shaking.

After making paint above, clean substrate, apply paint, dry (with no cure needed), and place into use.

Specifications

Active Ingredients	>99% MgO-SiO_2
Max Use Temperature	1600 C
Use Atmosphere	All
Fired Composition/Binder Phase	Glassy Carbon/ Magnesium Silicate
Hardness	Moderate
Liquid Carrier	Ethanol/Acetone
Water Resistance	Moderate
Ability to Suspend Solids	Moderate
Brookfield Viscosity (cps)	185 @2/60
Specific Gravity	0.82
Shelf Life (months)	>12
Coating pH	Not applicable
H F R Ratings	1-3-0
Substrate Use	All
% Volatiles	97

Safety Information

- Consult SDS before use.
- Avoid breathing of spray/vapors.
- For Industrial Use only.

Sizes and colors

BNSL Binder is a cloudy liquid.
Standard Size: 1 gallon Nalgene container.

CAUTION: DO NOT CONTACT WET COATINGS WITH MOLTEN METAL.